Bachelor's thesis

NTNU
Norwegian University of Science and Technology
Faculty of Engineering
Department of Energy and Process Engineering

Julie Helen Evenstuen
Pernille Sofie Pedersen
Ida Marie Thrane

Utilising the Potential in Thermally Activated Building Systems (TABS) to Optimise the Positive Energy Block (PEB) at Sluppen

Bachelor's thesis in Engineering, Renewable Energy
Supervisor: Jacob J. Lamb
May 2022

NTNU
Kunnskap for en bedre verden

Julie Helen Evenstuen
Pernille Sofie Pedersen
Ida Marie Thrane

Utilising the Potential in Thermally Activated Building Systems (TABS) to Optimise the Positive Energy Block (PEB) at Sluppen

Bachelor's thesis in Engineering, Renewable Energy
Supervisor: Jacob J. Lamb
May 2022

Norwegian University of Science and Technology
Faculty of Engineering
Department of Energy and Process Engineering

NTNU
Norwegian University of
Science and Technology

NTNU

Institutt for energi- og prosessteknikk

Bacheloroppgave

Project title (ENG): Utilising the Potential in Thermally Activated Building Systems (TABS) to Optimise the Positive Energy Block (PEB) at Sluppen **Oppgavens tittel (NOR):** Utnyttelse av potensialet i termoaktive dekker for å optimalisere den positive energiblokken på Sluppen	**Gitt dato:** 06.01.2022 **Innleveringsdato:** 20.05.2022 **Antall sider rapport / sider vedlagt:** 93/23
Gruppedeltakere: Julie Helen Evenstuen, Pernille Sofie Pedersen, Ida Marie Thrane	**Veileder:** Jacob J. Lamb **Prosjektnummer:** 22BIFOREN-001
Oppdragsgiver: TrønderEnergi AS	**Kontaktperson hos oppdragsgiver:** Mette Rostad

Fritt tilgjengelig: ☒

Tilgjengelig etter avtale med oppdragsgiver: ☐

Rapporten frigitt etter:

Preface

This bachelor thesis is written as a part of the Renewable Energy Engineering program at the Norwegian University of Science and Technology (NTNU) for the concluding semester of spring 2022. The thesis is written in collaboration with *TrønderEnergi*, with supporting data from Kjeldsberg.

We want to take this opportunity to thank Jacob J. Lamb, our supervisor at NTNU, for his weekly follow-up, helpful input, motivation, laughs and coffee. A thank you is also directed to *TrønderEnergi* for the opportunity to contribute to the +CityxChange project and for trusting our vision for the thesis. An extra thank you to Mette Rostad for her enthusiasm, encouragement and knowledge and Berhard Kvaal for guidance on behalf of *TrønderEnergi*.

Thanks to Thomas Berg Jørgensen and Truls Reitan Berthelsen at *Kjeldsberg* for a tour of the buildings and helpful insight, and Morten Fossum at *Statskraft Varme* for presenting the district heating network in Trondheim.

Finally, we want to thank the Department of Energy and Process Engineering (EPT) for creating an environment that allows us to contribute to our generation's biggest challenge, reducing the effects of climate change.

Trondheim, 19.05.22

Julie Helen Evenstuen Pernille Sofie Pedersen Ida Marie Thrane

Abstract

Buildings account for 40 % of the world's energy use, most of which is used for space heating and the operation of electrical equipment. Creating buildings with more efficient and environmentally friendly heating systems is therefore crucial to reducing greenhouse gas emissions. The +CityxChange project, a European Commission Horizon 2020 project, aims to build zero-emissions sustainable urban ecosystems with 100 % renewable energy sources. Four buildings at Sluppen, Sluppenvegen (SLV) 11, 13, 17B and 19 in Trondheim are in the process of becoming a Positive Energy Block (PEB), as a part of the +CityxChange project. The buildings hold offices, a food court, and a climbing centre.

This thesis aims to analyse ways of shaving power peaks and optimising energy usage by simulating PEB properties and utilising Thermally Activated Building Systems (TABS), heat pumps, and sector coupling to move and change heating demands and power peaks.

A literature review on TABS was conducted to create an overview of other experiences and better understand the pros and cons of TABS. TABS is not a widespread technology in Norway, and presently, three buildings have them installed, and two more are under construction. The flexibility of TABS can be used to shave power peaks, but it is complex to calculate accurately. However, several simple models have relatively high accuracy, especially for cooling systems.

A case study of Sluppen with the relevant technical specifications and system descriptions was performed. The current status of the Sluppen-system was mapped to conduct simulations in MatLab. Simple simulations characterised the peak shaving potential and moved heating loads from 07:00–16:00 to 20:00–05:00. Another simulation explored the opportunities of using sector coupling to lower electricity demand.

The Base Case showed that the system currently does not qualify as a PEB. However, Kjeldsberg has planned multiple measures to make sure the system soon becomes one. The heat pumps are the primary heat source for SLV 17B and SLV 19, and electrical equipment consumes the most electricity. Approximately 57 % of the heat consumed at SLV 17B gets distributed through the TABS. The peak shaving potential is most prominent around noon on weekdays, especially during the winter months.

In the TABS and heat pump simulations, the power peak reduction is around 11 % but the total energy demand increases. The potential is highest in the winter and lowest in the summer. In the sector coupling simulation, the power demand was decreased by 5 %, while the district heating demand grew dramatically by 235 %. Due to the district heating pricing model, this scenario has a competitive disadvantage compared to heat pumps. Additional PV installation is planned; however, according to the calculations, this will not make the system reach the PEB requirements. More renewable energy is needed to even out the production curve and conform to the consumption curve.

This thesis will contribute to TrønderEnergi's work in the +CityxChange project by providing an overview of the available data and implying what additional data needs to be collected. In addition, it will contribute with a theoretical base for optimising the system to become a PEB and give insight into TABS.

Sammendrag

Bygninger står for 40 % av verdens energibruk, hvorav mesteparten går til romoppvarming og drift av elektrisk utstyr. Å videre utvikle bygninger med mer effektive og miljøvennlige varmesystemer er derfor avgjørende for å redusere klimagassutslipp. +CityxChange-prosjektet, et European Commission Horizon 2020-prosjekt, har som mål å bygge bærekraftige nullutslipp- og urbane økosystemer med 100 % fornybar energi tilførsel. Fire bygg på Sluppen, Sluppenvegen (SLV) 11, 13, 17B og 19 i Trondheim er i startfasen av å bli en positiv energiblokk (PEB), som en del av +CityxChange. Bygningene består av kontorer, en mathall og et klatresenter.

Denne oppgaven analyserer ulike strategier for å kutte effekttopper og optimalisere energiforbruk. Dette gjøres ved å simulere de ulike egenskapene ved PEB-en; utnytte termoaktive dekker (TABS), varmepumper og sektor kobling for å flytte og endre varmebehov og effekttopper.

En litteraturstudie om TABS ble utført for å gi en oversikt over andre erfaringer og bedre forstå fordeler og ulemper med TABS. TABS er ikke en utbredt teknologi i Norge, og er per dags dato installert i tre bygninger, og er ytterligere planlagt i to bygg. Fleksibiliteten til TABS kan brukes til å kutte effekttopper, men det er komplisert å beregne eksakt. Imidlertid har mange enkle modeller høy nøyaktighet, spesielt for kjølesystemer.

Det ble gjennomført en casestudie av Sluppen, med fokus på systembeskrivelsene og relevante tekniske spesifikasjoner. Kartlegging av dagens situasjon på Sluppen (Base Case), ble gjort for å kunne gjennomføre simuleringer i MatLab. Enkle simuleringer karakteriserte potensialet for kutting av effekttopper ved flytting av varmelaster fra 07:00–16:00 til 20:00–05:00. En annen simuleringsanalyse undersøkte mulighetene for å bruke sektor kobling til å redusere elektrisitetsetterspørsel.

Base Case avdekket at systemet foreløpig ikke kan kvalifiseres som en PEB, men Kjelsberg har planlagt flere tiltak for å sikre at systemet oppnår dette i nær fremtid. Varmepumper er den primære oppvarmingskilden i SLV 17B og 19, og det er elektrisk utstyr som bruker mesteparten av elektrisiteten. Omkring 57 % av varmen som forbrukes i SLV 17B, leveres til TABS. Potensialet for å kutte effekttopper i næringsbyggene er mest fremtredende midt på dagen på hverdager, og i vintermånedene. I TABS- og varmepumpe simuleringene ble effekttoppene redusert med omtrentlig 11 % mens det totale energibehovet gikk opp. Potensialet var større på vinteren, enn på sommeren. I sektor kobling simuleringen gikk elektrisitetsforbruket ned med 5 %, og fjernvarmebehovet økte med 235 %. Prismodellen som brukes på fjernvarme gjør ofte bruk av varmepumper til den billigste løsningen.

Ytterligere installasjoner av solcellepaneler er planlagt, men dette er ikke nok for at systemet skal nå PEB-kravene. Det behøves mer fornybar energi for å jevne ut produksjonskurven og få den til å samsvare med forbrukskurven.

Denne oppgaven vil bidra til TrønderEnergi sitt arbeid i +CityxChange-prosjektet ved å gi en oversikt over tilgjengelige data og antyde hvilke tilleggsdata som må samles inn. I tillegg vil den bidra med et teoretisk grunnlag for å optimalisere systemet på Sluppen til å bli en PEB, og gi innsikt i TABS.

Acronyms, Symbols and Software

List of Acronyms

AMS	Advanced Measurement and Control Systems (Avanserte Måle- og Styringssystemer)
CAPEX	Capital Expenditure
COP	Coefficient Of Performance
DH	District Heating
DHD	District Heating Demand
DWH	Domestic Water Heater
EL	Electricity
ELD	Electricity Demand
EPC	Energy Plus Costumer
ESEER	European Seasonal Energy Efficiency Ratio
ESS	Energy Storage Systems
EU	European Union
GIA	Gross Internal Area
GFA	Gross Floor Area
HP	Heat Pump
LES	Local Energy Systems
LNG	Liquefied Natural Gas
LHS	Latent Heat Storage
LPG	Liquefied Petroleum Gas
NaN	Not a Number
NVE	Norwegian Water Resources and Energy Directorate
PCM	Phase-Change Materials
PEB	Positive Energy Block
PED	Positive Energy District
PV	Photo Voltaic
RES	Renewable Energy Sources
RME	The Norwegian Regulatory Authorities for Energy
SCOP	Seasonal Coefficient of Performance
SD	Industrial Control System (Sentral Driftskontroll)
SEER	Seasonal Energy Efficiency Ratio
SFP	Specific Fan Power
SHS	Sensible Heat Storage
SLV	Sluppenvegen
STC	Standard Testing Conditions
TABS	Thermally Active/Activated Building Systems
TES	Thermal Energy Storage
TESS	Thermal Energy Storage Systems
TSO	Transmission System Operator
UN	United Nations
VCRC	Vapor Compression Refrigeration Cycle
VHC	Volumetric Heat Capacity
ZEB	Zero Emission Building

List of Symbols

Symbol	Unit	Description
$EP_{H,0}$	$\mathrm{kWh/(m^2 \cdot yr)}$	Net Specific Heating Demand
K_1	-	Climate Coefficient
$\theta_{y,m}$	°C	Annual Average Temperature
q''	$\mathrm{W/m^2}$	Heat Flux
k	$\mathrm{W/(m \cdot K)}$	Thermal conductivity
T	K	Temperature
L	m	Wall thickness
h_c	$\mathrm{W/(m^2 \cdot K)}$	Convection heat transfer coefficient
ε	-	Emissivity
σ	$\mathrm{W/(m^2 \cdot K^4)}$	Stefan Boltzmann's constant
A	$\mathrm{m^2}$	Area
R	$\mathrm{m^2 \cdot K/W}$	Thermal resistance
Q	W	Overall heat transfer
U	$\mathrm{W/(m^2 \cdot K)}$	Heat transfer coefficient
r	m	Radius
m	kg	Mass
c_p	$\mathrm{J/(kg \cdot K)}$	Specific heat capacity
h	kJ/kg	Enthalpy
$\dot{m}$	kg/s	Mass flow
W	W	Work
COP	-	Coefficient of performance
P	W	Power
η	%	Efficiency
μ	$\mathrm{kg/(m \cdot s)}$	Dynamic viscosity
ρ	$\mathrm{kg/m^3}$	Density

List of Software

Program	Version
Matlab	R2022a academic use
Microsoft Excel	2022

Contents

List of Figures

List of Tables

1 Introduction

This section presents the background for the thesis, information about the +CityxChange project, the purpose and the limits of the thesis, along with the research questions and structure.

1.1 Background

This thesis is a part of the +CityxChange (Positive City Exchange) project. +CityxChange is a European Commission Horizon 2020 project focusing on building smart cities in the lighthouse cities of Trondheim (NO) and Limerick (IE), along with their distinguished follower cities Alba Iulia (RO), Pisek (CZ), Võru (EE), Smolyan (BG) and Sestao (ES). The cities are actively working to become leading cities in integrating smart, green and positive energy solutions. The goal is to achieve zero-emissions sustainable urban ecosystems, and a 100 % renewable energy city region by 2050. To achieve this, the exchange of information and experiences between project members and dissemination of findings to the public sector is crucial [1].

Sluppen is one of three pilot projects in the +CityxChange project in Trondheim. This area consists of six buildings, four relevant for this thesis, and will be developed into a positive energy block (PEB) within two years. The main goal of this pilot project is for the Sluppen area to become energy positive by 2030. To accomplish this, sector coupling and the connection between district heating and electricity for the heating systems in buildings must be sufficiently integrated [2].

The owner of the Sluppen +CityxChange project is *Trondheim Kommune*; however, the project is a collaboration between numerous partners [2]. Relevant partners for this thesis is *TrønderEnergi*, *Kjeldsberg*, NTNU and *Statskraft Varme*.

1.2 About Sluppen

Sluppen is a vital intersection for traffic from the south into the centre of Trondheim, which has made the area attractive for numerous businesses and industries. Historically, Sluppen was predominantly agricultural land that developed into an industrial area. Now, Sluppen is on the way into a new era, designed by *R. Kjeldsberg* to be a living district day and night, with new housing, offices, and retail and service areas. In addition, the district focuses on sustainability with future-oriented buildings of high quality and good environmental and energy properties [3].

This thesis will concentrate on four buildings at Sluppen, which will form a PEB. This includes Sluppenvegen 11, 13, 17B and 19. Figure 1.1 shows a picture of the mentioned buildings, with the limits of the PEB in this thesis. Sluppenvegen 11 and 13 hold "*Lager 11*" and "*Grip Klatring*", an old storage building that now offers street food, culture, experiences, and bouldering, all within the same building. While Sluppenvegen 17B (Stålgården) and 19 (Lysgården), hold modern offices in new, energy-efficient buildings [3].

Figure 1.1: *The buildings at Sluppen relevant for this thesis with limits for the PEB [4].*

1.3 Purpose of the Thesis

Kjeldsberg, in cooperation with TrønderEnergi, Statkraft Varme, Trondheim Kommune and NTNU aims to make Sluppen into a positive energy block (PEB). The development of PEBs contributes to the transition from linear to integrated energy systems. Furthermore, it contributes to reaching the UN's sustainability goals 7 – Affordable and Clean Energy, 9 – Industry, Innovation and Infrastructure, 11 – Sustainable Cities and Communities and 13 – Climate Action. TrønderEnergi is a significant hydropower and wind power actor in Trøndelag and works a considerable amount with future energy solutions. The Sluppen system is currently in the early stages of becoming a PEB. On this basis, the group and TrønderEnergi constructed a thesis focusing on evaluating the existing system and data to map the peak shaving potential in the buildings for use in future analysis.

1.4 Research Question

This thesis aims to assess how thermally activated building systems (TABS) affect heating demands at Stålgården (Sluppenvegen 17B) in Trondheim and how this can optimise the soon to be PEB at Sluppen. The goal is to simulate the properties of a PEB and analyse methods for shaving power peaks by utilising TABS, heat pumps and sector coupling. Future energy systems have to transition into more centralised systems to reach the global climate goal, where it is essential to utilise local resources and have a flexible system. Building and optimising the production and consumption patterns in PEBs are a method to achieve this.

1.5 Limits of the Thesis

This thesis is limited by the data provided by TrønderEnergi and Kjeldsberg. In multiple datasets, no data was available for January and February; therefore, all simulations and results start in March. Missing or erroneous data, such as room temperature and TABS meter, also limited the thesis. The inaccurate TABS meter data required the thesis to take a more

theoretical approach instead of a practical one. Missing room temperature data prohibited a proper flexibility analysis on the TABS.

Out of all the buildings at Sluppen, only four buildings are considered part of the thesis; Sluppenvegen 11, 13, 17B, and 19.

The +CityxChange project is an EU project with EU regulations, assumptions, and definitions that do not necessarily apply to the Norwegian power market. In this thesis, all of these have been disregarded.

The results (figures and numbers) presented in this thesis are our interpretation and are produced by us based on documentation from Kjeldsberg. The presented information can not be considered a complete representation of the actual system.

1.6 The Structure of the Thesis

Chapter 2 - *Theory* shall present the theoretical framework and concepts behind essential PEB structures, such as building regulations, TABS, heat pumps and PV panels. Along with a presentation on the energy market in Norway and the energy system in Trondheim.

Chapter 3 contains a literature review of thermally activated building systems both nationally and internationally. The basis of this thesis is the system at Sluppen, and in Chapter 4, the specifics of the case study are presented.

Chapter 5 - *Methodology* explains the data collection and treatment process, along with the method for the three peak-shaving simulations with TABS, heat pumps and sector coupling.

Chapter 6 - *Base Case – Results and Discussion* presents the current situation at Sluppen, while Chapter 7 - *Simulations – Results and Discussion* presents the results and discussion of the three simulations; TABS, HP, and Sector Coupling. Furthermore, Chapter 8 - *Future Aspects* discusses the future actions and estimations for the PEB.

Finally, in Chapter 10 - *Conclusion*, there will be a summary of the findings, followed by a list of references and appendices.

2 Theory

This section presents the theoretical framework for this thesis. The first part is an introduction to the Norwegian energy market and a definition of types of energy-efficient buildings, which provides context for efficient energy use in office buildings. Secondly, an introduction to the principles behind the TABS, such as heat transfer and thermal energy storage, is given before a description of TABS. Then, other technologies usually found in a PEB, such as heat pumps and PV panels, are described. Lastly, a presentation of the energy system in Trondheim is given, including the grid and district heating systems, along with smart grids and sector coupling.

2.1 Energy Market in Norway

The goal for Norway is to cut 50–55 % of emissions from greenhouse gases by 2030 [5]. More than 90 % of Norway's electricity production comes from hydropower, which means the possibility of emission cuts is higher in other sectors than power production.

Hydropower gives a high degree of flexibility but is vulnerable to arid years. To compensate, Norway has cables to neighbouring countries to have security in such years, which can also stabilise electricity prices. The different regions of Norway, shown in Figure 2.1, have various production capacities and potentials. Transmission lines between the regions are limited, making each region responsible for the majority of their production [7]. In this thesis, the emphasis will be on Trondheim, Trøndelag (within region NO3 in Figure 2.1), where the PEB at Sluppen is located.

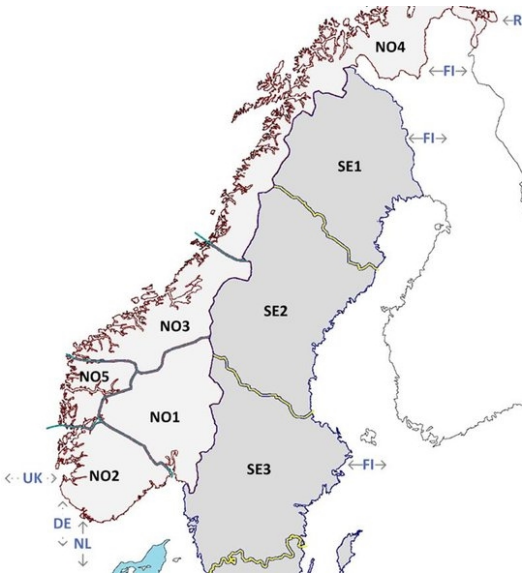

Figure 2.1: *Illustration of the Scandinavian NordPool price areas with external trade [6].*

Trøndelag's production is 70.7 % hydropower, 28.2 % wind power, and 1.2 % thermal power, plus cables connecting to Sweden. The largest city, Trondheim, had a net consumption of 2 721 GWh in 2020, where the service industry used about 35 % of the electricity [8]. This energy is primarily used in buildings for space heating, heating water, lighting, and operating electrical equipment [9].

Energy demand changes throughout the day and varies based on seasons. A base load typically provides the constant energy demand, and when it is high, the grid requires additional power to cover peaks [10]. Power peaks in the grid often happen in the morning when residents are getting ready for the day and in the afternoon when dinner is made, and laundry machines and dishwashers are in use. The size and duration of these peaks differ, but patterns are often visible when examining a specified region. A typical power load curve for residential areas is displayed in Figure 2.2a [11]. When multiple households follow this pattern, the power load will congest and may exceed the grid's limits. In these moments of congestion, the grid may not be able to deliver steady power due to the elevated power peaks. One solution would be to upgrade the excising grid, but designing an entire system based on peak values would be

unnecessarily expensive. Another solution is to either lower or move demand. Luckily, much of the energy use is not time-sensitive, and energy storage systems can spread consumption more evenly throughout the day. An example of this is thermal energy storage systems such as water heaters, which can warm up water at any moment and keep it hot throughout the whole day [12]. With a growing share of renewable energy in the power mix, the supply becomes unpredictable, and it increases the importance of a flexible and efficient system that uses the power when it is most readily available.

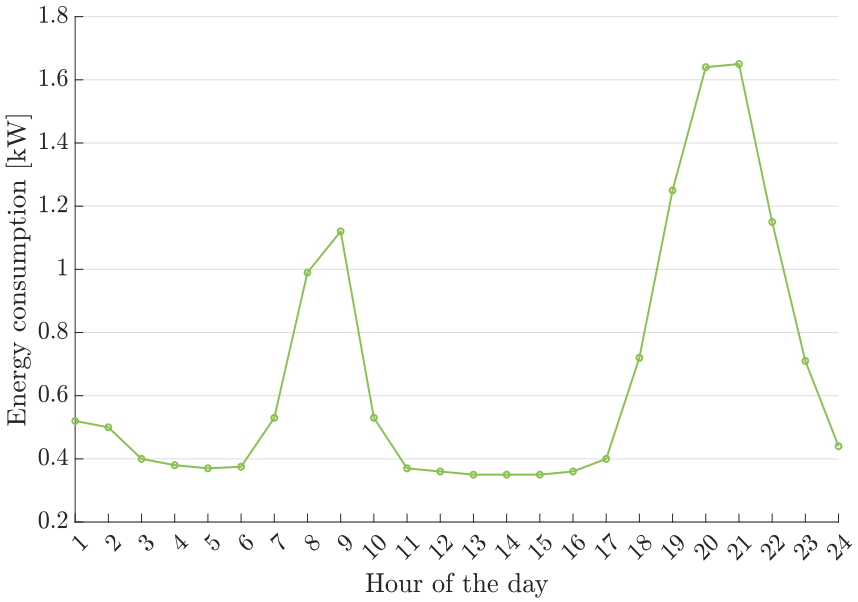

(a) Residential building, inspired by Energy Directorate (NVE) [11].

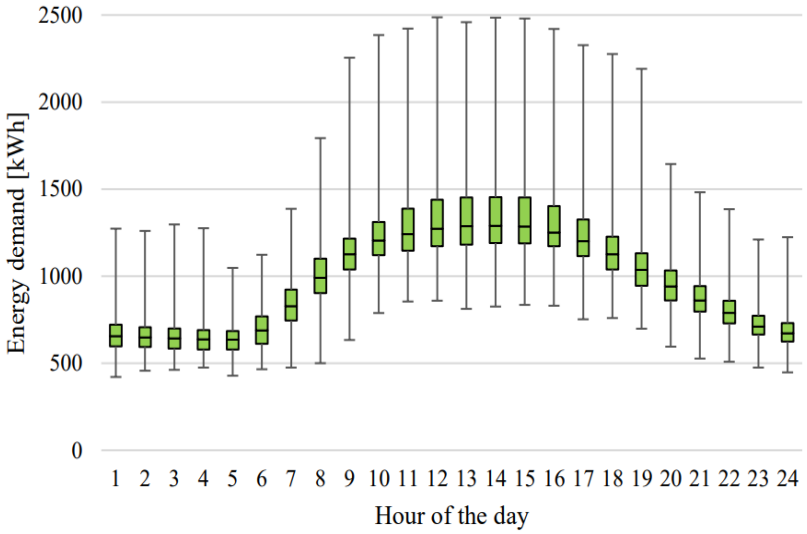

(b) Office building [13].

Figure 2.2: *Typical load profiles for residential and office buildings [11,13].*

On the other hand, office buildings have the opposite consumption pattern. As illustrated in Figure 2.2b, the demand is high during the middle of the day during work hours and decreases in the early and late hours of the day when people are at home [13]. The low demand during the night hours is present in the consumption pattern of residential and office buildings.

2.1.1 Electricity Consumption in Office Buildings

In 2016 the Norwegian Water Resources and Energy Directorate (NVE) published an analysis of energy use in commercial buildings. They found that the representative energy consumption for office buildings is 235 kWh/($m^2 \cdot yr$) [14].

Eight different office buildings built at various periods were considered in the analysis. The energy labels ranged from A to D, providing a range of consumption patterns. All the office buildings had district heating, and two had charging stations for electric vehicles [14].

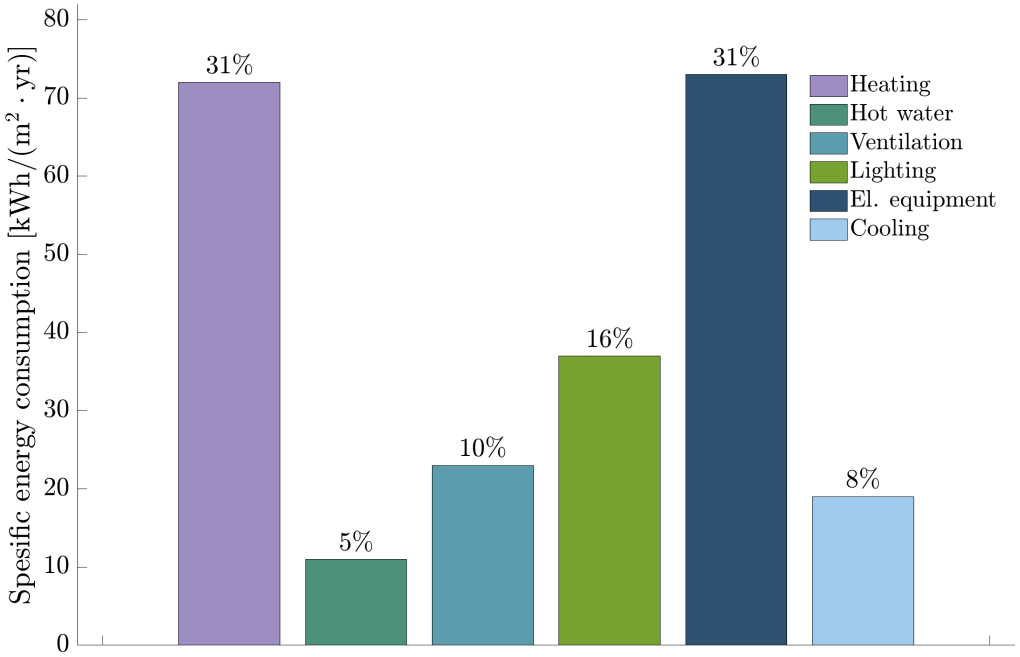

Figure 2.3: *Purpose-based energy use in office buildings in Norway during a year [14].*

Figure 2.3 shows the energy use divided by purpose in a representative office building in Norway. The space heating and operation of electrical equipment accounted for over 60 % of the energy, and the rest was for heating water, ventilation, lighting, and cooling. As can be seen, there is an enormous potential for energy savings by utilising more efficient heating systems and upgrading the building mass to have fewer thermal losses. There is also the potential to use the excess heat from electrical equipment for heating.

2.1.2 Electricity Consumption and Climate

Electricity consumption is dependent on several factors, such as area and building structure, but the largest impact is the changes in outside temperatures. The results from a study by Øystein Døhl in 1999 reveal that an average deviation from the normal of one degree colder in a month entails an increase in electricity consumption of 6 400 MWh per degree days of deviation, in total, an increase of just under 200 GWh monthly [15]. Figure 2.4 shows how the electricity consumption increases with a decrease in temperature. The data represents the monthly mean consumption [16] and mean temperature in Trøndelag for 2021 [17].

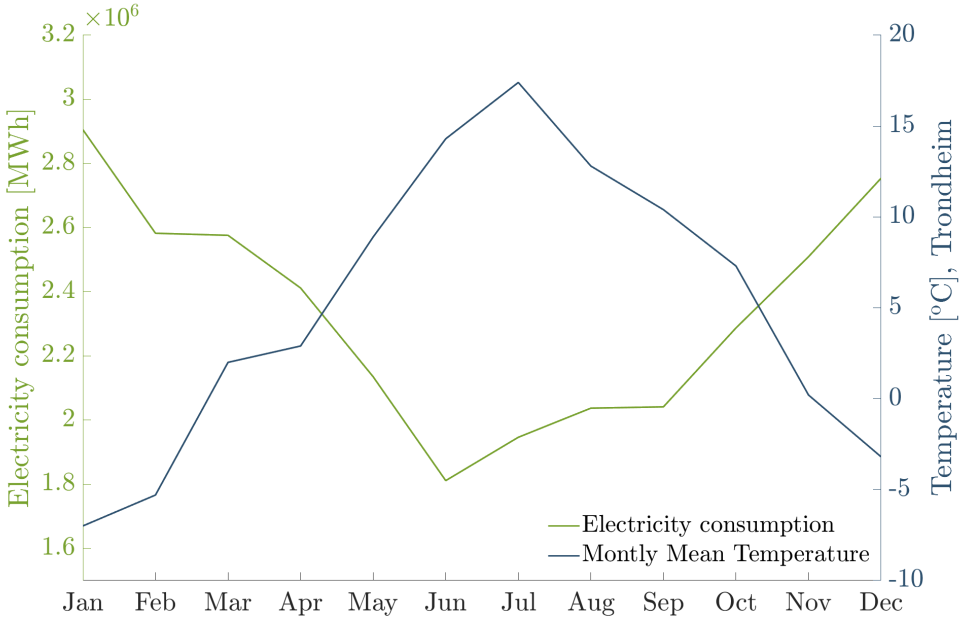

Figure 2.4: *Monthly mean consumption in Mid-Norway and the monthly mean temperature in Trondheim [16,17].*

2.1.3 Electricity Prices

In the last year, energy prices in parts of Norway have increased. This increase is due to less rain and the considerable changes in the European energy market caused by climate actions, and the dependency on energy imports from Russia. This increase also causes people to invest in more energy-efficient solutions. Self-sufficient regions with good transmission networks, such as North- and Mid-Norway, typically have lower prices than southern Norway. Figure 2.5 shows the average monthly spot price for electricity in Trøndelag from 2018 to 2021. Trøndelag's prices have been stable, except in 2020 when they were lower than usual [18].

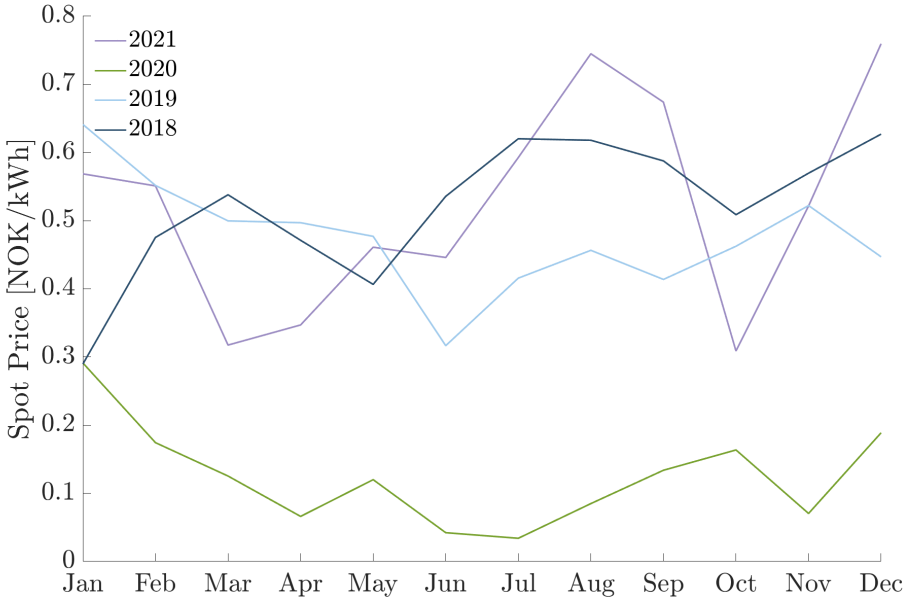

Figure 2.5: *Spot price in Trøndelag for 2018-2021 [18].*

2.1.4 Power Distribution in Norway

The price of electricity is determined by the market at *Nord Pool* and depends on supply and demand. Norway is part of a market-based power system in the Nordic and is incorporated into the power market in Europe. The grid operation is, however, strictly regulated. The power distribution grid is a critical infrastructure, and interruption, too high power load or low power supply can have severe consequences. One solution to lower the risk and face future challenges is to improve the grid further, but grid expansions are expensive. According to *Enova*, Norway is planning to invest 140 billion NOK into the power grid in the next few years [19,20].

There are plenty of power losses connected to electricity distribution in Norway. The total losses are around 7 % of the total power production, where 24 % of these occur in the central grid [21]. The most considerable losses can be found in the distribution grid [22]. The losses are dependent on the amount of current being transported, the distance it is being transported over, and the instantaneous grid load [23]. In the winter, power losses increase due to the increased demand for electric heating, putting a greater strain on the grid.

Customers who both consume and produce energy are called prosumers, or energy plus costumers (EPC) [24]. In Norway, EPC does not have to pay a fixed fee for feed-in (delivered energy) and can measure and settle feed-in and withdrawals at one measuring point. The regulation on control of network activities defines EPC as costumers with consumption and production behind the connection point where the input power at the connection point does not exceed 100 kW. An EPC may not have an energy-producing facility subject to a license or turnover that requires a trading license behind the connection point. If an EPC feeds in more than 100 kW on the grid, they violate the terms of being an EPC. Then they have to declare with the regulatory authorities for energy (RME) if they should be regulated as a transmission system operator (TSO) [25].

RME has recently developed a solution for housing associations to produce and share up to 500 kW of energy among themselves [26]. It is currently impossible to share surplus energy with neighbouring buildings unless the system is located in a housing association. This rule also applies to energy-positive commercial buildings and PEBs; the extra energy must be sold to the main grid and be further distributed by a TSO. The exception to this rule is Powerhouse Brattøra which recently, in 2022, got permission to sell energy to nearby customers in a pilot project [27].

2.2 Energy-Efficient Buildings

Buildings account for 40 % of the world's energy use; therefore, making them more efficient is crucial to stop climate change [28]. In this section, types of energy-efficient buildings, such as passive buildings, zero-emission buildings and energy plus buildings, will be presented.

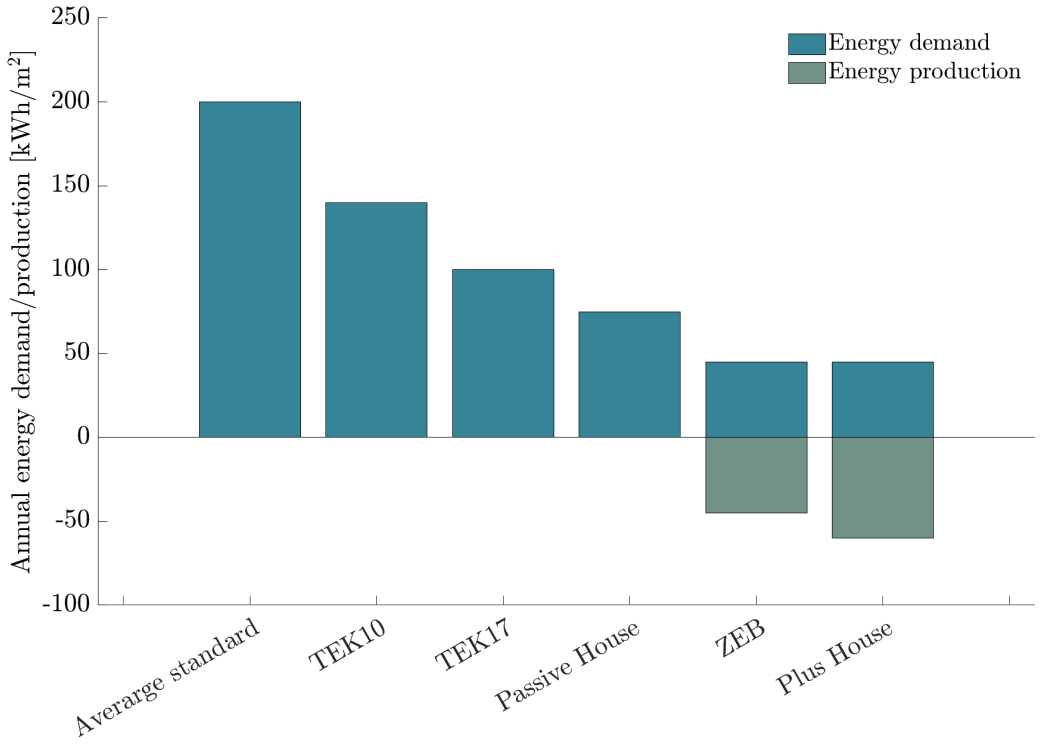

Figure 2.6: *Energy demand and production from buildings of different Norwegian standards [29].*

Figure 2.6 shows the demand and production of energy for the average building mass in Norway, the new requirements for buildings in TEK10 and TEK17, and the energy-efficient buildings; passive houses, zero-emission buildings and energy plus houses [29].

2.2.1 Passive Houses

A passive house is an energy-efficient building aimed at reducing all the conventional causes of heat loss, which requires proper insulation, no-air leakages and no thermal bridges. Measures such as well-insulated windows, correct orientation and heat recovery ventilation systems contribute to energy savings of up to 90 % compared to traditional buildings. The purpose is to make an energy-efficient, comfortable, affordable and environmentally friendly building all at the same time. Passive houses originated in Germany but are now widespread throughout Europe [30].

Passive houses have been tailored to Norwegian conditions and standardised for residential and commercial buildings in NS3700 and NS3701. The standards consist of requirements for the net energy for heating and cooling, as well as minimum requirements for building components. The requirements for commercial buildings from NS3701 are presented in Table 2.1 [31].

Table 2.1: *Minimum requirements for building components, systems and thermal leakage for passive office buildings, from NS3701 [31]*

Minimum values	
U-value windows and doors	≤ 0.80 W/(m$^2 \cdot$ K)
Normalised thermal bridge	≤ 0.03 W/(m$^2 \cdot$ K)
Heat recovery, ventilation	≥ 80 %
SFP-factor for the ventilation	≤ 1.5 kW/(m^3/s)
Leakage at 50 Pa	≤ 0.60 h^{-1}
Energy demand and management for lightning	Minimum 60 % of installed power for lightning is subject to the control system

For buildings over 1000 m^2 the highest net specific energy requirement for space heating [kWh/(m$^2 \cdot$ yr)] is given in Equation 2.1 [31].

$$EP_{H,0} + K_1(6.3 - \theta_{ym}) \tag{2.1}$$

where $EP_{H,0}$ is the net specific heating demand [kWh/(m$^2 \cdot$ yr)], K_1 is the climate coefficient, and θ_{ym} is the annual average temperature [°C]. For an office building $EP_{H,0}$ equals 20 kWh/(m$^2 \cdot$ yr), and K_1 equals 3.6, while the annual average temperature is calculated for the area of the building [31].

For an office building in Trondheim with an annual average temperature of 5.6°C [32] the net specific energy requirement for space heating equals 22.5 kWh/(m$^2 \cdot$ yr).

In addition, heating systems are required to have significant use of energy products other than electricity and fossil fuels. According to TEK-17 §14-4, buildings with over 1000 m^2 must have energy-flexible heating systems and be adapted for the use of low-temperature heating solutions [33].

2.2.2 Zero-Emission Buildings

Zero-emission buildings (ZEB) are energy-efficient buildings that aim to become net-zero. The building compensates for the total impact by producing on-site energy, depending on the level of ambition [34]. ZEBs can be divided into six categories, as follows:

- ZEB-O ÷ EQ: On-site energy production compensates for the emissions from energy use in operation, except for energy use for equipment/appliances.
- ZEB-O: On-site energy production compensates for the emissions from energy use in operation.
- ZEB-OM: On-site energy production compensates for the emissions from energy use in operation and materials.
- ZEB-COM: On-site energy production compensates for the emissions from energy use in operation, materials, and construction.
- ZEB-COME: On-site energy production compensates for the emissions from energy use in operation, materials, construction, and demolition.
- ZEB-COMPLETE: On-site energy production compensates for the emissions from materials, transport, construction, operation, and demolition.

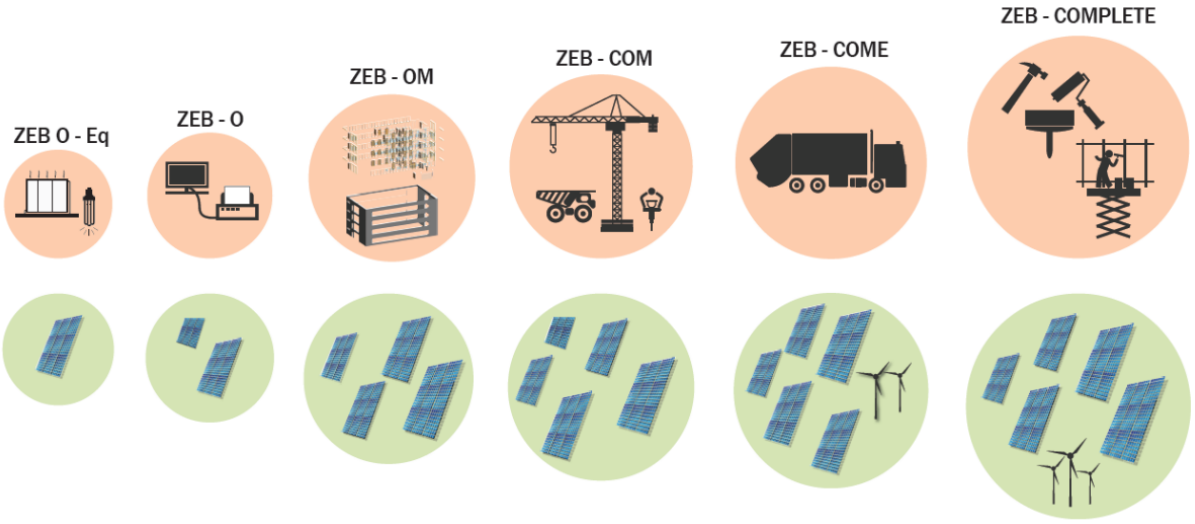

Figure 2.7: *ZEBs with different ambition levels and the required on-site renewable energy production [34].*

Figure 2.7 shows the different levels of ZEBs and how much the energy generation compensates for them. Generally speaking, the most common definition of a ZEB refers to becoming net zero in the operational phase of the building annually, ergo the ZEB-O [34].

2.2.3 Energy Plus Houses

Energy plus houses are buildings that generate more energy during their lifetime than what is involved in the production of building materials, construction, operation and demolition. Energy plus houses are similar to the ZEB-COMPLETE, except the building generates more energy than it needs, which can be distributed and sold to nearby buildings or grids. The energy is produced from means such as solar cells, solar collectors, and wind turbines [35].

2.2.4 Positive Energy Blocks

A Positive Energy Block (PEB) is an area with at least three buildings ($> 15\,000$ m^2) that produces more energy than it consumes in a year. It needs to include local renewable energy production and measures to reduce its energy demand. The buildings need to serve different purposes, such as housing, offices, or commercial spaces, to take advantage of sharing access energy and complementary energy consumption patterns [36].

In the case of Sluppen, Stålgården and Lysgården are considered a passive houses, Lysgården has energy production in the form of PV panels, and Lager 11 is a regular building. PV panels are scheduled to be installed at the remaining buildings. Together they will make up the PEB at Sluppen.

2.3 Heat Transfer

Heat transfer is defined as the transport of thermal energy due to a temperature difference. If there is a temperature difference within a medium or between mediums, heat will transfer from high to low temperatures. In general, heat transfer consists of three modes; conduction, which refers to heat transfer that occurs across a medium; convection, which refers to a heat transfer that occurs between a surface and moving fluids; and radiation, which refers to the emission of electromagnetic waves from a medium [37]. The three modes are illustrated in Figure 2.8.

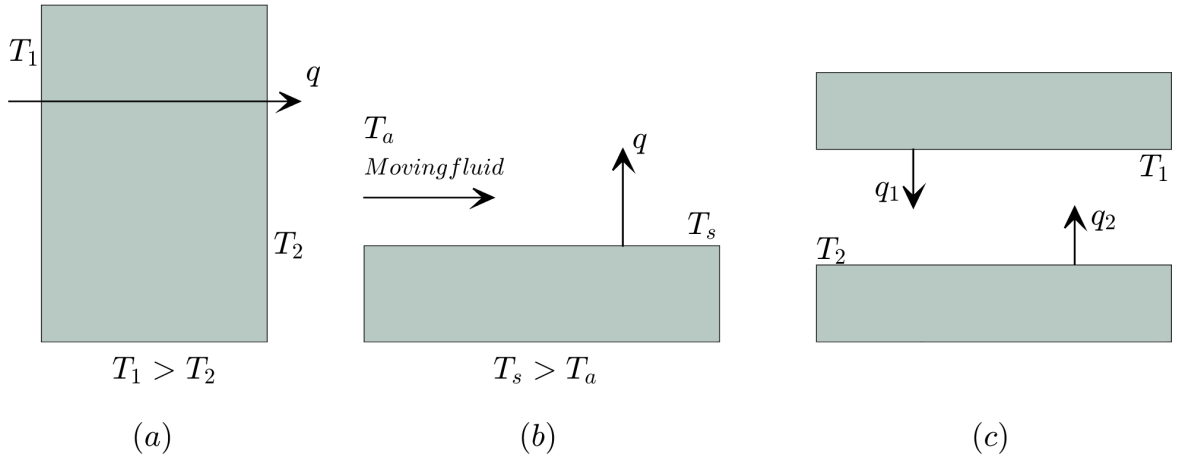

Figure 2.8: *Heat transfer modes: (a) conduction though a solid, (b) convection from a surface to a moving fluid, and (c) radiation between two surfaces [38].*

2.3.1 Conduction

Conduction is the transfer of energy from a more energetic to a less energetic molecule within a substance due to interactions between the particles. The interactions consist of random translational motion and the molecules' internal rotational motion and vibrations. The high-energy molecules have higher temperatures than the low-energy molecules. When colliding with other molecules, energy transfers to the lower energy, lower temperature molecule until a temperature equilibrium is achieved, as illustrated in Figure 2.9 [37]. Conduction can occur in liquid, gaseous, or solid objects.

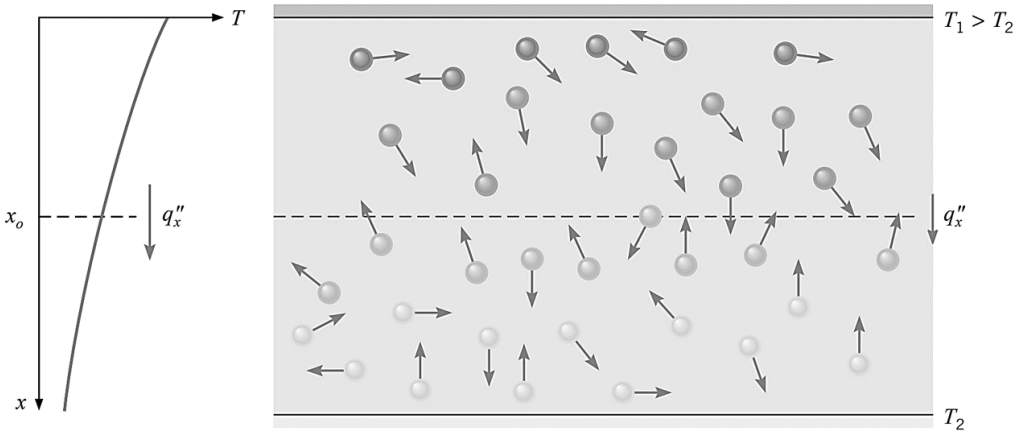

Figure 2.9: *Conduction heat transfer with diffusion of energy due to molecular energy [37].*

An example of conduction is a hot substance that heats the container it exists within. For a homogeneous medium, the heat transfer is described by Fourier's law:

$$q''_{cond} = -k\frac{\Delta T}{L} \tag{2.2}$$

where q_{cond} is heat flux [W/m^2], k is the thermal conductivity [W/(m $\cdot$ K)], ΔT is the temperature difference [K], and L is the wall thickness [m].

The thermal conductivity of a material (k) is defined as the heat transmitted through a unit thickness of a material. Therefore, it determines whether a material is suitable for insulation. Generally, solids have the largest thermal conductivity, followed by liquids, then gases. Table 2.2 shows the thermal conductivity of common materials [37].

Table 2.2: *Thermal conductivity of common materials [39]*

Material	Thermal conductivity [W/(m $\cdot$ K)]	Material	Thermal conductivity [W/(m $\cdot$ K)]
Air	0.025	Brick	1.30
Water, at 10°C	0.60	Glass	1.00
Water, at 20°C	0.598	Soft wood	0.13
Steel	50	Hard wood	0.18
Concrete, reinforced	2.30	Insulation	0.025–0.050

2.3.2 Convection

Convection is heat transfer that occurs between a surface and moving fluids. It consists of two mechanisms; energy transfer through random molecular motion and bulk motion of the fluid [37].

Convection can be forced or natural. Forced convection happens when external forces cause flows, such as mechanical devices or wind (Figure 2.10a). Natural convection can be naturally induced by buoyancy. Buoyancy is an upward force created by the different densities within the fluid [40]. An example of natural convection heat transfer is hot components on a vertical array of circuit boards transferring heat to the air (Figure 2.10b). The air temperature rises when it touches the hot components, thereby reducing the density of the air. Because some of the air is lighter than the surrounding air, buoyancy forces cause a vertical motion, causing hot air to ascend from the boards to be replaced by colder ambient air [37].

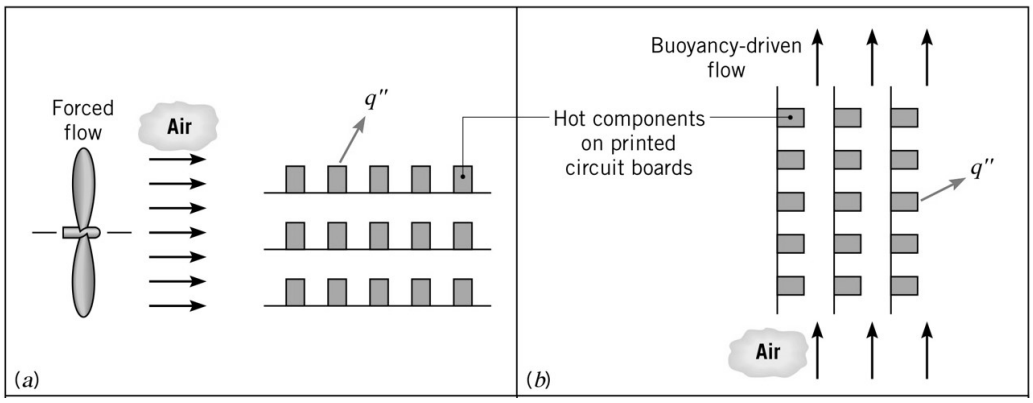

Figure 2.10: *Convection heat transfer processes. a) Forced convection, and b) Natural convection [37].*

Heat transfer by convection depends on the fluid, the state of this fluid, the temperature difference and the flow type, along with the surface temperature, geometry and roughness. These properties make convection a complex mechanism to calculate. A simplified Equation for the heat flux density, given by Newton's law of cooling (Equation 2.3) is given below [37].

$$q_{conv} = h_c(T_s - T_f) \tag{2.3}$$

where q_{conv} is the heat flux [W/m^2], h is the convection heat transfer coefficient [W/(m$^2 \cdot$ K)], T_s is the surface temperature [K], and T_f is the fluid temperature [K].

2.3.3 Radiation

Radiation is heat transfer from electromagnetic waves emitted from a surface, liquid or gas. The emissions are due to changes in electron configurations of the molecules in the medium. A surface will radiate waves over a spectrum of wavelengths. Surfaces with higher temperatures emit shorter wavelengths.

Surfaces can absorb or receive radiation from other surfaces, for example, radiation exchange between a large surface surrounding a smaller surface. The radiation exchange between them is given by Equation 2.4.

$$q_{rad} = \varepsilon\sigma(T_s^4 - T_{surr}^4) \tag{2.4}$$

where q_{rad} is the heat flux [W/m^2], ε is the emissivity, σ is the Stefan-Boltzmann's constant, equal to 5.6704$\cdot 10^{-8}$ W/(m$^2 \cdot$ K^4), T_s^4 is the surface temperature [K] and T_{surr}^4 is the surrounding temperature [K].

The emissivity is the efficiency of a surface in relation to an ideal radiator. An emissivity of 1 means the surface is a perfect radiator, and 0 means the surface is a perfect reflector.

Radiation can also be expressed as net radiation heat exchange, with Equation 2.5.

$$q_{rad} = h_{rad}A(T_s - T_{sur}) \tag{2.5}$$

where, $h_{rad} = \varepsilon\sigma(T_s + T_{sur})(T_s^2 + T_{sur}^2)$ and A is the area [m^2].

2.3.4 Overall Heat Transfer

All the heat transfer modes are present in a building structure. Heat transfer problems are often complex to calculate due to the complexity of heat. However, by assuming one-dimensional, steady-state conditions with constant conductivities, simpler Equations and analogies can be used.

For calculating the overall heat transfer through a structure, one must first define the thermal resistance (R). Thermal resistance is the material resistance against heat flow or conductance. Thermal resistance is like electrical resistance, except it is associated with the conduction of heat instead of the conduction of electricity. In general, the definition of thermal resistance is the potential heat transferred, divided by actual heat flux [37].

The thermal resistance for conduction and convection through a wall is shown in Equation 2.6 and 2.7.

$$R_{t,cond} = \frac{T_{s,1} - T_{s,2}}{q_x} = \frac{L}{kA} \tag{2.6}$$

where $R_{t,cond}$ is the thermal resistance [$\mathrm{m}^2 \cdot \mathrm{K/W}$], $T_{s,x}$ is the temperature, q_x is the heat flux, L is the thickness of the layer, k is the thermal conductivity, and A the area.

$$R_{t,conv} = \frac{T_s - T_\infty}{q} = \frac{1}{hA} \tag{2.7}$$

where $R_{t,conv}$ is the thermal resistance, T_x is the temperature, q is the heat flux, h is the convection heat transfer coefficient, and A the area.

A simplification is done by creating a network of thermal resistances, including both conduction and convection resistances, like the electrical circuits. The equation for the overall heat transfer Q is given in Equation 2.8.

$$Q = U \cdot A \cdot \Delta T \tag{2.8}$$

where U is the heat transfer coefficient [$\mathrm{W/(m^2 \cdot K)}$], and ΔT is the temperature difference.

The heat transfer coefficient (U), defined as the ratio of heat transfer through the unit area and temperature difference, is the inverse of the joint resistance for all the layers in the structure, hence Equation 2.9. Building standards usually supply requirements for U-values in structures such as windows, walls, and doors, for limiting heat transfer in buildings [37].

$$U = \frac{1}{R_{tot}} = \frac{1}{\Sigma R_t} \tag{2.9}$$

For TABS that include pipes, it is also relevant to look at the heat transfer for radial systems. In radial systems, the thermal resistances are the same as for the composite wall but divided by $2\pi r$, and L equals $\ln(r_2/r_1)$. Figure 2.11 shows an example of a simplified radial heat transfer system, where hot fluid flows through an insulated pipe. The network shows the resistances and the temperatures in the pipe [37].

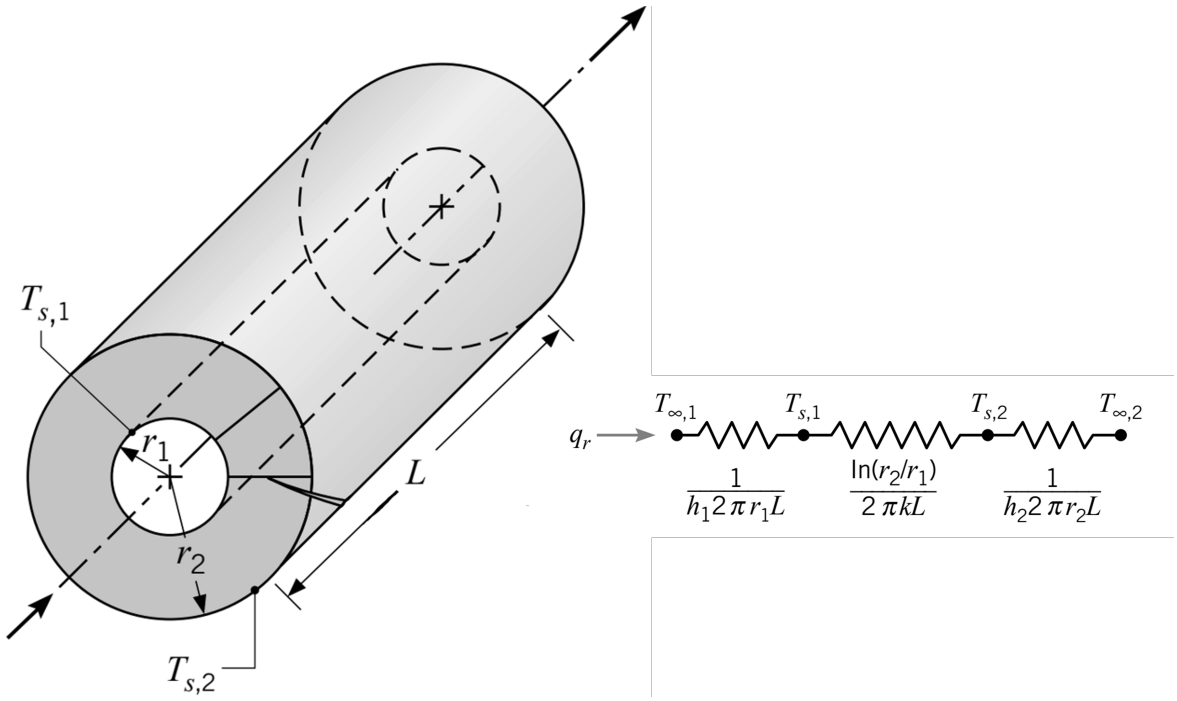

Figure 2.11: *Heat transfer within a pipe [37].*

2.4 Thermal Energy Storage

Thermal energy storage (TES) allows thermal energy to be stored and transferred. There are three main types of TES; sensible, latent, and thermochemical.

Sensible heat is heat that can be experienced (e.q., heat from the sun). It is the heat transferred to or from a substance which leads to a change in temperature [41]. Latent heat is the heat associated with phase transitions [42]. Thermochemical heat is the heat released or absorbed during a chemical reaction [43]. The essential characteristics of the three TES methods can be found illustrated in Figure 2.12.

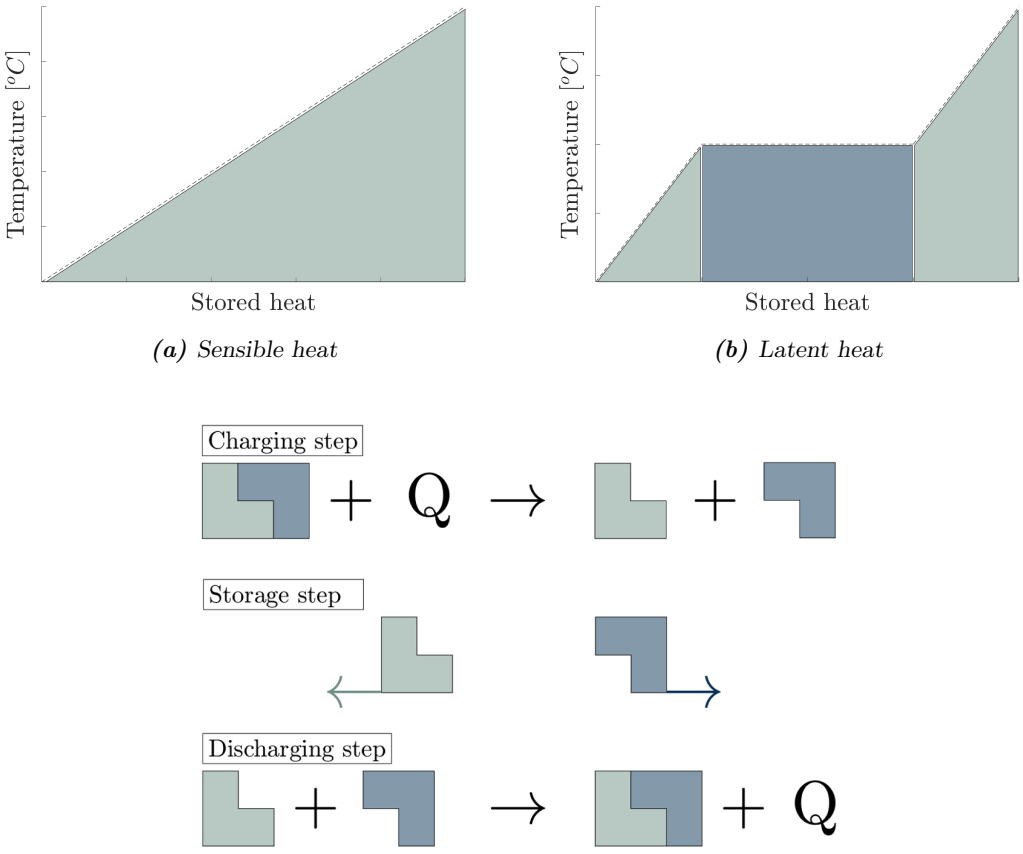

(a) Sensible heat

(b) Latent heat

(c) Thermochemical heat

Figure 2.12: *Methods of thermal energy storage, inspired by [44].*

As with any other energy storage system (ESS), TES can be used to shave load peaks by storing excess energy and releasing it during high demand periods. TES systems make it possible to respond quickly to short-term high load demands [45].

2.4.1 Sensible Heat

Sensible heat storage (SHS) is based on the heating or cooling of a storage medium. The cheapest and most commonly used medium is water; this makes SHS non-toxic. These systems take advantage of the temperature change, and the heat capacity of the storage medium [44].

The amount of heat stored (Q_s [J]) can be expressed as in Equation 2.10.

$$Q_s = \int_{T_0}^{T} mc_p \, dT \; = mc_p(T - T_0) \tag{2.10}$$

where m is the mass $[kg]$, and c_p is the specific heat capacity $[\mathrm{J}/(\mathrm{kg} \cdot \mathrm{K})]$ of the heat storage medium. T_0 is the initial, and T is the final temperature [K] .

As previously mentioned, water is the most commonly used material in SHS. When the water reaches its boiling temperature and vaporises, the heat capacity is cut in half.

$$c_{p_{vapor}} = \frac{c_{p_{liquid}}}{2} \tag{2.11}$$

The context provided in Equation 2.11 makes it so that water is only usable as a heat storage medium for low-temperature SHS. If the system's temperature exceeds 100°C, the medium has to be changed to oils, molten salts, or liquid metals.

As seen in Figure 2.12a, sensible heat directly changes the temperature of the material without affecting the phase. There is a direct link between temperature and the amount of energy stored.

Water has a specific heat capacity of 4 160 $\mathrm{J}/(\mathrm{kg} \cdot \mathrm{K})$. SHS systems generally have a capacity of 10–50 kWh/h and an efficiency of 50–90 % [44].

Figure 2.13 shows a simplified sketch of a sensible heat storage system. Hot water is stored in tanks and is amongst others, used for domestic water and heated flooring. Heat is supplied from solar collectors and a heat pump.

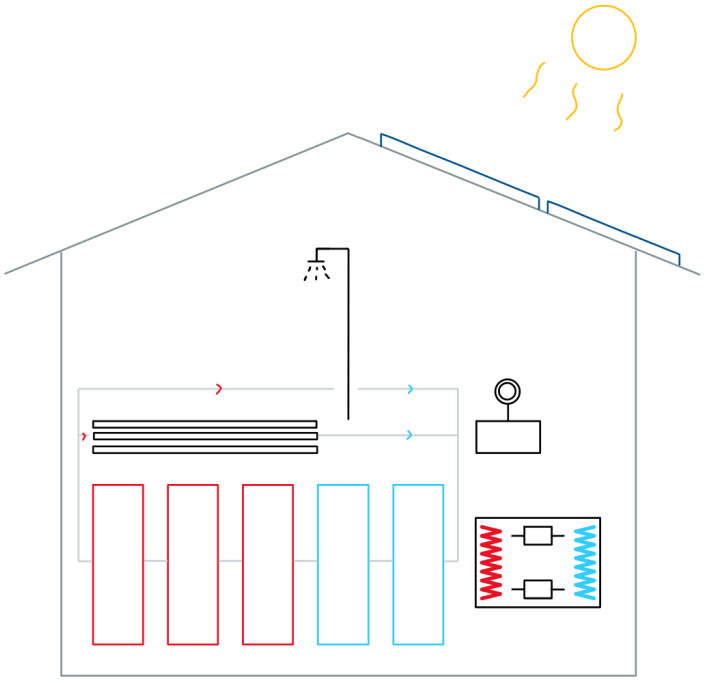

Figure 2.13: *Example of a sensible energy storage system, inspired by [46].*

Hot-water tanks are an established technology in these systems, which conserve thermal energy for later use. This method of TES is often used together with solar collectors and district heating.

2.4.2 Latent Heat

Latent heat storage (LHS) utilises Phase-Change materials (PCM) and their ability to absorb and release energy when their state of matter is changed. Latent heat is acknowledged as the enthalpy of fusion Δh_{fus}, which is presented in Equation 2.12.

$$\Delta h_{fus} = h_{liquid,T_m} - h_{solid,T_m} \tag{2.12}$$

Where h_{liquid,T_m} is the enthalpy in a liquid state, and h_{solid,T_m} is the enthalpy in a solid-state. Note that there is no change in temperature, ($\Delta T = 0$).

The part of Figure 2.12b where the amount of heat increases but the temperature stays constant, marked in blue, is latent heat. This heat is unnoticeable until the phase change, and the heat is released. Different salt and water mixtures are typical examples of PCMs [47].

Latent heat can be used to protect batteries from over heating. A PCM is placed around the cells as shown in Figure 2.14, when the temperature of the battery cells increase the surroundings change phase and absorb the heat [44].

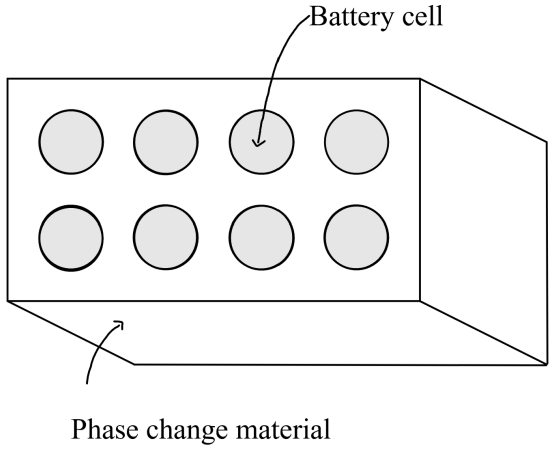

Figure 2.14: *Battery with latent heat storage, inspired by [48].*

LHS makes it so energy can be released at constant temperature and is used in thermal storage for solar energy and energy storage in building materials. These systems have a capacity between 50–150 kWh/h and efficiency of 75–90 %.

2.4.3 Thermochemical Heat

Thermochemical heat is the heat released or absorbed when two chemical components react. The amount of heat is equal to the reaction enthalpy (ΔH_r). The reaction is both exothermic (releases heat when $\Delta H_r < 0$) and endothermic (absorbs heat when $\Delta H_r > 0$). Thermochemical energy storage systems have a capacity of 120–250 kWh/h and an efficiency of 75–100 % [44].

2.4.4 Thermal Mass in Passive and Active TES

Thermal mass is the materials' ability to absorb, store and release heat. Materials with high thermal mass, such as tiles, brick, and concrete, can store larger amounts of heat. While materials with low thermal mass, such as wood and cloth, do not absorb and store heat well.

Thermal mass is also known as volumetric heat capacity (VHC), which is the product of the material's specific heat capacity and density. Table 2.3 shows the thermal mass of various materials [49].

Table 2.3: *Thermal mass of various materials [49]*

Material	Density [kg/m^3]	Specific heat capacity [kJ/(kg · K)]	Volumetric heat capacity [kJ/(m^3 · K)]
Water	1000	4.186	4186
Concrete	2240	0.920	2060
Sandstone	2000	0.900	1800
Brick	1700	0.920	1360

Thermal lag must also be considered when considering thermal mass. Thermal lag is the rate at which the material absorbs or releases heat. Materials that absorb and release heat slowly (for example, concrete and brick) have higher thermal lag than materials that absorb and release heat rapidly (for example, steel). The thermal lag is influenced by heat capacity, conductivity, the difference in temperature, the thickness of the material, surface area, texture, colour and surface coatings, and exposure to air. For most common building materials, the higher the thermal mass, the longer the thermal lag [49].

Passive thermal energy systems take advantage of the naturally available heat sources such as thermal mass. For example, concrete walls will absorb excess heat and release it when the temperature in the room drops. A visualisation of passive and active energy storage can be seen in Figure 2.15.

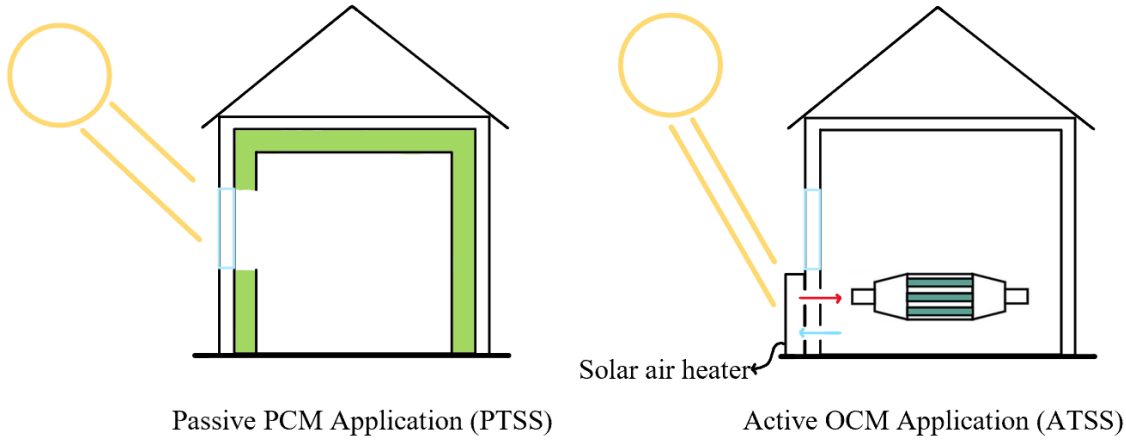

Figure 2.15: *Comparison between active and passive TES systems, inspired by [50].*

Active thermal energy systems are systems made to control the temperature in a room. These systems improve ESS and are commonly used in buildings to help shave power peaks. Domestic water heaters (DWH), air-conditioners, and ventilation systems are examples of active thermal energy systems [43].

Thermal masses, along with forecast-controlled temperature control in the concrete, can help optimise the utilisation of solar heat, actively and passively. For this to work, the thermal mass

needs to be exposed in the rooms that need heating or cooling. It must be passively exposed to hot or cool air through natural or mechanical ventilation or be activated, either by air or with water (TABS) [51].

2.5 Thermally Activated Building Systems

A thermally activated building system (TABS) heats or cools a building through integrated pipes in concrete floors. A TABS helps create an optimal indoor climate while minimising energy demand for heating and cooling. By utilising the thermal storage capacity of the concrete slab, peak loads of the building can be reduced [52].

The TABS circulates water, hot or cold, through the embedded pipes in the concrete. The water heats the concrete, which slowly releases heat into the rooms of the building due to its high thermal mass [52].

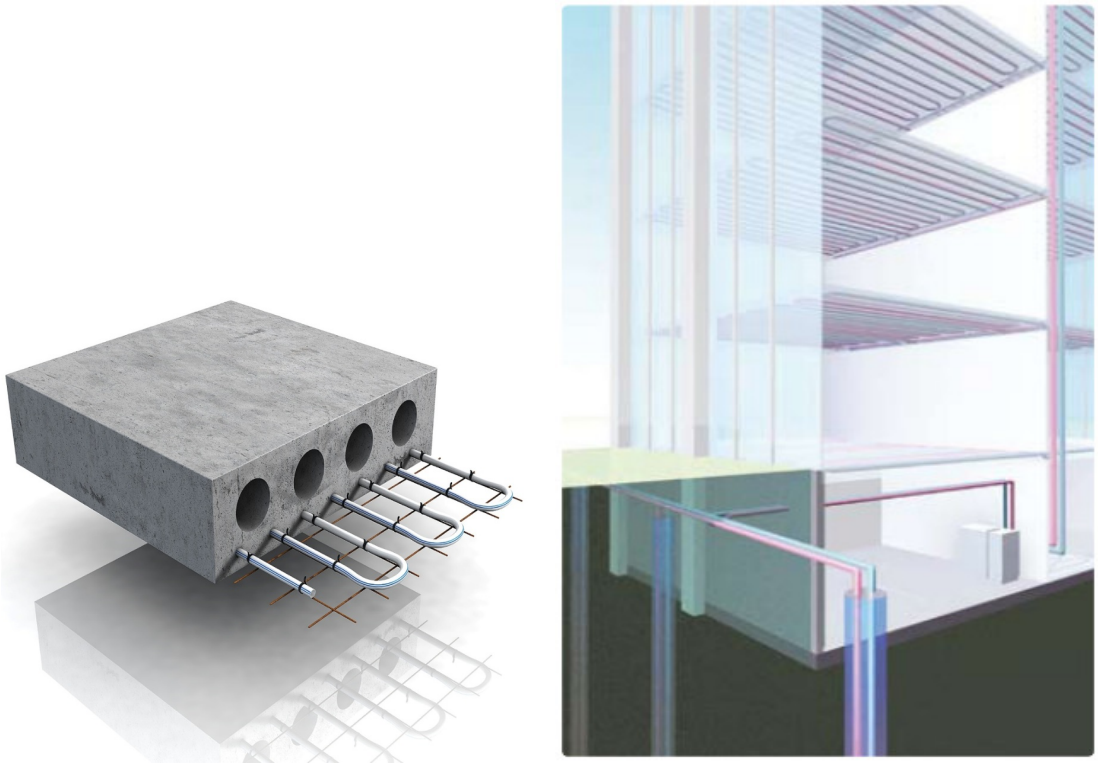

(a) *Principle drawing of TABS.* ***(b)*** *TABS embedded into the building structure.*

Figure 2.16: *Visualisation of how TABS are constructed and embedded into building structures [53].*

The Figures 2.16a shows concrete with the embedded pipes, and 2.16b the finished TABS embedded as floors and ceilings in a building. TABS are especially suited for buildings with multiple floors, such as office buildings [53].

The amount of thermal energy delivered or absorbed by the TABS is determined by the water mass flow rate and the difference between the supply and return temperature of the pipes [52]. Equation 2.13 defines the thermal energy from the TABS.

$$Q_{TABS} = \dot{m} \cdot c_p \cdot \Delta T = \dot{m} \cdot c_p \cdot (T_{supply} - T_{return}) \tag{2.13}$$

where Q_{TABS} [W] is the delivered or absorbed thermal energy by the TABS, $\dot{m}$ is the water mass flow rate, c_p [kJ/(kg · K)] is the specific heat capacity of water, and ΔT is the temperature difference between supply and return temperature [52].

To control the thermal energy delivered by the TABS, the supply temperature and/or the mass flow rate of the water can be changed [52].

The main advantages of TABS are increased comfort, reliability with fewer moving parts, and reduced energy use. An increase in thermal comfort is achieved by having a silent system without air circulation. They are dependable because of the integration into the building structure and the minimal need for maintenance. In addition, the TABS uses less energy by having an operating temperature close to the ambient environment [53].

TABS has a slow response time to changes in the supply temperature. Therefore, TABS works best as base loads and is not a reliable source for peak thermal loads. However, this property contributes to shaving electricity peak loads in a building, making it an advantage instead of a challenge [53].

2.6 Heat Pumps

A heat pump consists of a working fluid that flows through a vapour compression refrigeration cycle (VCRC). This cycle is reversible and can be used for both heating and cooling. The heat pump has an electric motor, a compressor, an expansion valve, and two heat exchangers. The heat exchangers function as both a condenser and an evaporator [54]. Figure 2.17 shows how the latter components are connected.

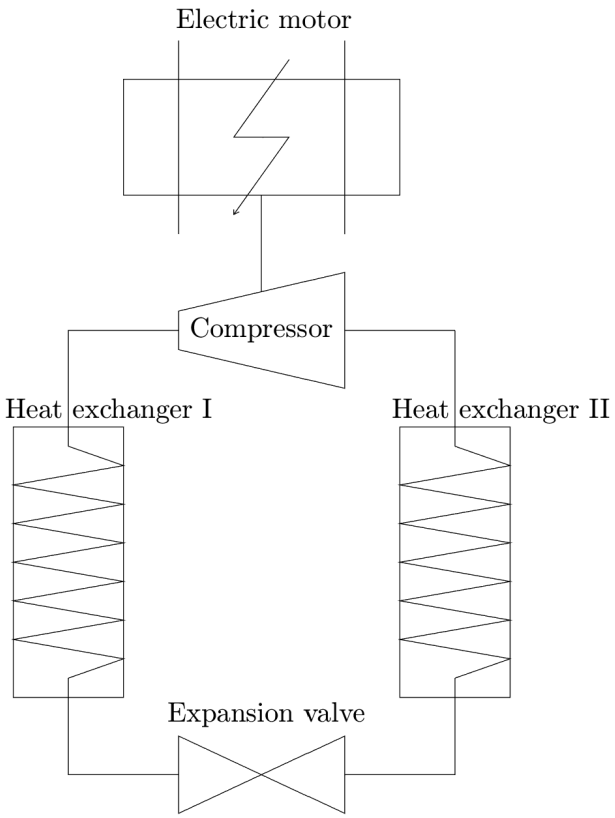

Figure 2.17: *Illustration of heat pump components and how they are connected, inspired by [55].*

2.6.1 Working Principle

The following explanation refers to the heating cycle. If the process were reversed, it would be cooling [54]. The temperature entropy diagram from the refrigeration cycle can be found in Figure 2.18.

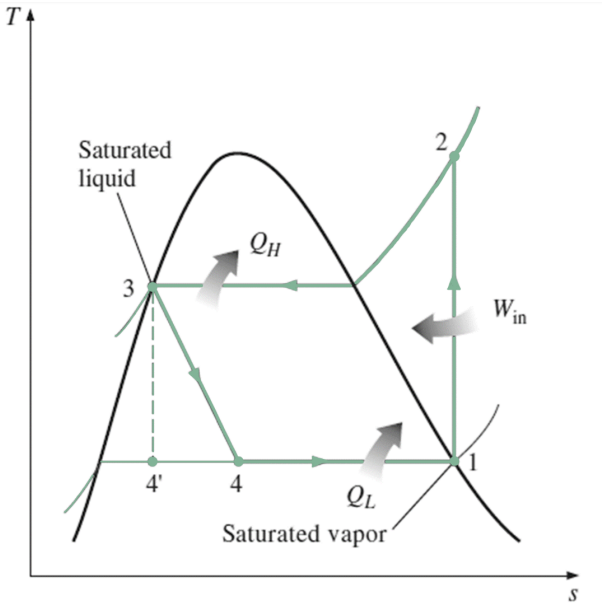

Figure 2.18: *T-S diagram of a refrigeration cycle [56].*

Heat ($\dot{Q}_{in}$), commonly from ambient air, is added to the process and used to evaporate the working fluid into a gas in the evaporator (Heat exchanger II in Figure 2.17). $\dot{Q}_{in}$ can be expressed using enthalpy, as in Equation 2.14.

$$\frac{\dot{Q}_{in}}{\dot{m}} = h_1 - h_4 \tag{2.14}$$

Where h_1 and h_4 are the enthalpies before and after the working fluid moves through the evaporator.

In the compressor, the working fluid is compressed by adding work ($\dot{W}_c$), expressed in Equation 2.15, from the electric motor. The compression increases the temperature from T_c to T_H.

$$\frac{\dot{W}_c}{\dot{m}} = h_2 - h_1 \tag{2.15}$$

Where h_2 and h_1 are the enthalpies before and after compression.

The working fluid then travels into the condenser (Heat exchanger I in Figure 2.17), where the fluid is condensed back into a liquid and heat ($\dot{Q}_{out}$) at temperature T_H is extracted from the cycle, and often used to heat a room. $\dot{Q}_{out}$ can be calculated as shown in Equation 2.16, using the enthalpies h_2 before and h_3 after condensation.

$$\frac{\dot{Q}_{out}}{\dot{m}} = h_2 - h_3 \tag{2.16}$$

The newly condensed liquid goes through the expansion valve, where the temperature reduces back to T_c. This process does not have any impact on the enthalpy, as shown in Equation 2.17.

$$h_4 = h_3 \tag{2.17}$$

where h_4 is the enthalpy after, and h_3 is the enthalpy before expansion.

Equations 2.14–2.17 are meant for an ideal cycle where $h_4 = h_3$, and this will often not be the case in real-life applications. The actual step 4 will have the same temperature as the ideal one but a higher entropy, as Figure 2.18 illustrates.

2.6.2 Performance

The Coefficient of Performance (COP) also known as the efficiency, shown in Equation 2.18, indicates the relationship between the electricity supplied and heat extracted from the cycle. The COP factor is dependent on the pump speed and varies with the outside temperature [55].

$$COP = \frac{Q_{useful\,heat}}{Q_{electric}} \tag{2.18}$$

If the energy output of the heat pump is known, the coefficient of performance can be used to calculate the electricity load the heat pump had on the local grid. Sometimes it is helpful to look at COP for a whole year. The Seasonal Coefficient of Performance (SCOP) gives that information. It takes into account changes in temperature and humidity and gives a more holistic view of the heat pump's performance. The Seasonal Energy Efficiency Ratio (SEER) can also be helpful. SEER shows the relationship between the pump output and the applied power during a cooling season [57]. The European Seasonal Energy Efficiency Ratio (ESEER) is considered a highly accurate metric and describes the real-climate energy efficiency of the heat pump. It is based on the energy efficiency ratio (EER) [58]. The EER represents the cooling output during cooling season and is calculated in the same way as COP [59].

Another performance measurement is the fouling factor: the theoretical resistance to the flow in the heat due to a fouling substance on the surface, or a layer of dirt film built-up over time. It is usually specified by the user and designer based on the experience of operating the heat exchanger [60]. The fouling factor formula can be seen in Equation 2.19.

$$R_f = \frac{1}{U_d} - \frac{U}{U_1} \tag{2.19}$$

where R_f represents the fouling factor, and U_d and U_1 are the reciprocal of the heat transfer coefficient before and after cleaning.

2.6.3 Working Fluids

The working fluid used in heat pumps is commonly known as refrigerants. Liquid-to-vapour phase change refrigerants utilise the heat obtained from a substance at low temperature to undergo a phase change and emit heat. During this process, the refrigerant transfers the latent heat produced in the phase change to a substance with a higher temperature [61]. There are multiple chemical compounds that can be used as refrigerants. The refrigerant should fulfil the following criteria to be suited for use in heat pumps [62]:

- Boiling point below $0\,^oC$
- Stable usage under operating conditions
- Reasonable condensation pressure and critical temperature
- Low gas flow rate
- Low global warming potential

- Non-toxic
- Non-flammable
- Be detectable in case of leakage
- Affordable
- Recyclable

The working fluid will directly affect the COP and has to be selected carefully. When choosing a refrigerant, the freezing temperature must be fitting for the conditions it will operate in, preventing the liquid from freezing and thereby clogging the pipes [63]. Refrigerants can be problematic since they generally are flammable, toxic, and cause depletion in the ozone layer. Therefore, it is essential to consider the environmental effects of the working fluid.

R134a, **R407c**, **R410a**, **R600** (butane), **R600a** (isobutane), and **R717** (Ammonia) are common refrigerants [62]. The first number indicated the number of carbon atoms, the second is the number of hydrogen atoms, the third is the number of fluorine atoms, and a lowercase letter indicates the specific isomer [64].

2.6.4 Types

Heat pumps are typically divided into three main categories: mechanically driven, heat-driven, and heat transformers [65]. Mechanically driven heat pumps are the most commercial ones [66]. They can also be divided into categories based on how they source and deliver heat. The most common types are presented in Figure 2.19.

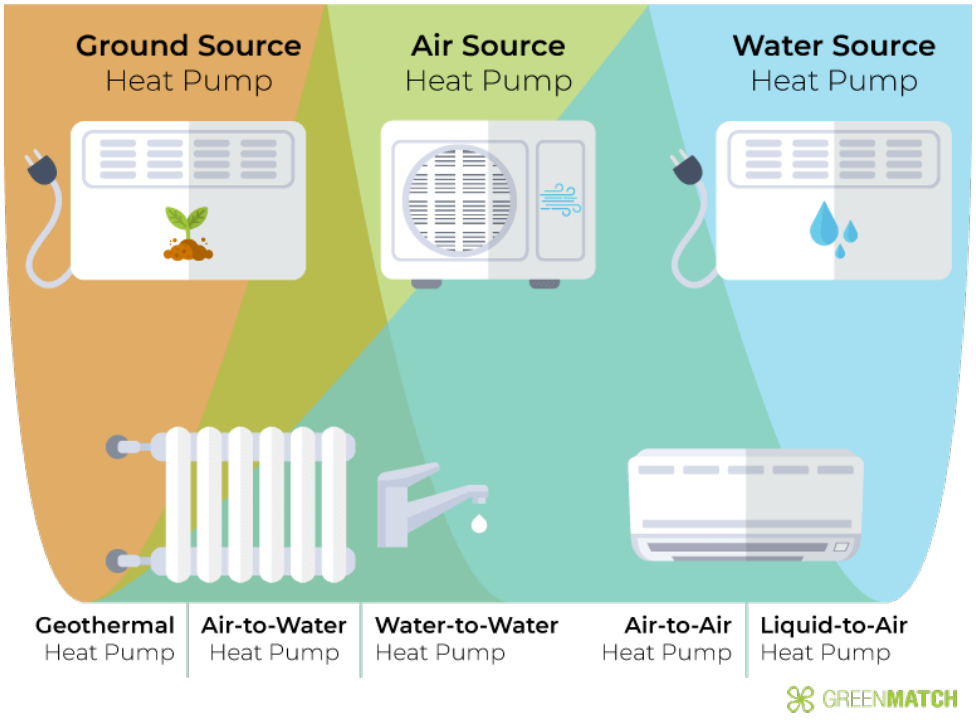

Figure 2.19: *Illustration of different heat pump types [67].*

Figure 2.19 shows three different heat sources for heat pumps; ground, air, and water. A ground source heat pump uses geothermal energy as a heat source. An air-air heat pump derives heat

from ambient air and delivers hot air, while a water-water heat pump derives heat from water (e.g., a lake) and delivers waterborne heat. An air-water heat pump utilises the heat in the outside air and delivers waterborne heat and a liquid-to-air heat pump derives heat from liquids and delivers warm air [55].

2.7 Photovoltaic Cells

Photovoltaic (PV) cells take advantage of the photovoltaic effect. When sunlight shines on the boundary layer of semiconductor materials, the energy from the sunlight (a photon) releases an electron from the material. Photovoltaic cells force this electron to travel through an external circuit, seen in Figure 2.20, to neutralise the negative charge made by the photovoltaic effect. Electrons moving through the wire generate current [68].

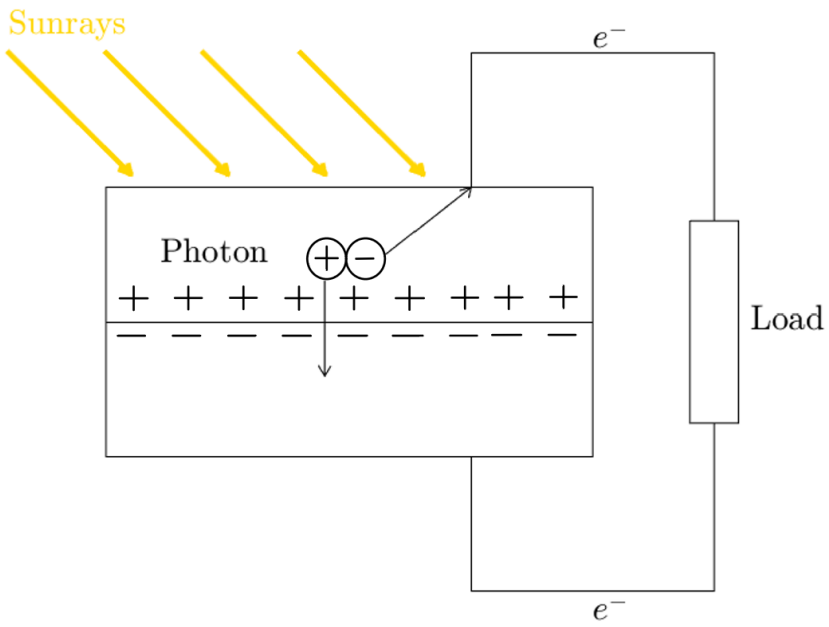

Figure 2.20: *Simple sketch of a photovoltaic cell with an external load, inspired by [69] .*

The amount of energy produced from a PV panel is dependent on the efficiency of the panels. The efficiency can be calculated using Equation 2.20.

$$\eta = \frac{P_{max}}{A \cdot 1\,000\,W/m^2} \tag{2.20}$$

where P_{max} is the maximum power from the panel [W], A is the area of the panel [m^2], and the maximum total irradiance at standard testing conditions (STC; 1 000 W/m^2).

Commercial PV panels usually have an efficiency ranging from 16–23 % [70], depending on the type. These numbers are constantly changing as technology evolves.

PV panels are an easy way to generate renewable energy on-site without leaving a permanent impact on nature. They are relatively easy to install, and the panels can be placed anywhere from rooftops to walls or even on the ground. The required maintenance is minimal due to the absence of moving parts. These factors make PV panels an excellent way to achieve net-zero goals in buildings and positive energy blocks.

The use of solar energy, particularly in combination with energy storage, can provide security of supply to a system. The most prominent challenge solar energy faces in Norway is presumably that PV panels produce the most energy when demand is at its lowest. The production curve generally looks like the one presented in Figure 2.21. The daily production presents with a similar curve as the yearly production.

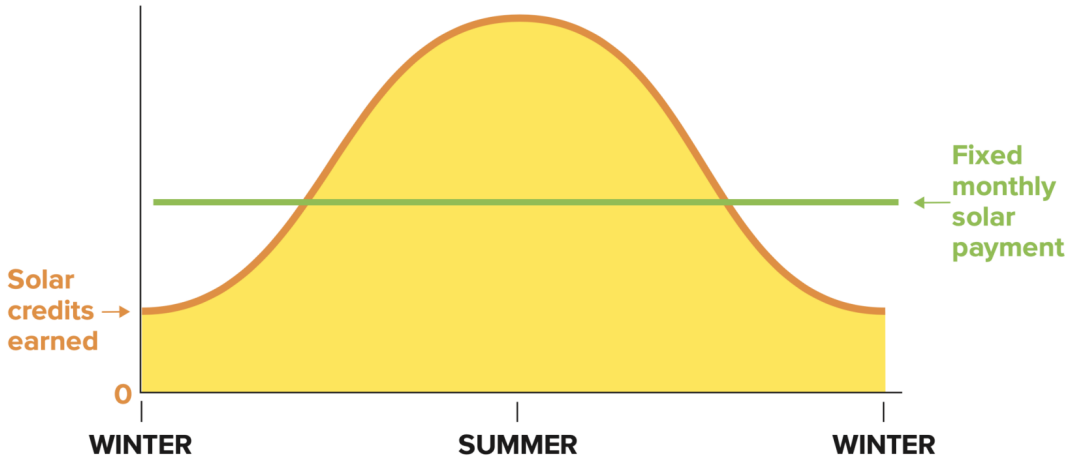

Figure 2.21: *Typical yearly energy production from PV systems [71].*

It is apparent that the production peaks during the day and are highest during the summer months. Figure 2.2a shows the average monthly load profile for a block of flats. It becomes apparent that residential areas usually have power load peaks in the morning and evening, which does not match with the PV production profile [72]. Office buildings, schools, and kindergartens, on the other hand, experience load peaks during the day [13]. This is quite the opposite of a residential building and shows similarities to the production curve presented in Figure 2.21. These characteristics make office buildings especially suitable for solar energy.

2.8 District Energy

District heating (DH) and cooling systems, also known as urban energy, utilise local heat and fuel resources that normally go to waste. It involves the heating of water in a Heat Production Plant, as seen in Figure 2.22. The heated water leaves the production plant, travels to the customers, and returns at a lower temperature. District heating is a method of meeting the cooling and heating demand in urban areas with a citywide distribution network that transfers the heating or cooling from facilities that are central supply units [73]. The customer receives the heat in their exchange unit. Customers use the heated water to provide heating through radiators, heated tap water and heat through pipes located under the floor. District heating is also commonly known as community heating or remote heating network and is defined as renewable energy by the Directive of the European Parlament [74].

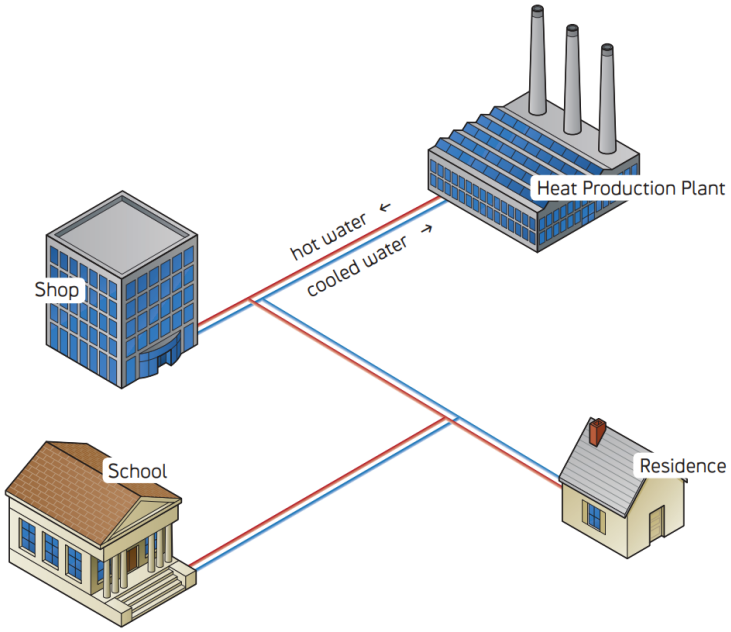

Figure 2.22: *Illustration of Heat Production Plant and distribution system [75].*

District heating is produced by energy recovery of waste, biofuels by chips and demolition materials, fossil gas, biogas, solar heating, fossil oil and bio-oil, waste heat from industry, heat pumps, and electricity [76]. Waste is the most common energy source. The baseload in district heating in Norway is based on renewable energy sources. Peak load is the additional heat when the baseload, the primary heating source, no longer covers all the heating needs. Therefore it is necessary to supplement with peak loads. This heat demand usually arises when the source of primary heating can no longer provide us with the heat that the system needs. This problem mainly occurs in winter when the demand is higher. Traditionally the peak load has been based on fossil energy sources, contributing to Norwegian climate emissions [77].

District energy is a regulated sector in Norway and plays a vital role in the principles of efficient investment in the energy infrastructure. A district heating system is most common in urban areas due to the capital expenditure (CAPEX) of pipe connection and network, market heat demands and access to a suitable cheap heat source. This urban localisation of the district energy is a positive contribution to minimise the capital investment and for the district energy to be competitive in the market. Pipelines are expensive therefore, it is more cost-effective to centralise the system [73].

2.8.1 Circular Economy

District energy contributes positively to the circular economy, considering the socio-economically efficient energy supply. A circular economy is defined as retaining and utilising products and resources efficiently and for as long as possible. Preferably, in a cycle, whereas few resources as possible are lost [78]. A reused, repaired, the improved or recycled product reduces the trend. In contrast, it is estimated that half of the total greenhouse gas emissions are related to how natural resources are managed and extracted. District energy utilises sources, such as recovered heat from waste, that would otherwise be lost and are an essential part of the transition from linear to circular economy [79].

The goal of a circular economy is to have no waste, and according to the Waste Framework Directive made by the European Commission, seen in Appendix A, waste recovery should be one of the last options. However, an average European accumulates five tons of waste each year, and in Norway, waste incineration is an essential part of the national waste management system [80]. In Norway, waste heat from waste incineration accounts for just under half of the energy sources in the district heating supply. Furthermore, in Europe, district heating is responsible for reducing at least 2.6 % of the total amount of the total CO_2 emissions, at least 113 million tons of CO_2 [81].

2.8.2 Price Model

The price model for different customers, private and commercial, are seen in the DH in Table 2.4 – 2.7. This structure of a price strategy does not fluctuate due to the demand and when the DH facilities have to use peak loads. According to the article, *District heating cost fluctuation caused by price model shift*, there is a need for a restructure of the pricing model to keep the competitiveness and increase transparency [77]. NVE has stated that they think a new pricing strategy for DH in Norway would be beneficial [82]. Today, the total DH price is a combination of a power cost, an energy cost and a volume cost, shown in Equation 2.21 [83].

$$DH\,Price = Power\,Cost + Energy\,Cost - Volume\,Cost \tag{2.21}$$

The power cost applies to industries with high power outages and is presented in Table 2.6. This price varies from summer to winter [84].

The energy cost consists of the monthly average spot price for the supply, grid rental, taxes, and surcharges. The Tables 2.4, 2.5 and 2.7 show the energy cost of DH for private customers, housing associations and the industry [84]. The price is based on the average monthly spot price because the District Heating Act of 1986 states that district heating should not cost more than electricity in the area. However, this premise is old and does not reflect today's energy system [85]. Grid rent is the charge consumers pay for receiving electricity into their homes [86]. Private customers and housing associations also have to pay a statutory contribution to the Enova energy fund through the Enova tax in addition to the consumption tax [87]. Power suppliers are required to purchase electricity certificates, and this cost is passed on to the costumers [88].

The volume cost is a reduction in cost if the DH company receives the desired ΔT in return from the customer. This equals a discount of 6 øre/kWh and adds a volume cost of 3.13 NOK/m^3 of water flowing through the building. This reduction only applies to housing associations and the industry [84].

Table 2.4: *DH pricing for private costumers [89]*

Private Customers - Energy Cost
Monthly average for the supply area, spot + Energy price grid rental, incl. Consumption tax and Enova tax + Surcharge incl. electricity certificate
Total energy component per kWh

Table 2.5: *DH pricing for housing association [90]*

Housing Association - Energy Cost
Monthly average for the supply area, spot + Energy price grid rental, incl. Consumption tax and Enova tax + Surcharge incl. electricity certificate – Deduction volume-linked (Nov-Feb)
Total energy generation per kWh (March - Oct) Total energy generation per kWh (Nov - Feb)

Table 2.6: *DH pricing for the Industry [83]*

Industry - Power Cost
Summer (May-Oct), Winter (Nov-April) 0–99 [NOK/kW $\cdot$ month] 100–399 [NOK/kW $\cdot$ month] $>$ 400 [NOK/kW $\cdot$ month]
Total energy generation per kWh (March - Oct) Total energy generation per kWh (Nov - Feb)

Table 2.7: *DH pricing for the Industry [83]*

Industry - Energy Cost
Monthly average for the supply area, spot + Energy price grid rental + Surcharge incl. electricity certificate + Consumption tax – Deduction volume-linked (Nov-Feb)
Total energy generation per kWh (March - Oct) Total energy generation per kWh (Nov - Feb)

2.9 Energy Infrastructure in Trondheim

The district heating main production is located at Heimdal, in Trondheim. The network runs from Heimdal to Ranheim with substations located at Nidarvoll, Marienborg, Dragvoll, Lilleby, Øya, Brattøra, Ladehammeren and Midtbyen, as seen in Appendix B.1. The largest costumer are the Norwegian University of Science and Technology (NTNU), Lerkendal Stadium, Nidardos Cathedral and St. Olavs Hospital.

In 2020, approximately 6.1 TWh of district heating and 192 GWh of district cooling were produced. Where 618 GWh is for district heating in Trondheim, and 13 GWh is for district cooling, as seen in Figure 2.23. The sector diagram illustrates the different district energy sources that were used in 2020 [91]. Recovered heat represents the most significant share with 81 %.

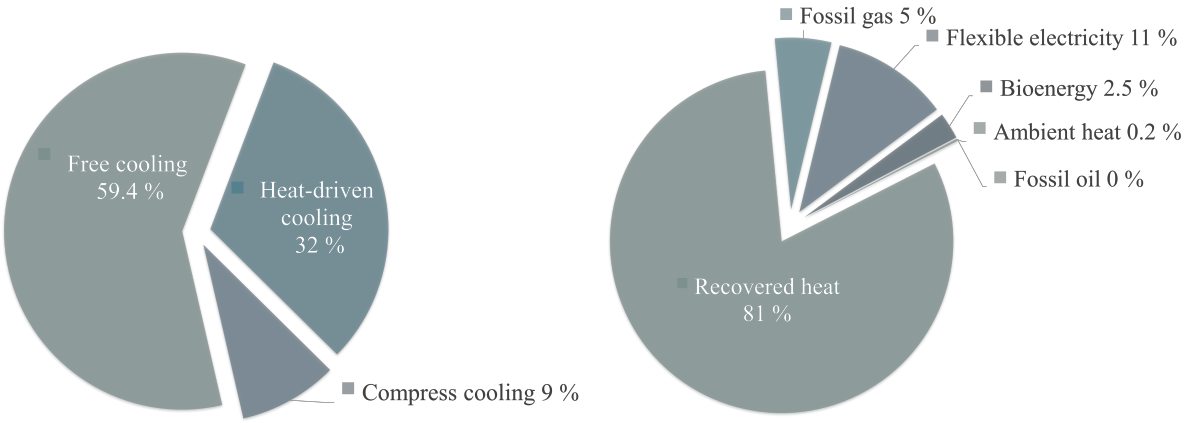

(a) District cooling. *(b) District heating.*

Figure 2.23: *District heating and cooling sources displayed in sector diagrams for Trondheim, 2020 [91].*

In Trondheim, most district heating energy is sourced from solid waste, as seen in the Table 2.8 for baseload, and electric boilers are the biggest top load and power reserve. The waste that arrives at the Heimdal production plan comes from the whole of Central Norway, from the North of Dovre in the south to Saltfjellet in the North. The plant at Heimdal can burn more than 200 000 tonnes of waste every year.

Table 2.8: *Renewable energy sources in Trondheim for DH, according to Statkraft Varme [91]*

Baseload Production	
Wasteheat from waste incineration	80 MW
Wasteheat from Rockwool	1 MW
Biofuels	9 MW
Biogas	1 MW
Heat pump	1 MW
Sum	92 MW

The facility at Heimdal follows strict requirements in order to avoid gaseous- and particle pollution. Many Norwegian buildings used to have oil boilers installed, but DH has replaced them as the waterborne heating system after the ban from 2020 [75]. In 2017, Statkraft installed a new

bio-oil boiler with a capacity of 10 megawatts and collaborated with Rockwool in Trondheim to purchase waste heat, as seen in Table 2.9. With this collaboration, surplus heat from Rockwool factories in Trondheim and Moss warms the inhabitants of both cities [92,93].

Table 2.9: *Top load and power reserve for DH, according to Statkraft Varme [91]*

Top Load and Power Reserve	
Electric boilers	90 MW
Bio-oil	10 MW
Natural gas (LNG)	30 MW
Propane gas/butane gas (LPG)	75 MW
Oil boilers	50 MW
Sum	230 MW

Through closer interaction between the thermal system and the power system, District energy can potentially play an important role in future Trondheim and other cities. By covering the need for heating and cooling, district heating can facilitate that other energy needs can be covered with electricity without having to strengthen the power supply to the area in question [80].

Smart districts in Trondheim are the first in the world in 2022 to buy and sell electricity in the neighbourhood. The energy system and the solutions have been developed in a collaboration between NTNU researchers, the business community and the municipality [94].

2.10 Energy Systems

There is a growth of energy production from renewable energy sources, and an increased focus on Local Energy Systems (LES) [95]. An Energy system is defined as a facility for transmission, consumption distribution or generation of energy in a well-defined system. Facilities can include energy production such as solar energy, wind power, and utilisation of heat pumps and district heating [96].

The electricity distribution grid will have to adapt to the future demands such as varying powerload and uncertainties. Smart energy system is an important part of the future solution of tomorrows energy supply. It is considered to be a key element to reach the climate goals by 2050, defined the by European Commission.

The EU aims to reform the European Energy System with an Integrated Energy System. Today, the energy system is often more linear, and energy flows in one direction, as seen on the left side of Figure 2.24. The goal is to integrate the energy system with a more efficient and *circular system*, as illustrated on the right side of Figure 2.24, focusing on reusing waste energy. Two other characteristics of an integrated energy system are a cleaner power system and a cleaner fuel system with more LES and direct electrification of the end-users such as transport, buildings, and industrial heating. This kind of integration promotes a circular energy system, increasing the usage and implication of renewable energy sources and promoting innovative projects within this field. This integrated energy system helps Europe reach the goal of being climate neutral by 2050 and make Europe more competitive and sustainable [97].

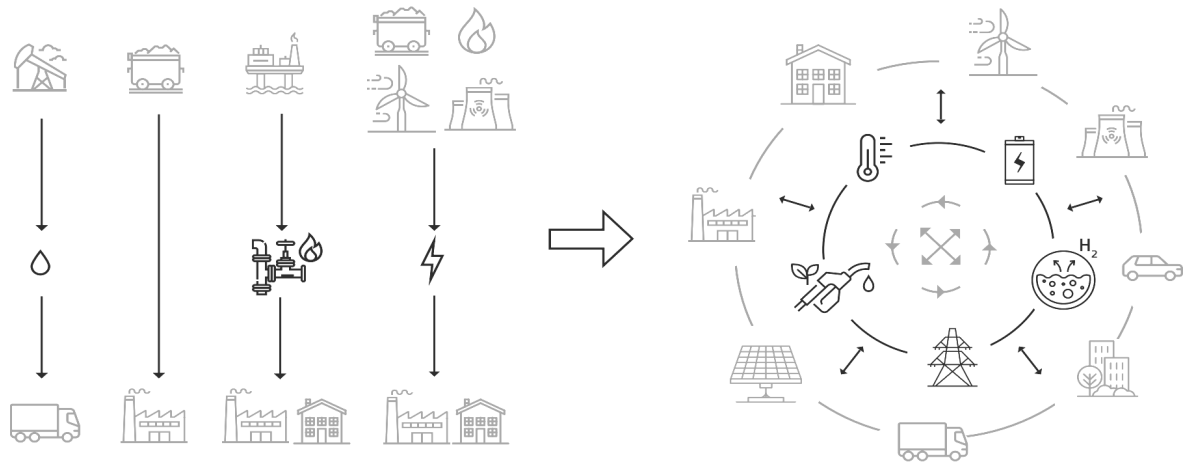

Figure 2.24: *Linear vs. smart integrated renewable energy system [97].*

2.11 Sector Coupling

Combining heat and power, a simultaneous generation and integration of heat and electricity are called sector coupling. It refers to the integration and interconnection of the power supply sector and the energy demand sector, and enables renewable energy across energy-consuming sectors. Such as heating and electricity both in the industry, transport and buildings. Sector coupling is a highly relevant concept that gives valuable flexibility and grid-balancing opportunities. It is about connecting the energy sectors and optimising them together [97].

Sector coupling can be used to balance demands and supply by enabling renewable to be used across a broader range of applications. It plays a vital part in adapting energy markets and infrastructure to a more integrated and complex structure [97]. Through sector coupling, emissions can be reduced, fossil fuel can be avoided and it can help to optimise and balance the energy system [98].

3 Literature Review on TABS

This section contains a literature review on TABS internationally and nationally. The implementation of TABS started in central Europe in the 1990s to provide cooling in new office buildings. Since then, the TABS technology has evolved into a combined heating and cooling system and has spread to other parts of Europe, North America, and East Asia [99]. In 2012 an ISO standard for dimensioning and calculation of dynamic heating and cooling capacity of TABS was published, and an updated version was published in 2021 [100]. TABS did not arrive in Norway until 2014, when two separate office buildings installed TABS almost simultaneously [101].

The international review is based on four articles with different aspects of the TABS's influence on the building. Romaní et al. [102] presented a summary of the simulation and control strategies from published papers. Michalak [103] measured the performance and temperature in the rooms where TABS are installed. Namai et al. [104] surveyed employees about thermal comfort, and Rijksen et al. [105] researched the TABS's ability to reduce the peak requirements.

The national review is based on an article from 2016 discussing the two first buildings in Norway with TABS integrated [101], Sandstuveien 68 and Stålgården, along with two master theses from NTNU about a newly finished building and one that is about to be constructed [106,107].

3.1 International Experiences

Romaní et al. summarised the main characteristics of TABS and presented the developed simulation and control strategies for TABS published prior to 2016. The findings reveal that many simplified models simulated have good accuracy in the application range, even though detailed numerical methods give the most accurate results. Control of supply temperature with heating and cooling curves is common for most TABS. More advanced control includes calculating energy supplied from the heating and cooling curves [102].

Michalak measured the performance of TABS in an office room in a Southern-Polish passive building from July 2019 to November 2019 during regular operation to describe the thermal comfort. The TABS were used for both heating and cooling. During the heating season, the water supply temperature varied from 22 °C to 30 °C. The supply temperature was raised a few hours before opening hours and decreased later in the day to compensate for internal heat gains from activities within the building. During the cooling season, the water supply temperature ranged from 16 °C to 22 °C. The obtained results of the study revealed that; the floor surface temperature varied from 20.6 °C to 26.2 °C, and the average vertical air temperature varied from 22.5 °C and 23.1 °C. The temperature difference between the floor and the ceiling was between - 0.9 °C and 6.3 °C, confirming good thermal conditions. There was no discussion of using TABS for peak-shaving despite the adjustments made during the heating season [103].

Namai et al. investigated the thermal comfort in an office building located in the urban area of Tokyo, Japan. Employees were surveyed four times about their thermal comfort over two years, with the operation controlled by on/off criteria. The findings showed that most scenarios maintained thermal comfort. However, intermittent operation and a high setpoint temperature of 23 °C of room air in the cooling mode provided the most optimal operation in terms of energy savings [104].

Rijksen et al. researched the TABS's ability to reduce the peak requirements for cooling in a building in the Netherlands by activating TABS for cooling only during the night. The findings showed that TABS could reduce the Chiller cooling capacity by 50 % for a building with 30 % glass in the facade but only 14 % for a building with 50 % glass in the facade. The nighttime operation resulted in a load shift of the cooling demand. For the first building with 30 % glass, the temperature increased by under 2.5 K, preserving the building's thermal comfort [105].

3.2 National Experiences

Stålgården was one of the first buildings in Norway to install TABS and is often referred to in other Norwegian projects or articles. In 2016 "VVS aktuelt" authored an article about the two buildings with TABS in Norway, where they contacted the technical chief Tonny Øien at Kjeldsberg Eiendom. The internal loads were different than first assumed, and the building needed more heating and less cooling. Therefore, the TABS produced more heat than they were designed for. Another early experience was that the outdoor climate did not strongly affect the indoor climate. Øien stated that when they tested turning off the TABS in the winter, three days passed until the building reached a critical temperature of 22 °C. It was further noted that the circulation of water was steady, which is optimal for pump operation, providing a suitable base load for the building [101]. The article does not mention the data behind these finds.

The same article mentions the first building to install TABS, Sandstuveien 68. Sandstuveien 68 is a passive house built in 2014 with TABS installed for cooling and has experienced operational challenges connected to specific design weaknesses in the current building [101].

Since 2015 a few other projects with TABS have been planned. Such as the Deichman Library in Oslo finished in 2019, an office quarter in Tromsø currently in building stage four [106], and the new government quarter to be completed in 2029 [107]. As of today, May 2022, no experiences or data have been published for these buildings.

4 Case Study – Sluppen

This section presents each of the buildings at Sluppen along with the technical specifications for components central to the PEB. The documentation needed to describe the system was delivered by Kjelsberg. General characterisations and descriptions from the relevant documents are included in this section.

4.1 Sluppenvegen 17B

Stålgården (2015) at Sluppenvegen 17B is a passive house with a Gross Floor Area (GFA) of 13 130 m^2 spanning over eight floors, with an energy label of A. The building contains about 8 000 m^2 of TABS, which provides heating and cooling. The building is connected to a district heating system, as seen in Appendix C, and also has ventilation systems and heat pumps that produce heat [108]. On the roof at Stålgården, 666 m^2 of PV panels are scheduled to be installed to contribute to local energy production.

4.1.1 Heat Distribution

For Stålgården, the heat distribution systems were complex, and for this thesis, the system description was simplified. The constructed flowchart in Figure 4.1 illustrates the heat distribution system in Stålgården and is labelled with the relevant variable names seen in the code in Appendix E. Due to limitations in this project and access to data, the system used for further work is defined as *System 17B_1*.

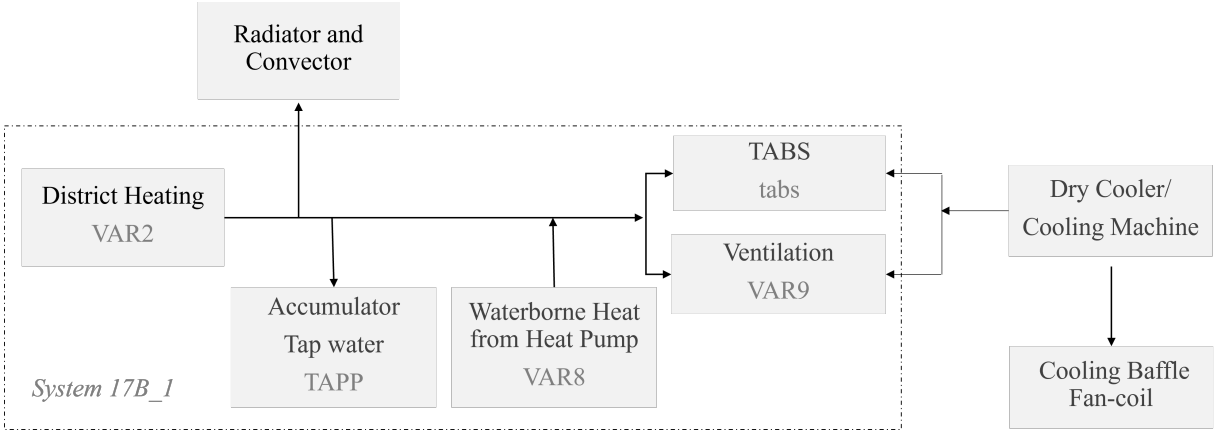

Figure 4.1: *A simplified flowchart of the heating distribution in Stålgården. "VAR2", "TAPP", "VAR8", "tabs" and "VAR9" are variable names implemented in the methodology and seen in the Appendix E. "System 17B_1" is the defined system that is used in the project.*

4.1.2 Heat Pump

SLV 17B has one air-to-water heat pump which supplies waterborne heat to the building. The heat is delivered both via TABS, radiators and convectors. The heat pump has a fouling factor of 0.044 m^2 K/kW. The function description for the heat pump can be found in Table 4.1. Where T_o is the outside temperature. The air-to-water heat pump function description operates with two seasons, summer and winter, and the function is dependent on the outdoor temperature.

Table 4.1: *Function description for the air-to-water heat pump at SLV 17B*

Season	Time of day	Function	Temp
Summer	Day	$T_o >$	20 °C
	Night	$T_o >$	15 °C
Winter	Day	$T_o <$	5 °C
	Night	$T_o <$	0 °C

Operating conditions for the heat pump are displayed in Table 4.2. The leaving fluid temperature is the fluid temperature that exits the heat pump and enters the heating distribution system in the building. In contrast, the return temperature is the temperature exiting the cooled or heated building and returning to the heat pump. The heat pump extracts heat from the building by supplying a cooler leaving temperature of 13 °C for cooling and adds heat to the building by supplying a warmer leaving temperature of 31 °C for heating.

Table 4.2: *Operating conditions for the air-to-water heat pump at SLV 17B*

Operating Conditions		Cooling	Heating
Return fluid temperature	[°C]	17	27
Leaving fluid temperature	[°C]	13	31

The technical data for the heat pump performances; capacity and power input, is presented in Table 4.3. The capacity and power input are higher for cooling than heating for the heat pump at SLV 17B. The difference in capacity is 80.75 kW, and the difference in power input is 14.97 kW.

Table 4.3: *Technical data for the air-to-water heat pump at SLV 17B*

Performances		Cooling	Heating
Capacity	[kW]	270.96	190.21
Power input	[kW]	66.37	51.4

Different efficiency ratios for the HP can be seen in Table 4.4. The *COP* is the coefficient of performance, *EER* is the Energy Efficiency Ratio, and *ESEER* is the European Seasonal Energy Efficiency Ratio. Different performance measurements for the heat pump and are explained in Chapter 2.6.2.

Table 4.4: *Efficiencies for the air-to-water heat pump at SLV 17B*

Type	Value
COP	3.7
EER	4.08
ESEER	3.83

The heat pump unit uses HRC R410A refrigerant; both compressors and heat exchangers have been optimised for the refrigerant at SLV 17B. The heat pump consists of two independent refrigerant circuits to improve power output. Appendix D shows the pressure enthalpy diagram for the refrigerant, in SI units. The heat pump is equipped with four compressors arranged in pairs to fit the two refrigerant circuits. The evaporator is a *brazed stainless steel plated*-type heat exchanger. It has a 19 mm thick insulation layer and is fitted with a film-type electric heater on the external surface to prevent the unit from freezing.

4.1.3 TABS

All office floors of SLV 17B are equipped with TABS that receive thermal energy from both the heat pump and district heating. Fine-tuning of local temperature is done using ventilation.

The TABS are relatively simple to regulate, with the supply temperature and/or flow rate of water being adjusted based on the outdoor temperature. The TABS are turned off during the day and used for cooling at night in the summer, and they are continuously on in the winter to provide heating, except for certain heating zones where the TABS are turned off. The function description of these are presented in Table 4.5. The TABS can be used for heating and cooling. Depending on the season, the operating temperatures lie between 22 °C to 25 °C close to the desired room temperature. The thermal lag of the concrete is why the TABS can operate with a relatively small ΔT.

Table 4.5: *Function description for the TABS at SLV 17B*

Season	Time of day		Function	Temp
Summer	Day	(10:00–22:00)	Stop	—
	Night	(22:00–10:00)	$T_o >$	0 °C
Winter	Day	(10:00–22:00)	$T_o <$	- 8 °C
	Night	(22:00–10:00)	$T_o <$	0 °C

4.2 Sluppenvegen 19

Lysgården (2019) at Sluppenvegen 19 is one of the world's most modern office buildings with production of solar energy and advanced heat pumps. The building has a GFA of 12 000 m^2 spanning over six floors [108]. Lysgården has an energy label of A, and is built after passive house standards.

4.2.1 Heat Pump

There is one air-to-water heat pump and one cooling unit at SLV 19. Only the heat pump will be considered in this thesis. The fluid flowing through the heat pump is *Water + Ethylene Glycol 30 %*, and it has a fouling factor of 0.044 m^2 K/kW . The operating conditions for heating and cooling are listed in Table 4.6.

Table 4.6: *Operating conditions for the heat pump at 19*

Operating conditions		Cooling	Heating
Return fluid temperature	[°C]	12	42
Leaving fluid temperature	[°C]	7	47

The heat pump takes heat from the building by supplying a cooler leaving temperature of 7 °C for cooling and adds heat to the building by supplying a warmer leaving temperature of 47 °C for heating. This heat pump has a higher difference between the leaving temperature for cooling and heating than the heat pump at SLV 17B.

The performances and the efficiencies for the heat pump at SLV 19 can be found in Table 4.7. The heat pump has a relatively high efficiency and a high SCOP.

Table 4.7: *Performances for the heat pump at 19*

Performances		Cooling	Heating
Capacity	[kW]	267	198
Power input	[kW]	69.7	82.5
Full load efficiency	(EER/COP)	3.83	2.41
Integrated full load efficiency	(COP)	—	2.1
Seasonal efficiency	(SEER/SCOP)*	4.05	3.48
Energy efficiency class	(EER/SCOP)	B	A+

(*) SEER : According to commission regulation (EU) N° 2281/2016 for comfort chillers
SCOP : According to commission regulation (EU) N° 813/2013 for low temperature heat pumps

4.2.2 PV Panels

Lysgården has a PV system consisting of 456 mono-crystalline panels installed on the roof. The panels are placed with an east/west orientation, with a tilt of 10 degrees from the rooftop. They are connected in strings of 12, and one converter is connected to 19 strings. An illustration of the existing PV panels can be seen in Figure 4.2.

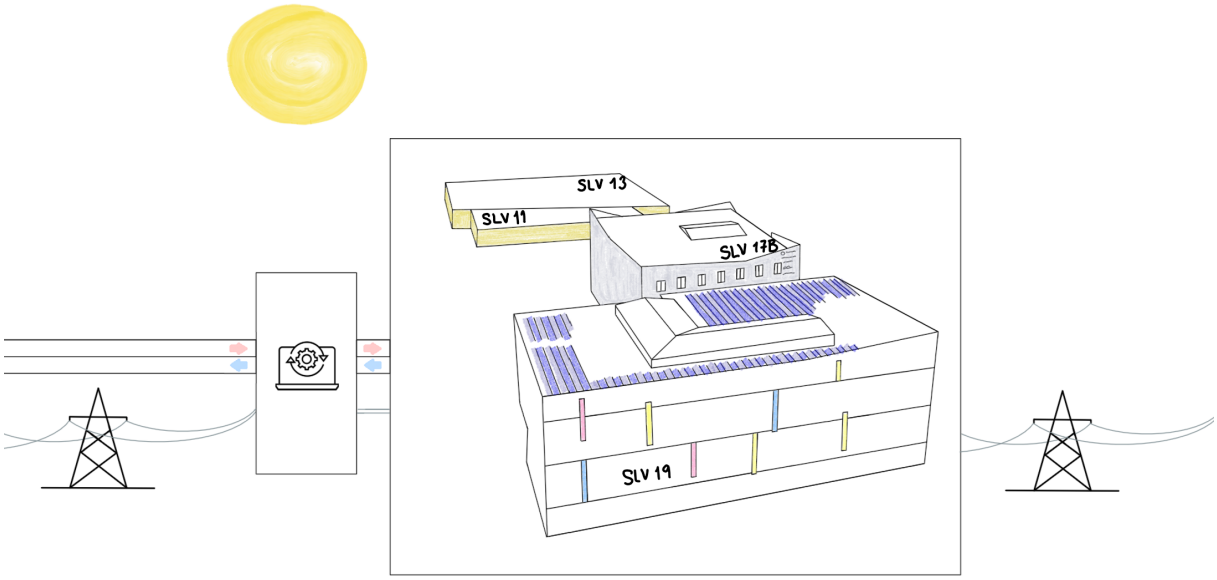

Figure 4.2: *Sketch of the PEB at Sluppen.*

Table 4.8 displays electrical data for the PV panels. The nominal power presented gives the system an installed capacity of 177.84 kWp. Two inverters are installed at 36 kVA each, which are connected to the main board and deliver 400 V of voltage.

Table 4.8: *Electrical data for the PV panels at 19*

Electrical data			
Nominal Power	P_{nom}	390	W
Efficiency	η	22.1	%
Rated Voltage	V_{mpp}	64.6	V
Rated Current	I_{mpp}	6.05	A
Open-Circuit Voltage	V_{oc}	75.3	V
Short-Circuit Current	I_{sc}	6.55	A

4.3 Sluppenvegen 11 & 13

Sluppenvegen 11 (1975) and 13 (2005) are connected and have a total GFA of 8 676 m^2 divided over two floors. The buildings hold a few heat pumps and are connected to the district heating network. Other than that, they do not have any energy-efficient measures, hence giving them an energy label of F [108]. SLV 11 contains a food court and SLV 13 holds a climbing centre.

4.4 Rye Microgrid

Rye Microgrid is located at a farm at Byneset just outside of Trondheim. The farm has 600 m^2 of PV panels installed in three rows. The microgrid collaborates with TrønderEnergi, and the PV production will be added to the system at Sluppen. The motivation for adding a remote system to the Sluppen system is to provide an additional *local* power supply to reach PEB requirements [109].

4.5 Aims of Study

This thesis aims to provide an overview of the current production and consumption pattern at Sluppen and scenarios for peak shaving in 17B using TABS, heat pumps, and sector coupling. Estimates for the future actions at Sluppen will also be explored.

5 Methodology

This section describes the methodology used to obtain the results for this thesis, based on the information from Case Sluppen, Section 4. It presents the raw data and how it has been processed and implemented. Furthermore, it describes the data flowchart and how the data is connected. An explanation of the written code used to conduct the simulations and the data treatment is also provided.

5.1 Data and Software

Kjeldsberg Eiendom provided the raw data which creates the basis for the thesis. Kjeldsberg Eiendom has also supplied relevant system descriptions and arranged a physical tour of the four relevant buildings to support understanding of the data and technical system flow. The provided data had a detailed function- and system description of all components in the buildings, and the relevant information is described in the Section 4, Case Study–Sluppen. In addition to this, weather and irradiation data have been gathered from *Norsk KlimaService Senter* and *NASA*. *Statkraft Varme* has also supplemented with an overview of the district energy infrastructure in Trondheim.

For the purpose of this thesis, the simulation software *MatLab* was chosen. MatLab is a matrix-based software tool that provides mathematical computing power to analyse data, develop algorithms and create models and other applications. MatLab has no defined modelling method but provides the user with the flexibility to create functions and self-made models. The program supports several interfaces to other languages and embedded systems. For this project, the data was mainly imported from *Microsoft Office Excel*, a spreadsheet generation, maintenance and printing program. Excel can enter numbers and data into a large table of cells in any scheme the user wants to create forms, reports and calculations.

Data on electricity demand was collected from AMS meters for each building, while the rest of the main meter data came from the SD system. Electricity demand includes heat pumps, computers, coffee machines and everything else in the building that uses electricity. The raw data is treated confidentially. The measured data retrieved from the SD system of the building is fragile at certain points. Some meters do not provide values, and some have not recorded particular hours. As a result, some of the data had to be approximated, but this will be stated where applicable.

Additional to raw data collected for the Base Case for the existing grid, data from the solar panels at Rye microgrid from 2021 is available. The plan is to redirect the energy from these panels to the future PEB. The PV data from Rye is measured with a higher frequency than hourly intervals. The systems at Rye consist of three rows of panels, each with a separate meter. Further PV calculations and estimations have also been conducted.

5.1.1 System Definition

To better understand the methodology, Figure 5.1 presents a simplified data flowchart describing the used data and how it is connected. The Figure visualises the origin of the provided data based on the meters available for the defined PEB.

The meters in Figure 5.1 represents provided data sets. The contained data of these data sets is not limited to what is displayed in Figure 5.1. Not all meters and sub-meters at Sluppen are used in this project due to periods of lacking data and time limits. The main meter contains yearly data on DHD and ELD from all the buildings. The SLV 19 meter contains ELD and PV production from SLV 19, and the sub-meters at SLV 17B contains data from 2021 for all heat distributed in *System 17B_1* defined in Figure 4.1.

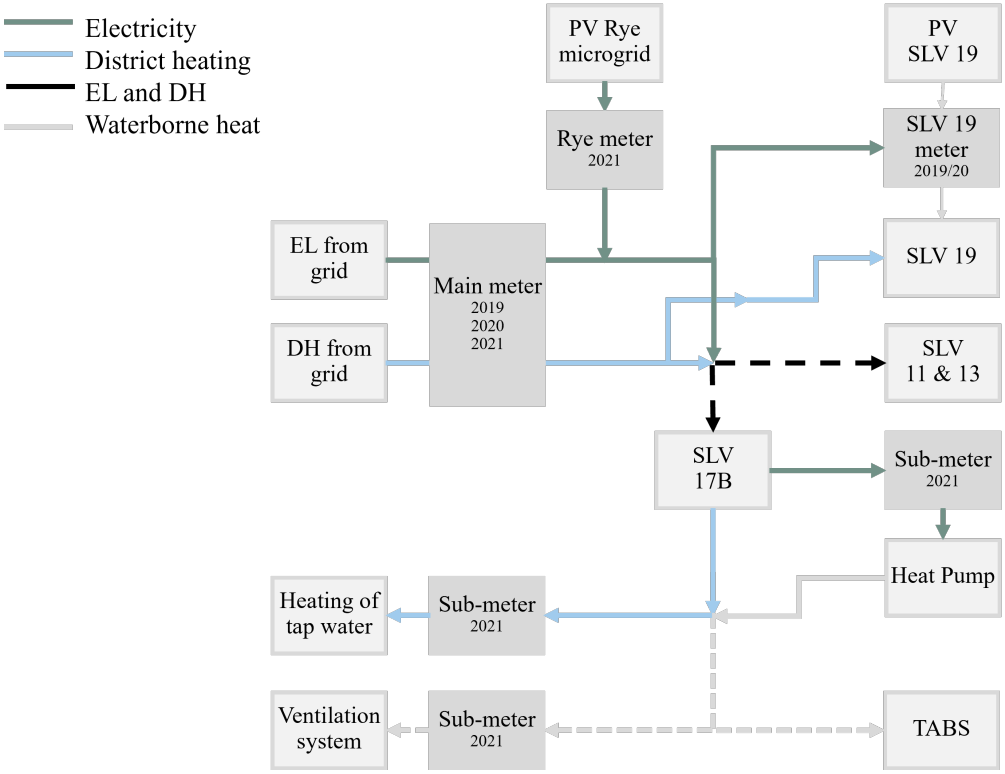

Figure 5.1: *Illustration of the flow of data available for the system.*

5.1.2 Data Selection and Treatment

Before using the raw data, it had to go through a data selection process and treatment. A data selection process determines the appropriate data type and considers its issues. It is crucial to process raw data carefully to correctly interpret them and ultimately avoid erroneous results in the prediction. For this assignment, the data is treated to be organized in an hourly resolution.

The raw data had missing values at the beginning of the year. Therefore, it was determined that the matrices would start on the 1st of March (00:00), and end on the 31st of December (00:00). Data from some meters skipped a measurement during daylight saving in the fall, and these hours were removed from the matrices that had them to match the provided data. The standard size for the matrices with the latter points accounted for became 7320×1 for the hourly resolution. There are also occasional outages in the data, and these values were fabricated using estimation.

Each section below refers to which appendix and lines in the code the text describes.

Temperature Data

Lines 6–13 in appendix E:
Weather data was collected from *Norsk klima senter* for the weather station at *Risvollan* in Trondheim (SN68230), from 01.03.21 to 31.12.21. This data was imported into MatLab as "w3". The correct hours were extracted, and the format was changed to an array to allow further manipulation. Furthermore, "w3" was run through a function (lines 15–25) to change the commas "," to periods ".", before it was saved for later use.

Main Meters

Lines 27–65 in appendix E:
The data from the main meters at Sluppen was loaded into MatLab, and the relevant columns and rows were located, extracted and converted into arrays. This process was done for all the buildings in the PEB for the years; 2019, 2020 and 2021. The data available from the main meter can be seen in Table 5.1.

Table 5.1: *Overview of accessible data from the main meters*

Address	Electricity Demand	District Heating Demand
11	x	x*
13	x	x*
17B	x	x
19		x

*District heating demand for Sluppenvegen 11 & 13 is measured by the same meter, and therefore has one common matrix.

Production Profile

Lines 67–103 in appendix E:
The production profile for Sluppenvegen 19 was then created. The data was loaded into MatLab, and the correct columns were fetched. As Table 5.1 shows, the main meter did not record electricity demand from Sluppenvegen 19, but because of the PV system, Lysgården has its meter, where this data was found. However, the values in this file were measured from 01.09.19 to 31.08.20. A new file was created (line 75) in Excel to make this file match the other matrices. The values from 2020 (01.01.20–31.08.20) were placed at the beginning of the file, while values from 2019 (01.09.19–31.12.19) were filled in at the end.

The data for electricity demand at Sluppenvegen 19 and solar production was then fetched and converted to arrays. The electricity demand was saved to be used in the load profile.

The additional PV production matrix was loaded into the script, converted to kWh and added to the production from Lysgården to create the production profile. The treatment of the additional PV production is described in Section "Additional Solar Production". The newly created matrix had some disproportionately large values, which were removed using for and if loops (lines 92–103).

Load Profile

Lines 105-129 in appendix E:
The matrices created in "Main Meters" were used to create the load profile, which was done both for the total system and the individual buildings. First, the total load profile was created by calculating the yearly average values from each address for both electricity and district heating before all these matrices were summed. The individual load profiles were created by making matrices based on the address and not years, which was done in "Main Meters". These matrices were 7320x3 and contained all the data from the main meter for each building.

Sub-Meters

Lines 131–169 in appendix E:
The file containing information from the sub-meters at Sluppenvegen 17B was loaded into MatLab. The relevant columns and rows were found and extracted for electricity consumption and delivered heat (lines 137–150). The prominent peaks created by the inrush current were removed by running them through a self-produced function, which can be found in lines 171–176. An estimation on heat delivered to the TABS was done in line 163, based on the energy balance ($VAR8 + VAR2 = VAR9 + TAPP + tabs$) of *System 17B_1* described in Figure 4.1. Negative values were removed from the matrix using the for and if loop in lines 165–169.

Additional Solar Production

Lines 1–36 in appendix F:
Additional solar production from Rye was also to be taken into account. There were three columns of production data, and the resolution did not match the rest of the data. The mean value for the solar production data was found over every hour to achieve an hourly resolution (lines 7-15) before the three columns were summed (line 19). Assumptions were made to fill in the missing data (lines 20-35).

5.2 Simulation

With the system definition from Figure 5.1 in mind, three main scenario analyses were conducted. The first viewed the possibilities for peak shaving based on changing the consumption pattern of the TABS. It looks into how much the peaks could be shaved if the use of TABS were moved from 07:00–16:00 to 20:00–05:00 the day before. This is possible since the TABS can store thermal energy for about two days. The second analysis was done to move the heat pump usage, which can be regulated throughout the day. The peaks were moved in the same time intervals as in the first simulation. The third one was done based on improving the sector coupling. It looks into extremes for the system to give theoretical maximum values. Each analysis was conducted for a week in the first month of every season and for the whole year.

5.2.1 TABS

The respective code can be found in appendix G.
The necessary data was loaded into the script, and the indexes for the week that would be analysed were found and saved as a variable (*index_march*). The variable *index_march* started at 00:00 Monday and ended at 23:00 Sunday for the second week of March. The peak hours (*ph*), which are defined as the hours between 07:00 and 16:00, were found using the *peakhours*

function (lines 146–160), and multiplied by the matrix containing the estimated values for heat delivered to the TABS. A new *index_march* was defined starting 00:00 Sunday and ending 23:00 Saturday for the same week as before. This *index_march* was used to fetch the corresponding values for electricity demand.

To account for the additional hours on Sunday, 24 empty cells were added to the end of EL_march. A valley hours matrix vh was created by adding 12 empty cells to the beginning and end of ph so it start s at 20:00 on Sunday. Valley hours are values that will fill the valleys that appear before the peak, while ph will shave the peaks. vh was also multiplies by 1.1 to make up for heat losses associated with TES when moving the load. A new ph was created by adding 24 empty cells at the beginning to add inn the hours for the first Sunday.

When EL_march, ph, and vh had the same number of cells, vh was added and ph was subtracted from EL_march. The description function shown in lines 162–184 was then used to display the mean, minimum, maximum value and sum of the new and old electricity demand. This process was repeated for June, September and December. Lastly, the method described was applied for the whole year (lines 95–143). The peakhours function was replaced with the code in lines 100–126, to account for the whole year.

5.2.2 Heat Pumps

The respective code can be found in appendix H.
The same method was performed as in Section 5.2.1, only this time for the heat pumps ELD. The HP can be regulated as needed, an there are therefore no heat losses associated with heat production. The heat produced by the HP must however be stored in the TABS, and the same ten percent as in the previous section was therefore added to the valleys to account for heat loss. It is best for the heat pump not to be completely turned off, so ten percent of the peaks were not shaved, so that the HP can stay on and just be regulated.

5.2.3 Sector Coupling

The respective code can be found in appendix I.
The necessary data was loaded into the script. The matrix containing DH data (FJV) had some errors from the inrush current which were removed using the *peakdelete* function (lines 93–98). The variable *index_march* was created, and the corresponding cells were fetched from the matrices containing electricity and district heating demand. The electricity demand for the heat pump was subtracted from the total demand and saved as a variable (EL). The heat from the HP was added to the DH demand and saved as $HEAT\_IN$. When moving demand from the HP to DH, Equation 2.18 describes the relation between the current and hypothetical demand, where $Q_{useful\,heat}$ stays constant and the moved demand has to be multiplied by the COP. The variables were described using the describe function, defined in lines 100–104. The process was repeated for September and December. In June the heat pump was used for cooling, this was accounted for by not subtracting the cooling demand from the total electricity demand (lines 32–43), since cooling had to be done by the HP and cannot be moved to DH. This was also taken into account when repeating the process for the whole year (lines 76–90).

5.3 Future Aspect – PV Estimation

The respective code can be found in Appendix J.
Estimation was done to demonstrate how the planned PV installations will affect production. Irradiation data was collected for Sluppenvegen 11 from NASA and loaded into the script. Data on existing production was also fetched from the script found in Appendix E. The relevant areas and efficiencies were defined before estimation was done using Equation 2.20. When plotted against the total electricity demand, it became apparent that the production had to be 2.5 times larger to cover the demand during summer. This optimised production was found by summing the total estimated production and multiplying it by 2.5 (line 22).

6 Base Case – Results and Discussion

This section presents and discusses data from the current system at Sluppen and the specifics for SLV 17B, the only building with TABS installed.

Figure 6.1 shows the daily total ELD and DHD for all the buildings, along with the temperature from 2021 and the existing solar production from SLV 19 and Rye. The figure plots the mean values for 2019, 2020, and 2021. The national covid-lockdowns could have influenced the data in March 2020, autumn 2020, spring 2021, and winter 2021. The general recommendation to work from home during 2020 and 2021 also has impacted the data.

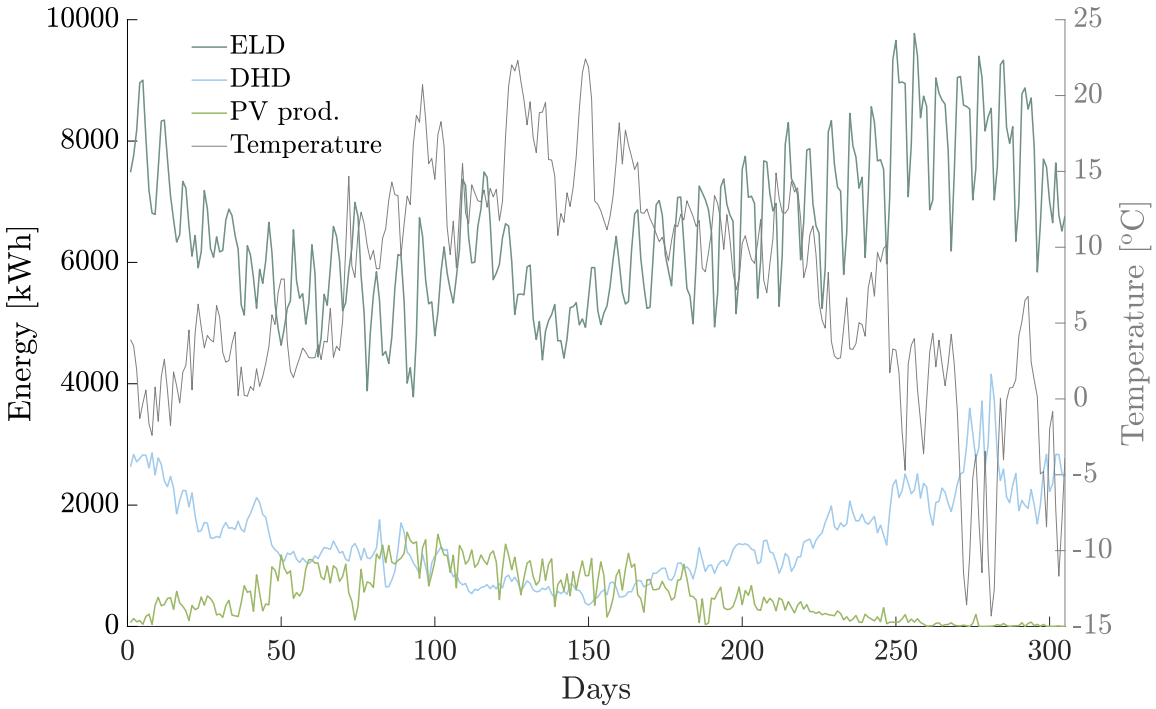

Figure 6.1: *The average, daily total ELD, DHD, and PV production, for 2019, 2020 and 2021.*

The electricity demand is high in early spring, lowers in the summertime, and rises again in autumn and winter. The increasing demand around 100 days corresponds with an increase in temperature, and consequently, cooling demand rises. The shared summer vacation is probably causing the valley around day 150, and the winter holidays are believed to be the reason for the dip at the end of the year.

The DH demand has a similar curve to the electricity demand, with peaks in the spring and wintertime. The demand is relatively stable in the summer and is affected by the shared summer vacation. The larger peaks in the cooler seasons are likely due to larger drops in the outside temperatures.

The PV production peaks in the summer and has close to no production towards the end of the year. The shifting weather is presumably some of what caused the daily variations in the production curve. There is a large gap between production and consumption in the system, and the PV panels are not close to covering the consumption any day of the year. Therefore the

system does not fulfil the criteria for being called a positive energy block.

Figure 6.2 shows the yearly (March–December) consumption of electricity and district heating per building. The data is from 2021, except for ELD for SLV 19, which is the sum of demand from September 2019 to August 2020.

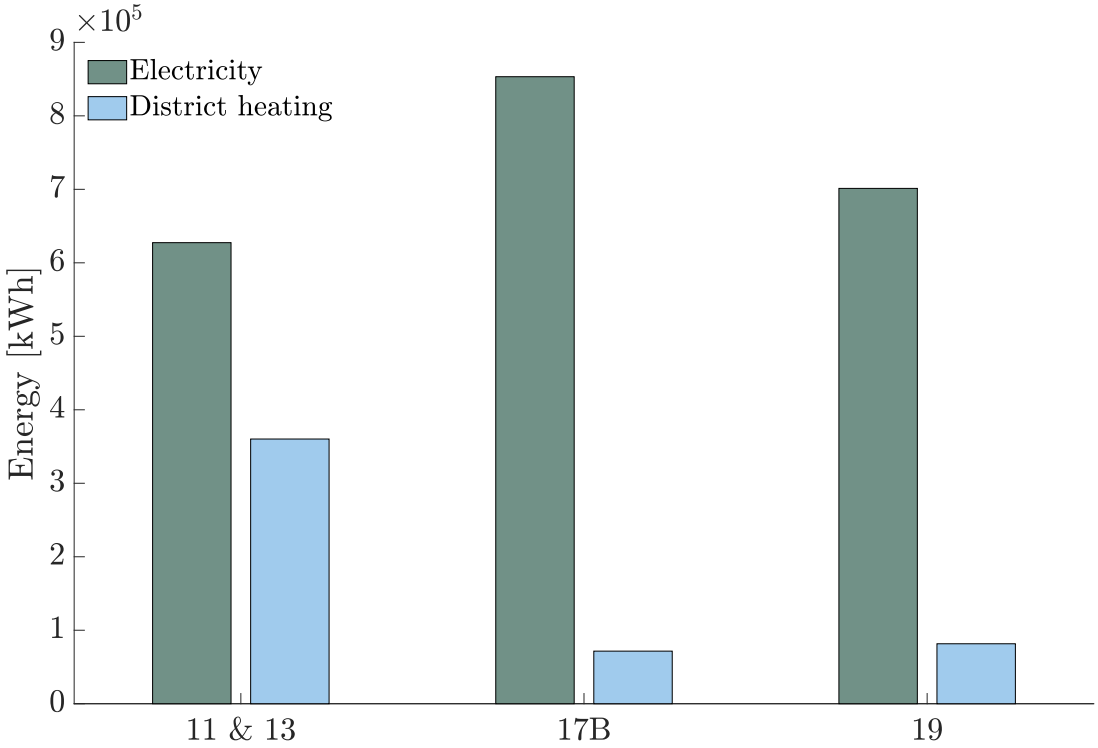

Figure 6.2: *EL and DH demand per building.*

For the ten considered months, SLV 17B has the highest electricity demand with 853 251 kWh/yr and the lowest district heating demand at 71 572 kWh/yr, while SLV 11 & 13 have the lowest electricity consumption with 627 421 kWh/yr and the highest DH consumption at 360 215 kWh/yr. SLV 19 consumes on 701 179 kWh/yr of EL and has a DH demand of 81 600 kWh/yr.

SLV 17B is the building with the largest GFA and therefore has a higher EL consumption than the other buildings, while SLV 19 has a smaller GFA by about 1 000 m^2 and therefore has a lower electricity demand. Both SLV 17B and 19 are office spaces, which require a large amount of electricity for electrical equipment and heating. The latter buildings inhabit highly efficient heat pumps, making it cheaper to use HPs for heating than DH, which explains why the DHD is substantially lower for SLV 17B and 19 vs SLV 11 & 13.

SLV 11 & 13 have the lowest GFA and electricity demand. However, the buildings are old, less efficient and have more heat losses, with an energy label of F. This means that they generally require more energy to cover the heating demand, and this partly explains their high DHD. SLV 11 & 13 have a different consumption pattern than SLV 17B and 19 because they are used as food courts and climbing centres, not offices. The food court probably requires more tap water, which increases the DH demand further.

In Table 6.1 the total yearly (January–December) energy consumption for each building at Sluppen including data from January and February, is presented. This table is the calculated total consumption by Kjeldsberg and is not representative of the datasets used in previous results and upcoming simulations.

Table 6.1: *Yearly total energy consumption (ELD + DHD) including January and February for 2021*

Building	Electricity demand [kWh/yr]	District heating demand [kWh/yr]	Total energy consumption [kWh/yr]
11 & 13	566 454	368 943	953 397
17B	924 111	104 759	1 028 870
19	758 731	95 177	853 9089

The relation between the different buildings DHS and the electricity demand for SLV 17B and 19 is consistent with Figure 6.2. January and February, two months with high demands for heating, increase the demands for all elements, as expected. With the exception being ELD for SLV 11 & 13. The demand shown in Figure 6.2 for March through December is much higher than the total consumption for January through December in Table 6.1. The significant differences in total consumption indicate an error in the 2021 dataset for SLV 11 & 13 or the Kjeldsberg calculation.

6.1 SLV 17B

SLV 17B is the building with the most available data due to the sub-meter connected to the TABS. The large utilisation of waterborne thermal energy consisting of DH and HP heat makes it suitable for sector coupling. The following plots are all based on data from the sub-meters at SLV 17B and only contain data from 2021.

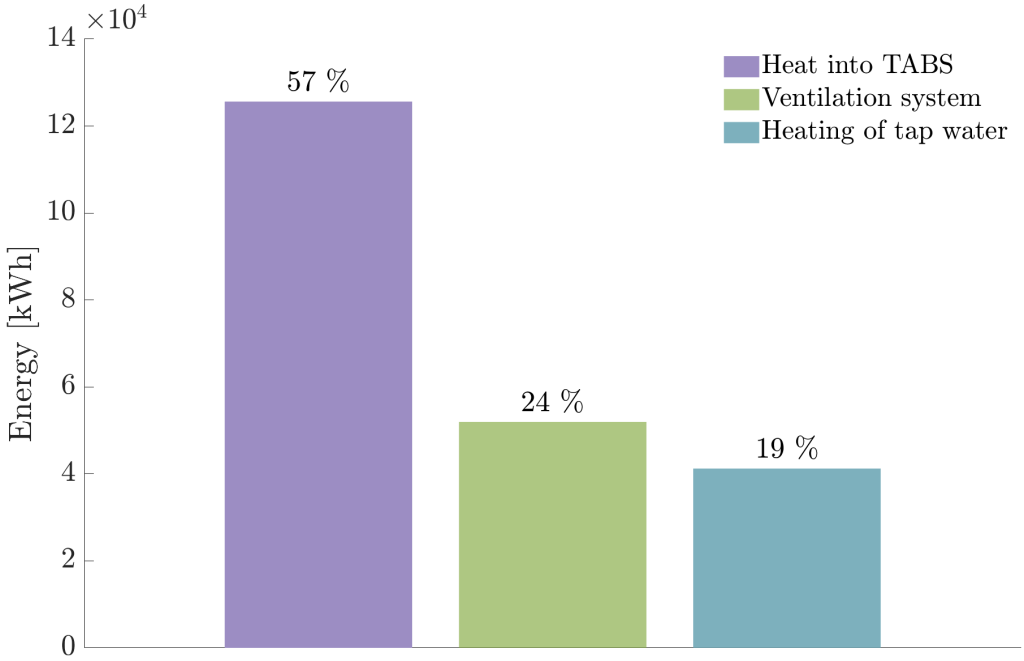

Figure 6.3: *Purpose-based heat energy use in 17B.*

Figure 6.3 shows the consumption of heat divided by purpose. The TABS use 57 % of the heat, 24 % is for ventilation, and 19 % go to heating of tap water. Tap-water uses only district heating, ventilation uses mainly HP, and the TABS uses an unknown mix of both DH and HP.

The TABS utilises most of the thermal energy entering the system at SLV 17B and is the primary heating source. Ventilation covers the remaining heating demand, while tap water is not used for heating the building. Therefore there is a considerable potential to lower power peaks for this building by regulating the TABS.

Figure 6.4 shows the demand for electricity and district heating, the thermal energy delivered from the heat pump and the net electricity use. The Figure displays one week, Monday through Sunday, in each season; spring, summer, autumn and winter. The net electricity use represents the electricity demand for non-heating purposes, and the electricity demand is the total electricity demand including electricity used for heat pumps.

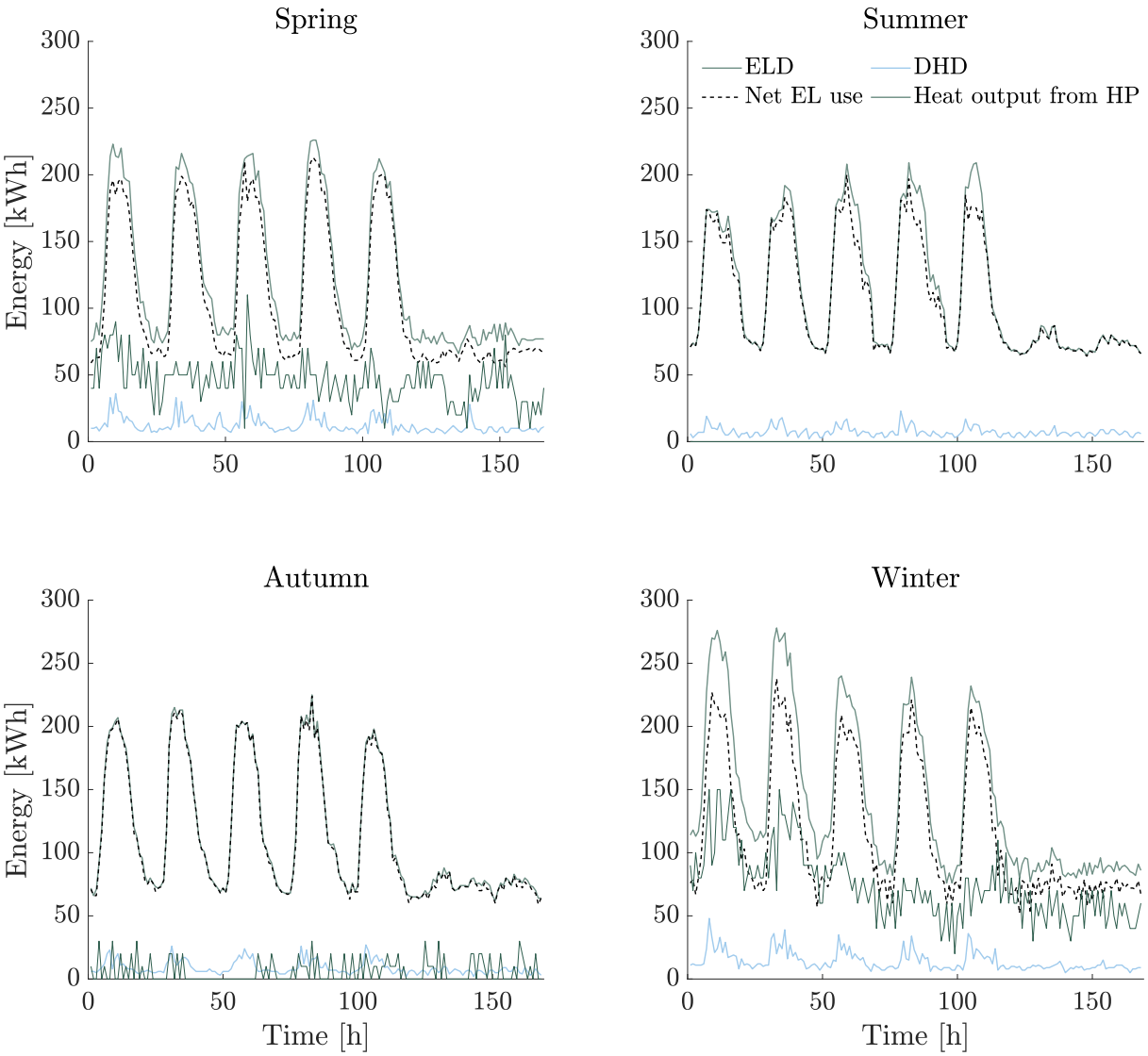

Figure 6.4: *Electricity demand, and heat outputs from HP and DH from one week each season.*

The shape of the curves indicates high demand during the day and low demand during the night on weekdays. At the weekend the demand is low because the office is less used. The power

peaks appear around noon, as expected according to the load characteristics for office buildings (Figure 2.2b). The shape of the curve is equal for all seasons but with higher midday demand in the colder seasons.

The net electricity demand is almost equal to the net electricity consumption during the weeks of summer and autumn when heating demands are lower because of higher ambient temperatures. During the winter and spring weeks, there is a significant gap between them, representing the potential for flexibility in the production of thermal energy from other sources than electricity.

The DHD is relatively stable but increases in heating peak hours during all seasons. The heat output from the heat pump has peaks consistent with peaks in the electricity demand during spring and winter, implying that the heat pump is used for peak heating loads. Peaks in DH demand are likely due use of DH for purposes other than just heating tap water. The heat output from the HP changes with the outdoor temperatures and heating demands. The outdoor temperature defines the SCOP and thereby influences the heat pump's power consumption. Heat outputs are high in the winter and spring and low during summer and autumn, as expected from the demand curve for Trondheim (Figure 2.4).

Figure 6.5 shows the electricity demand of the HP, the thermal energy delivered for heating and cooling, and the outdoor temperature for Trondheim. The heating outputs are highest when the temperature is low, and when the temperature is high, the heat pump switches to cooling mode. The thermal outputs and the COP for the HP change with the seasons.

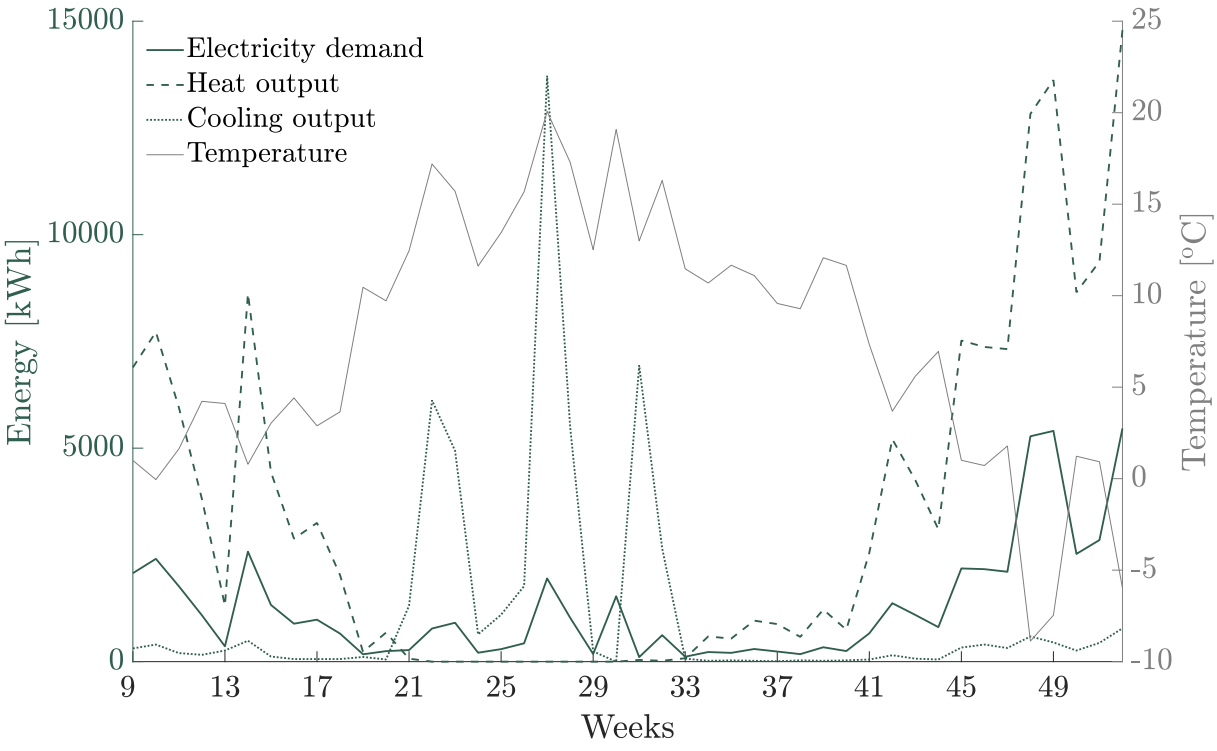

Figure 6.5: *Heating and cooling characteristics for the HP at SLV 17B.*

The COP, visible as the relation between electricity in and thermal energy out of the HP, varies greatly throughout the year. The heating COP is most significant during late autumn and winter, and the cooling COP is highest during the summer. This change in COP was expected

based on the theory and corresponded with the temperature. Figure 6.5 demonstrated that the HP utilises the thermal energy in the ambient air in an efficient matter, which is consistent with the high efficiency factors presented in Table 4.4. There is a clear connection between the outdoor temperature and energy output from the HP, which corresponds with the theory.

The Figure also shows that less energy is needed for cooling than heating. The cooling peak is higher than the highest heating peak, even though the energy demand is lower when the cooling peak is reached vs when the heating peak occurs. An equal amount of energy would cool more than it would heat, which is consistent with the theory and the capacities displayed in Table 4.3.

There is no heating demand from the HP during the summer weeks. However, there is a slight cooling demand throughout the year, probably caused by the cooling of electrical equipment by the tenants.

The share of the total ELD used by the HP for heating and cooling purposes is displayed in Table 6.2. The winter has the highest share use, and the autumn has the lowest.

Table 6.2: *Share of electricity used for heating (HP)*

Season	Share
Spring	12 %
Summer	5 %
Autumn	1.6 %
Winter	19 %
Mean whole year	6.6 %

In winter and spring, electricity is used for heating. The summer has low demand because of the higher temperatures and the shared summer vacation but is used for cooling in the warmest summer weeks, which can be seen in Figure 6.5, and is why the summer share is larger than the autumn one. During autumn, the heating demands increase slowly but stay relatively low.

It becomes apparent that the yearly share of energy used for heating is relatively small compared to the shares for office buildings seen in Figure 2.3. This is, however, anticipated since the buildings are very energy-efficient with an energy label of A.

7 Simulations – Results and Discussion

This section contains the results and discussion of the three simulations; TABS, HP, and Sector Coupling. All results represent data from 2021 since the sub-meter, shown in Figure 5.1, only holds data from this year. Note that the yearly energy consumption differs for TABS and HP versus Sector Coupling because the two first datasets include one more day (28.02.21) due to load shifting, which the sector coupling does not regard.

7.1 TABS

In this simulation, the load from the TABS is moved using the code displayed in Appendix G. The load is moved back from Monday (07:00–16:00) to the prior Sunday (20:00–05:00). The TABS themselves do not produce energy, and the demand has to be covered by either DH or HP production.

Figure 7.1 contains weekly plots, plotted from Sunday through Saturday. The peak shaving potential if the load of the TABS is shifted is presented in Figure 7.1 for spring, summer, autumn and winter. Ten percent heating demand has been added to the valleys to compensate for heating losses when moving the load. These ten percent is an estimated value and may not correctly represent a real-life situation. This percentile requires more research for more accurate outcomes in further development of the simulation.

Figure 7.1a shows the current and hypothetical demand curve for a week in March when moving the TABS load. Irregular hour-long peaks in the heat pumps electricity demand can be observed in Figure 6.4. These have most likely further propagated and affected the curve for TABS heat consumption since the hypothetical curve in Figure 7.1a shares these inconsistent variations.
The power peaks appear skinnier in March than in the other seasons, especially at the beginning of the week. Since the simulation is not optimised for this kind of variations, as it moves load based on set time intervals, some reductions in the demand can be disregarded. The results may have been different if the load shifting was optimised for each specific peak and not time. This method does not have a significant impact on the highest peak value in March, which according to Table 7.1 only reduces the peak by 16 kW.

The losses associated with this method of peak shaving increase the heating demand. These losses can be covered by district heating as to not affect the ELD. Solar energy could probably cover parts of the increases in demand.

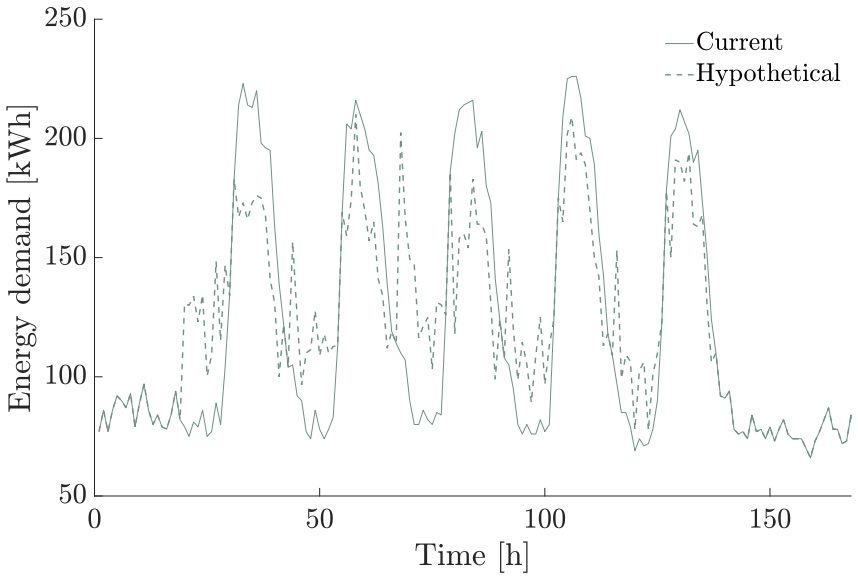

(a) One week in March.

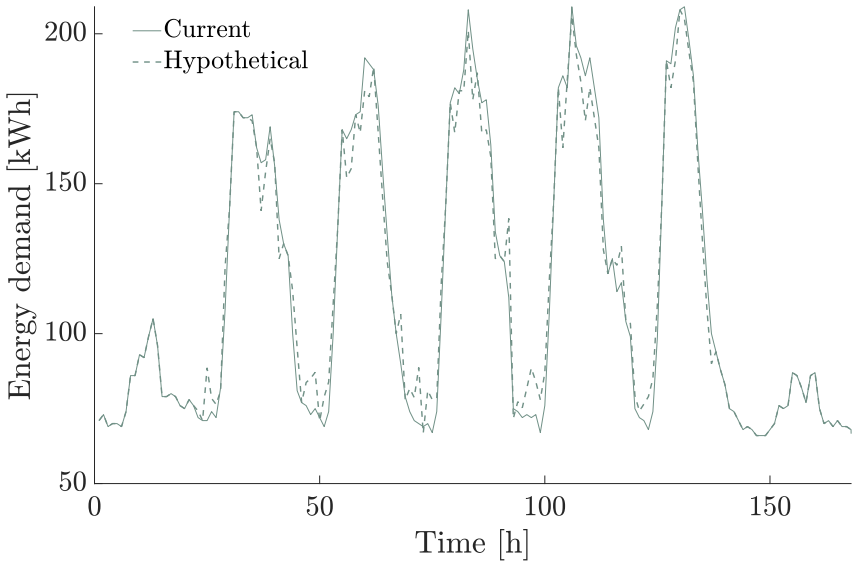

(b) One week in June.

Figure 7.1: *Peak-shaving potential with TABS for each season.*

Figures 7.1b and 7.1c show the current and hypothetical demand curve for a week in June and September when moving the TABS load. In the weeks of summer and autumn, the current and hypothetical demands are approximately the same. Table 7.1 emphasises the fact that this method is not particularly effective during summer, as it only increases the total heating demand. The method performs better during autumn than in the summer but the impacts on the peaks still are not major for autumn compared to spring and winter.

PV production peaks during the summer months and could probably reduce the EL load on the grid. A downside of moving the demand to the night is that it can not be covered by solar production, this problem could however easily be solved with battery ESS as there are many available technologies for short term energy storage.

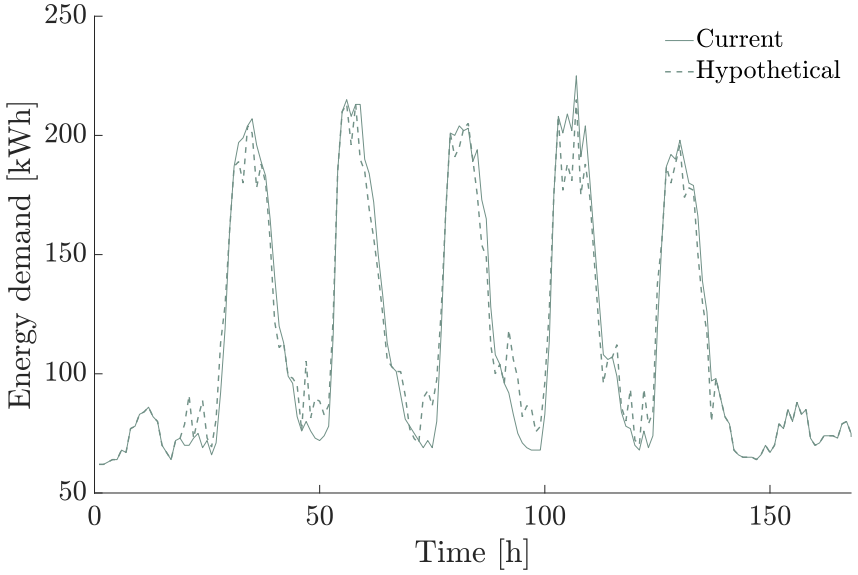

(c) One week in September.

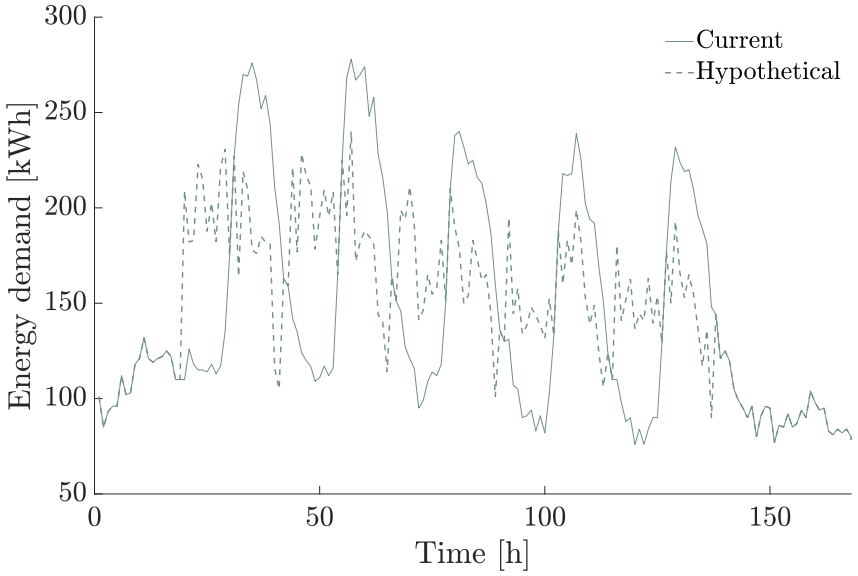

(d) One week in December.

Figure 7.1: *Peak-shaving potential with TABS for each season.*

Figure 7.1d shows a relatively even hypothetical curve with descent peak reduction compared to the current curve. The hypothetical curve indicates much less variation in December than in March, and the difference between the highest peak and lowest valley is significantly reduced.

The daily power peak grows during the week, which is most likely due to passive thermal energy storage. When the building is heated on Monday and electrical equipment starts to produce heat as people are working, heat is stored in the building's thermal mass. Due to the thermal lag described in Section 2.4.4, the heating demand declines throughout the week. The method of peak shaving used in this section is definitely most effective during December when the heating demands it at its highest.

Table 7.1 describes the main characteristics of the curves plotted above. It depicts that heating demand generally increases while the peak value decreases, and that the mean and minimum values remain almost unchanged. It should be noted that cooling is not taken into account and that the changes in total demand are due to the losses which appear when implementing TES. The change is most noticeable in December, where the highest peak is reduced from 278 to 240 kWp, and the weekly heating demand is increased by 311 kWh/week.

Table 7.1: *Overview of heating demand, with and without using TABS for peak shaving*

Month	Version	Mean [kWh/h]	Minimum [kWh/h]	Maximum [kWp]	Sum [kWh/week]
March	I	106.1	66	226	20 371
March	II	106.97	66	210	20 538
Difference		+ 0.87	0	- 16	+ 167
June	I	99.76	66	209	19 154
June	II	99.94	66	208	19 189
Difference		+ 0.18	0	- 1	+ 35
September	I	100	62	225	19 200
September	II	100.27	62	215	19 251
Difference		+ 0.27	0	- 10	+ 51
December	I	127.93	76	278	24 562
December	II	129.54	77	240	24 873
Difference		+ 1.61	+ 1	- 38	+ 311

I = current
II = hypothetical

It becomes clear that the potential for change, and heating demand are directly correlated in this simulation.

The lack of room-temperature data makes it unclear how changing the heating source will affect the amount of energy needed to reach comfortable temperatures. This should be researched and taken into consideration in the project's further development.

If this method of peak shaving was implemented for the whole year, the yearly changes would be those displayed in Table 7.2. The highest peak during the year is reduced by 30 kW, equal to about 10 %. The total yearly energy demand on the other hand rices by 4 090 kWh/yr equal to about 0.5 %.

Table 7.2: *Yearly changes in energy demand and peak value, using TABS for peak shaving*

Version	Yearly energy demand [kWh/yr]	Highest peak [kWp]
I	855 010	278
II	859 100	248
Difference	+ 4 090	- 30

The figures reveal that most of the reduction occurs in the winter when the energy demand is highest in Norway, as can be seen in Figure 2.4. During winter, it is critical to lessen the peaks to minimise the load on the power grid. January and February are, as previously mentioned, not taken into account in this calculation. These months are, together with December, the months with the highest energy demand and would most likely have a considerable impact on the results. Since the weather for January and February is the most similar to December and the method is most effective in December, it is reasonable to assume that the results from these months would be similar to the ones from December.

7.2 Heat Pump

This section presents and discusses results from the simulation where peak-shaving was done by shifting when the HP was being used. In order to produce heat before the actual heating demand appears, the HP will have to take advantage of the thermal energy storage characteristics in the TABS. When moving the HP load, ten percent was left on the peaks to keep the HP on during the whole day. Doing this makes it so the HP does not have to be turned on and off, and inrush current is avoided. Ten percent was also added to the valleys to account for heat loss when storing thermal energy. These percentiles are rough estimates, which should be tweaked to better reflect reality.

The results represent the peak-shaving potential for one week each season, Sunday through Saturday, and are presented in Figure 7.2 and Table 7.3. The load is moved approximately half a day back, beginning Sunday at 20:00.

For a week in March, which can be seen plotted in Figure 7.2a, the highest peak is reduced from 226 to 214.3 kWh according to Table 7.3. There is a noticeable change between the current an hypothetical curve and the hypothetical curve is a bit more even than the current one. The distance between peak and valley is reduced every weekday, but it is most prominent at the beginning of the week. These result is consistent with the results from the TABS simulation.

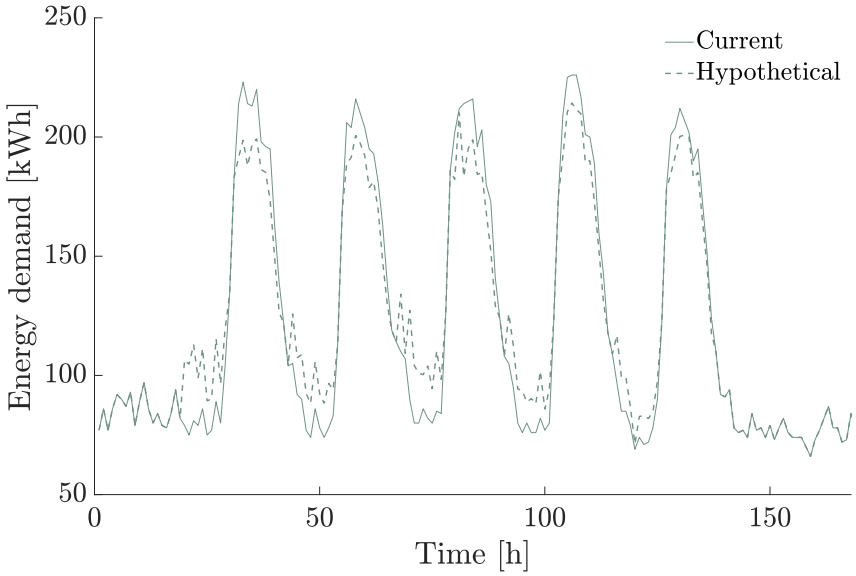

(a) One week in March.

Figure 7.2: *Peak-shaving potential with HP for each season.*

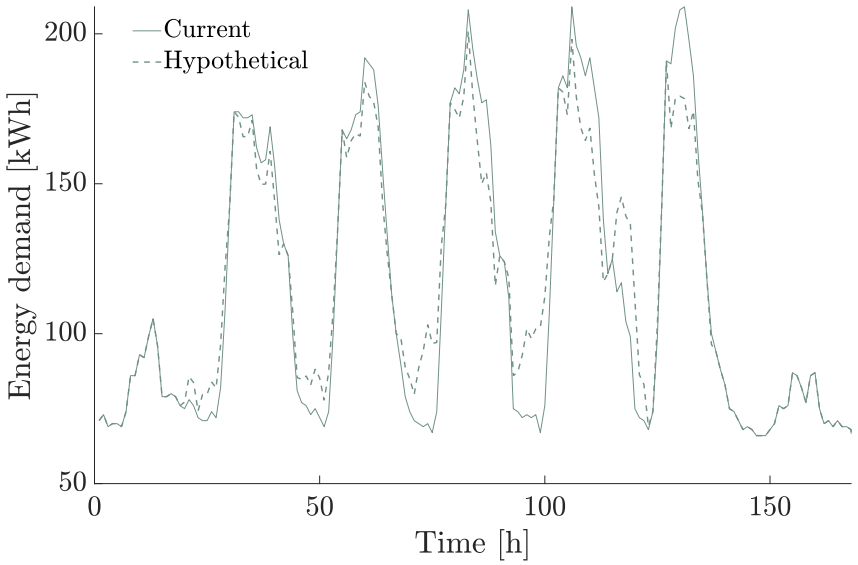

(b) *One week in June.*

Figure 7.2: *Peak-shaving potential with HP for each season.*

Figure 7.2b shows the results for June. The difference between the current and hypothetical curve is more significant in this simulation, Figure 7.2b, than they were in the previous one, Figure 7.1b. This difference is most likely due to the fact that the heat pump can also be used for cooling, which the TABS simulation did not consider. After all, the TABS simulation considers a combination of DH and HP, while the HP simulation only considers the HP. The valley filling on Thursday evening is considered odd since the Thursday peak is shaped differently from the others, with a broader bottom. The fourth peak, representing Thursday, has a broader bottom than the other ones. This results in an odd valley filling, once again since the simulation is based on set time intervals. This method reduces the peaks in June, but due to the slim nature of the top of the peaks on Wednesday and Thursday, this is not always visible in Figure 7.2b. These results do however, only regard one week at a time and the results of this week may vary greatly from the nearby weeks. To correctly evaluate the simulation a longer period of time should be taken into consideration.

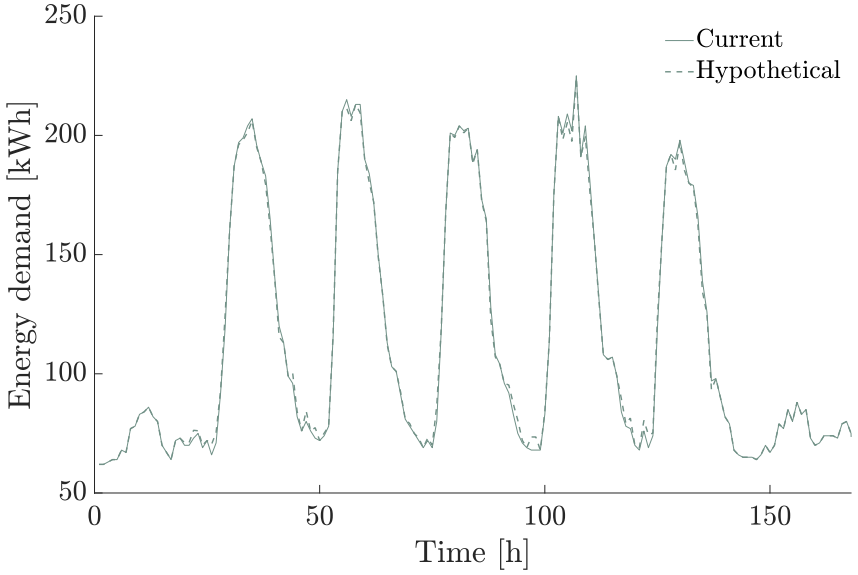

(c) One week in September.

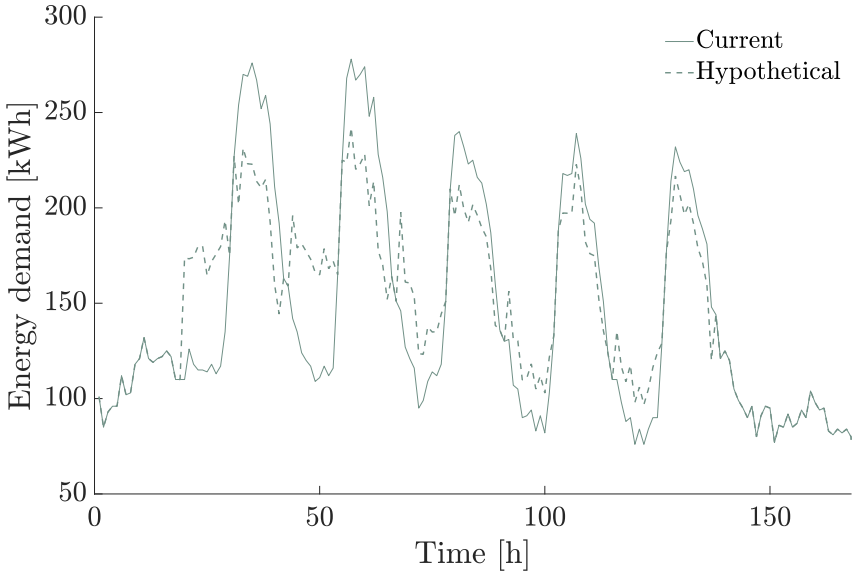

(d) One week in December.

Figure 7.2: *Peak-shaving potential with HP for each season.*

In September, Figure 7.2c shows almost no peak shaving potential. The peaks and valleys in the the current curve overlaps with the hypothetical curves. This result corresponds with Figure 6.5 which shows low heating demand from the HP during this week (week 35).

The results for December are similar to the results from the previous simulation, presented in Figure 7.1d. The hypothetical curve shown in Figure 7.2d is more even than the current one, and the difference between the highest peak and lowest valley is significantly reduced. The heating demand decreases as the week goes on due to passive thermal heat storage, discussed in Section 7.1. The highest peak in December is reduced from 278 to 242 kW according to Table 7.3. This difference equals an approximately 13 % reduction while the energy demand is increased by around 1.5 %.

Table 7.3 gives an overview of some critical values describing the results from this simulation. The results are similar to those presented for the TABS simulation, in Table 7.1. The difference is that the HP method includes cooling from the HP, this mainly affects the results in June when the cooling demand is high (illustrated by Figure 6.5). The changes are most prominent in December. The values for June and March are relatively similar, which emphasizes the impact cooling demand has on the ELD. Peak reduction is barley noticeable in September and underlies that the peak shaving potential is dependent on the heating demand.

Table 7.3: *Overview of heating demand, with and without using HP for peak shaving*

Month	Version	Mean [kWh/h]	Minimum [kWh/h]	Maximum [kWp]	Sum [kWh/week]
March	I	106.10	66	226	20 371
March	II	106.89	66	214.3	20 523
Difference		+ 0.79	0	- 11.7	+ 152
June	I	99.76	66	209	19 154
June	II	100.52	66	200.8	19 299
Difference		+ 0.76	0	- 8.2	+ 145
September	I	100.00	62	225	19 200
September	II	100.10	62	224.1	19 220
Difference		+ 0.10	0	- 0.9	+ 20
December	I	127.93	76	278	24 562
December	II	129.74	77	242	24 910
Difference		+ 1.81	+ 1	- 36	+ 348

I = current
II = hypothetical

Table 7.4 shows the changes throughout the whole year with this method of peak shaving. The simulation reduces the peak by about 12 % and increases the yearly energy demand by about 0.2 %.

Table 7.4: *Yearly changes in energy demand and peak value, using the heat pump for peak shaving*

Version	Yearly Energy Demand [kWh/yr]	Highest Peak [kWp]
I	855 010	278
II	857 070	244
Difference	+ 2 060	- 34

Having data for January and February would probably, also for this simulation, cause larger change in Table 7.4, as the method seems to be the most effective during winter. Table 6.1 showed that the total energy demand in SLV 17 was 1 028 870 kWh/yr in 2021, which means that solely 83 % of the demand is accounted for in these simulations. By having data for January and February, the demand would be significantly higher and the potential for peaks shaving, which seems to increase with heating demand, would rise. Figure 6.5 showed that the heat pump

is effective when the temperature is low, and should work well in January and February.

Figure 2.2a shows that residential buildings typically experience a power peak in the evening. Moving the load to the previous evening will interfere with this residential peak and create an even more prominent peak. This is a side effect of isolating the system from its surroundings in the simulations. Therefore, the optimal time to receive the load should be researched, and the simulations optimised to consider the total grid.

7.3 Sector Coupling

This simulation explores the possibilities of utilising sector coupling to lower power demand by changing the ratio of DH and EL in the energy mix and turning off the heat pump. No load-shifting occurs, as the goal is to change the energy source and not time of consumption. This section will present and discuss the outcomes of the simulation.

Figure 7.3 shows a significant increase in DHD and an evident decrease in ELD this particular week in March. The relation between these two will represent the COP factor and seem to be approximately equal to the COP factor displayed in Table 4.4.

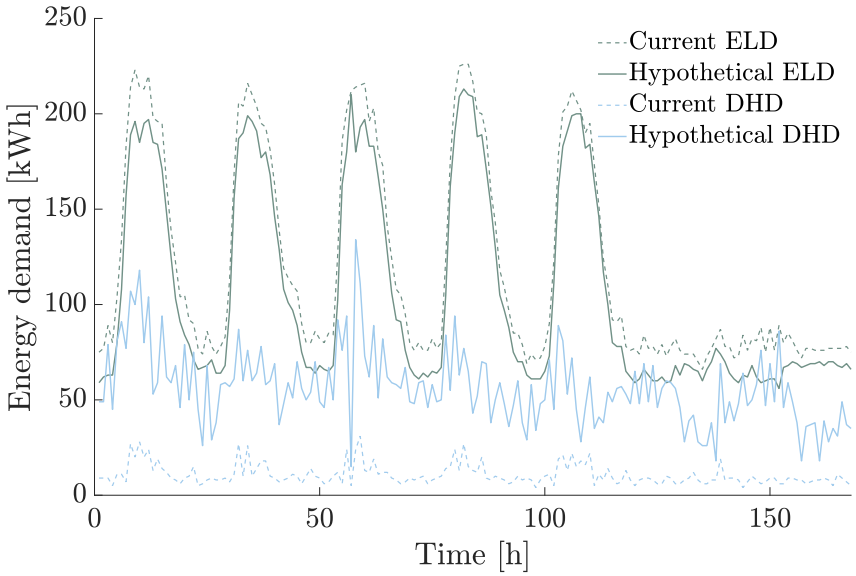

(a) One week in March.

Figure 7.3: *Peak-shaving potential with Sector Coupling for each season.*

The decrease in ELD varies from day to day and is most noticeable at the beginning of the week; this may be due to the passive TES in the building, which lowers the heat demand throughout the week. The difference between the highest peak and the deepest valley stays relatively constant during the workdays. There is an even decline in ELD during the weekend without significant changes between the current and hypothetical curve shape. On the other hand, the hypothetical DHD groves in magnitude and fluctuates more than the current one. The odd peak in ELD for the HP mentioned in Section 7.1 is visible in this Figure as the peak in DHD at around 58 hours.

The ELD is a bit lower in Figure 7.3b but the DHD is unchanged, which indicates that the heat pump cools the building during June. The DH network can not currently contribute to cooling, and DH can therefore not replace the change in ELD.

Figure 7.3c reveals small changes in both ELD and DHD, which are inconsistent and merely last for a couple of hours at a time. The size of these changes which become evident in Table 7.5, suggests that this method is not particularly effective for neither June or September.

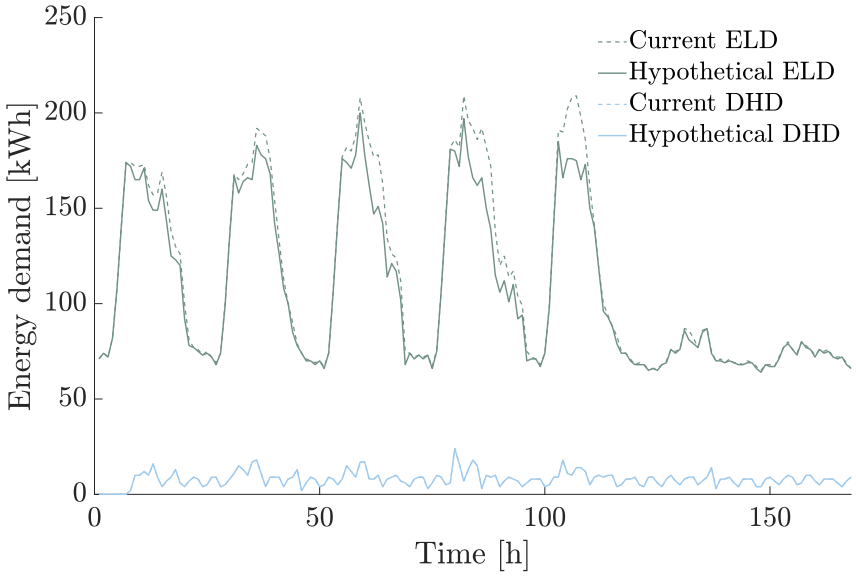

(b) One week in June.

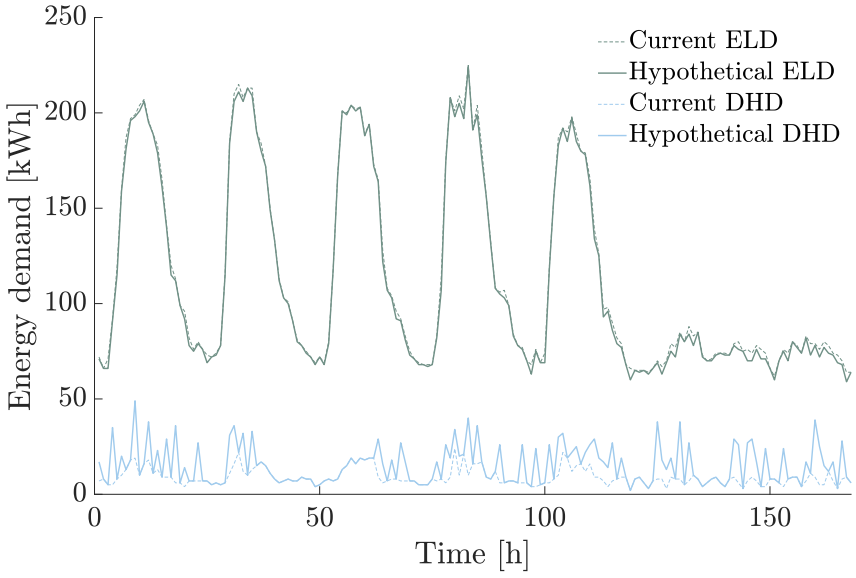

(c) One week in September.

Figure 7.3: *Peak-shaving potential with Sector Coupling for each season.*

The method used in this section is, like the other ones, the most effective in December. The hypothetical ELD has more of a consistent shape than the current curve. The difference between peaks and valleys decreases and stays relatively consistent throughout the week. The DHD, on the other hand, has unpredictable peaks during the day, which fluctuate in magnitude during the week. The DHD is higher at the beginning of the week and gets lower as the week progresses. The

change between current and hypothetical DHD is prominent during the weekend, considering both value and shape. The hypothetical ELD and DHD are similar in magnitude during the weekend and valleys, which is a considerable change from the current curves.

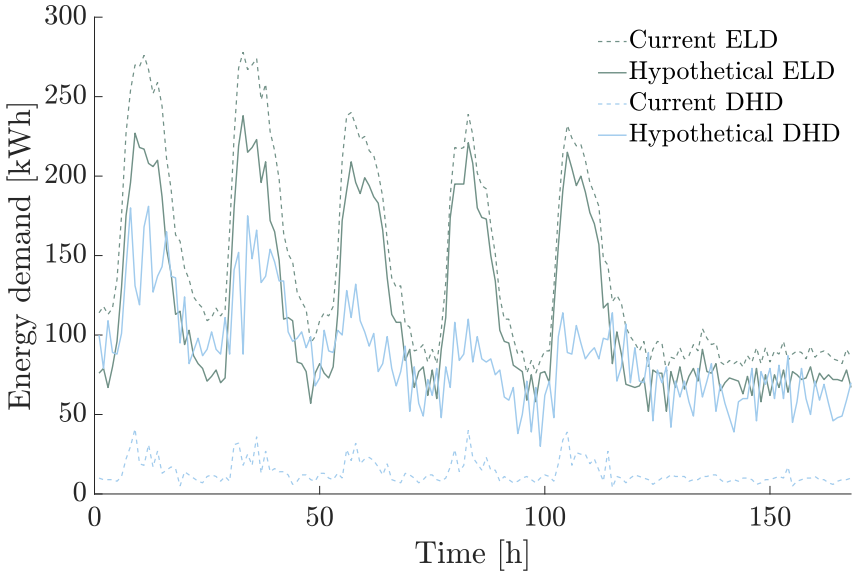

(d) *One week in December.*

Figure 7.3: *Peak-shaving potential with Sector Coupling for each season.*

Table 7.6 shows characteristics of the figures above and visualises changes in total energy demand and powers peaks. The ELD and DHD changed the most in December, DHD increased by about 84 %, and ELD dropped almost 20 %.

Table 7.5: *Monthly values for electricity and district heating demand, when using sector coupling*

Month	Version	What	Mean [kWh/h]	Minimum [kWh/h]	Maximum [kWp]	Sum [kWh/week]
March	I	EL	120.49	66	226	20 243
	II	EL	106.21	56	213	17 843
	I	DH	10.738	4.0	31	1 804
	II	DH	56.690	15	134	9 524
June	I	EL	112.94	65	208	18 974
	II	EL	107.43	64	200	18 974
	I	DH	8.0179	0	24	1 347
	II	DH	8.0179	0	24	1 347
September	I	EL	114.61	62	225	19 225
	II	EL	112.82	59	224	18 954
	I	DH	9.0	2.0	24	1 512
	II	DH	15.071	2.0	49	2 532
December	I	EL	142.69	76	278	23 972
	II	EL	115.32	52	238	19 373
	I	DH	13.696	4.0	41	2 301
	II	DH	87.863	30	181	14 761

I = current
II = hypothetical

Table 7.6 demonstrates how EL and DH demands and peaks would change if this simulation was applied to the whole year. It is clear that there is a dramatic increase in DHD, and the ELD is reduced by five percent. The electricity peak is also reduced noticeably. The relation between the rise in DHD and the decline in ELD corresponds with the theory and the COP presented in Table 4.4.

Table 7.6: *Yearly changes in EL and DH demand and peak value, using sector coupling*

Version	Yearly electricity demand [kWh/yr]	Yearly DH demand [kWh/yr]	Electricity peak [kWp]	DH peak [kWp]
I	853 250	63 842	278	41
II	806 840	214 300	248	181
Difference	- 46 410	+ 150 458	- 30	+140

The limitations of the existing DH systems should be considered when deciding whether a DHD of this size is realistic. If the DH system has to be expanded to account for the increase in demand, it is unclear if the five percent decrease in ELD is worth the cost, as these procedures are pretty expensive. However, an advantage this method holds over the two other presented is that by not changing the time of consumption, there are fewer losses, which again contributes to lower demand.

To not cause such a high DHD, it is possible to combine the presented methods where DH takes more of the load, but the heat pump is still in use. In this case, the time of occurrence for peaks in both the EL and DH grid should be researched to find a cost minimising solution that works around these peaks.

Figure 7.3 shows that the energy input for the same amount of heating output is significantly lower when using the HP, making it a lucrative option when the EL prices are low. However, as the system moves towards becoming a PEB, it has to lower its ELD. Not using the HP is a step in that direction since it is one of the only EL-consuming components that the building owner can control.

7.4 Comparison of the Simulations

Table 7.7 sums up the impact the TABS, and HP simulation had on the system in SLV 17B.

Table 7.7: *Yearly change in energy demand and electricity peaks for the TABS and HP simulations*

Simulation	Change in energy demand	Power peak reduction
1 TABS	+ 0.5 %	- 11 %
2 Heat pump	+ 0.2 %	- 12 %

The difference between the two simulations in Table 7.7 is relatively small. The HP simulation has a slightly lower increase in energy demand and a somewhat higher peak reduction than the TABS simulation. However, the methods used in the simulations were reasonably similar, and therefore the small difference makes sense.

Table 7.8 shows the impact the sector coupling simulation had on the system. The changes in EL peaks are similar for all the simulations. The changes are most noticeable in Table 7.8 due to the large increase in DH. The smallest peak is achieved with the heat pump simulation, but the most even curve is achieved during December with the TABS simulation. This can be seen in Figure 7.1d.

Table 7.8: *Yearly change in electricity and district heating demand and peaks for the sector coupling simulation*

Simulation	Change in ELD	Change in DHD	Chang in EL peak	Change in DH peak
3 Sector coupling	- 5 %	+ 235 %	- 11 %	+ 340 %

The implementation of peak shaving measures does not have to be limited to one of the mentioned simulations. A combination of the three could be used. For example, heat could be distributed to the TABS at night (20:00 to 05:00), and a profitable mix of electricity use for the HP and DHD could be found. This way, the increase in DHD would not be as massive as the one presented in Table 7.8 but the system would still get some the benefits of peak shaving presented in Table 7.7.

8 Future Aspects

This section contains estimations on PV production and calculations regarding whether the planned development of the project will reach PEB requirements or not. Additional power production with PV panels is scheduled to be installed at SLV 11, 13 and 17B soon. Therefore, the future potential and the gap between the current, future and required production are presented and discussed.

Other measures for reaching the requirements for becoming a PEB, such as controlling the demand by moving heating loads, utilising more district heating, connecting Sluppen to other systems and sector coupling, are also discussed.

8.1 PV Production

Figure 8.1 shows the existing PV production at SLV 19 and Rye, along with the estimated future potential from PV panels scheduled to be installed at SLV 17B and 11.

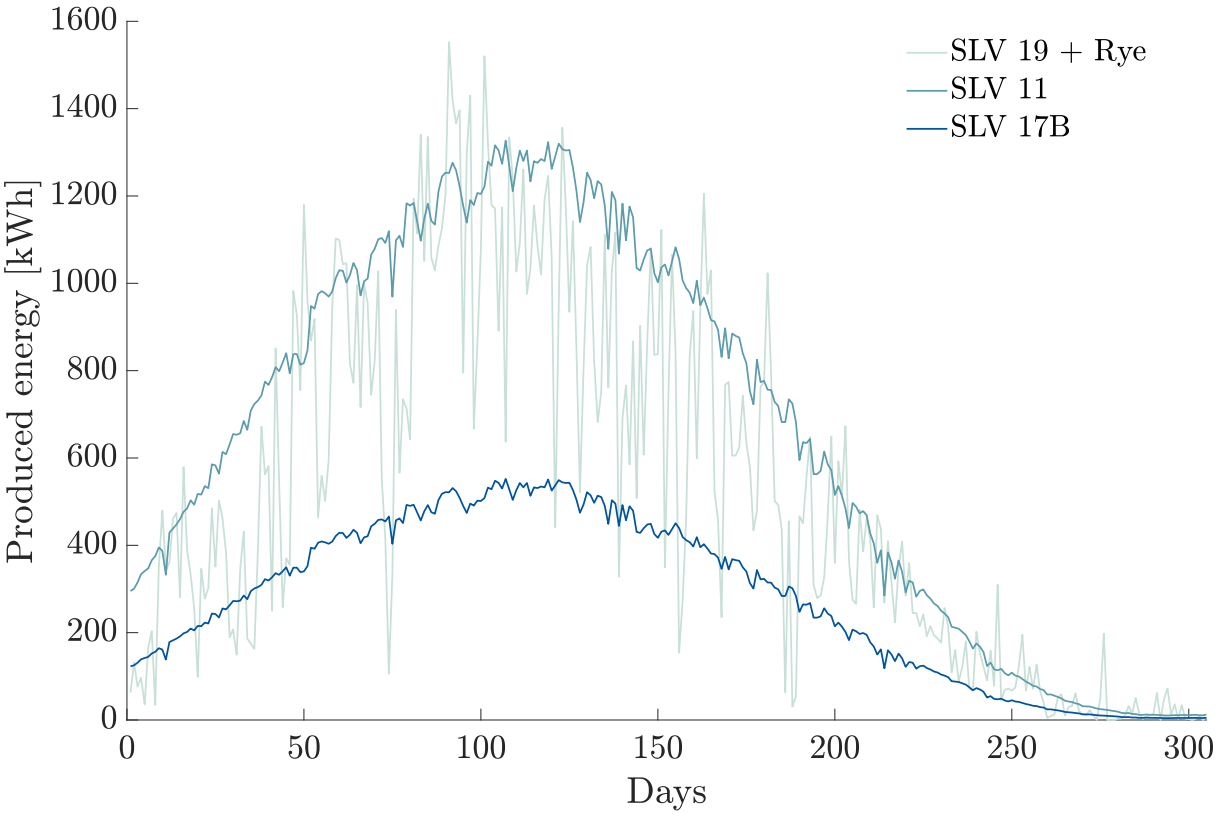

Figure 8.1: *Existing PV production from SLV19 & Rye, and estimated production for the scheduled panels at SLV 17B and 11.*

The production in Figure 8.1 matches the shape of the theoretical curve presented in Figure 2.21. The existing production at SLV 19 and Rye experiences numerous daily variations. As expected, PV production is low in months with few daylight hours and high in months with more. Weather conditions, shadows on the panels, meter errors, or data errors can all cause considerable daily variations in PV production. PV production is directly related to the amount of sunlight available and cloudy, rainy, and snowy days thereby directly impacting production. SLV 19 and Rye have, in total, four sensitive meters that can malfunction and fail to register the correct production.

The SLV 19 and Rye data measurements have varying resolutions on the meters. Consequently, errors could have occurred during the conversion from data every couple of seconds to data every hour, and during the merging of the two data sets. MatLab may also have contributed to errors in the data sets used for simulations in the form of import or code errors.

The estimated production for SLV 11 and 17B is calculated with Equation 2.20, with irradiance data from NASA and the efficiency of the PV panels at SLV 19 presented in Section 4.2.2. This simplified equation does not consider the weather conditions, tilt and orientation, shadows cast by dust or nearby structures, or other losses. The potential displayed in Figure 8.1 is significantly higher at SLV 11 because the building has a larger roof area than 17B. The total yearly estimated PV production equals 442 280 kWh. In reality, the PV output will be lower than estimated.

Figure 8.2a shows the total estimated production from the existing and planned PV panels at the PEB plotted with the total electricity demand. The net electricity demand equals the difference between the electricity demand and total production. Solar energy is produced throughout the whole year, including some in December. The yearly electricity consumption for the buildings equals 1 997 300 kWh from March to December, which means the planned, estimated electricity production only covers about 22 % of the consumption. There is a noticeable reduction in ELD during the summer when using solar energy, but the system does not at any hour deliver surplus energy to the grid. However, the production at SLV 17B does cover the electricity consumption of the HP. There was no data available for the HPs at SLV 11 & 13 and 19, but assuming the PV production does cover the electricity consumption of the HP for the other buildings as well, the buildings will, based on what is presented in Section 2.2.2, qualify as a ZEB-O-EQ.

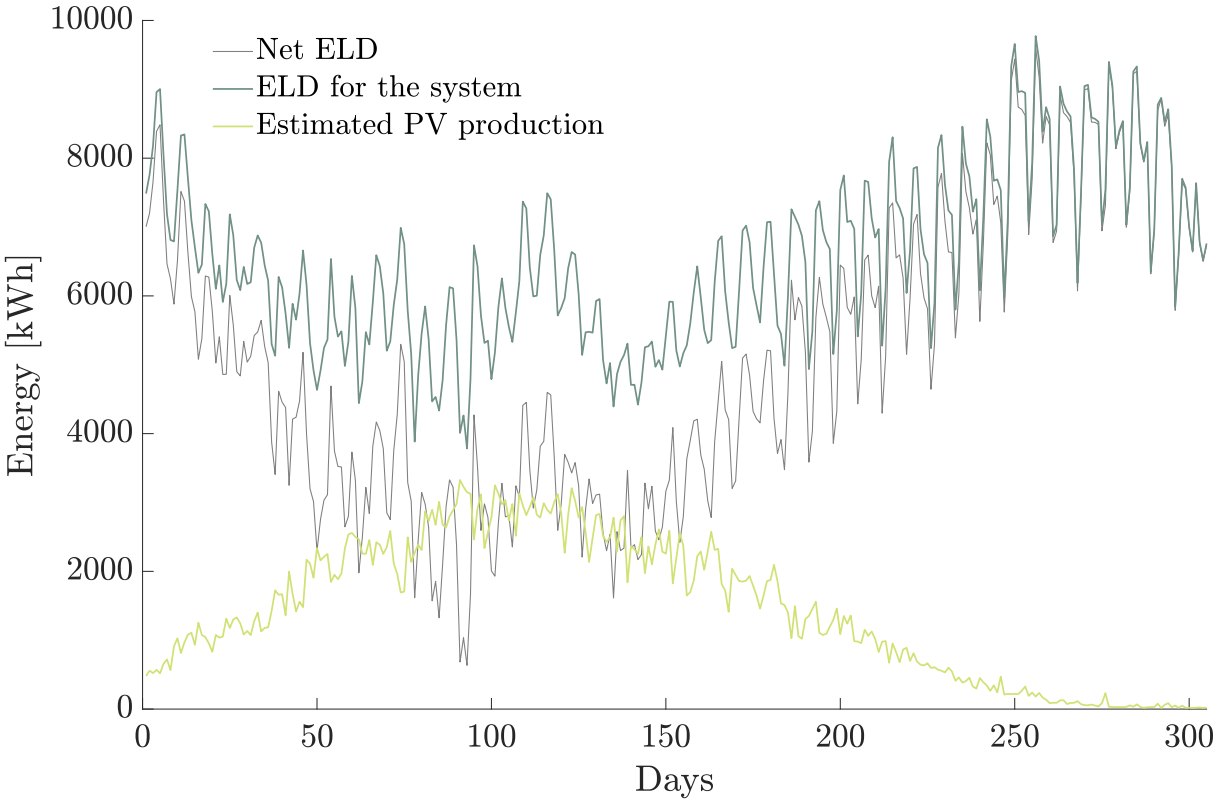

(a) *Estimated future solar production and current electricity demand.*

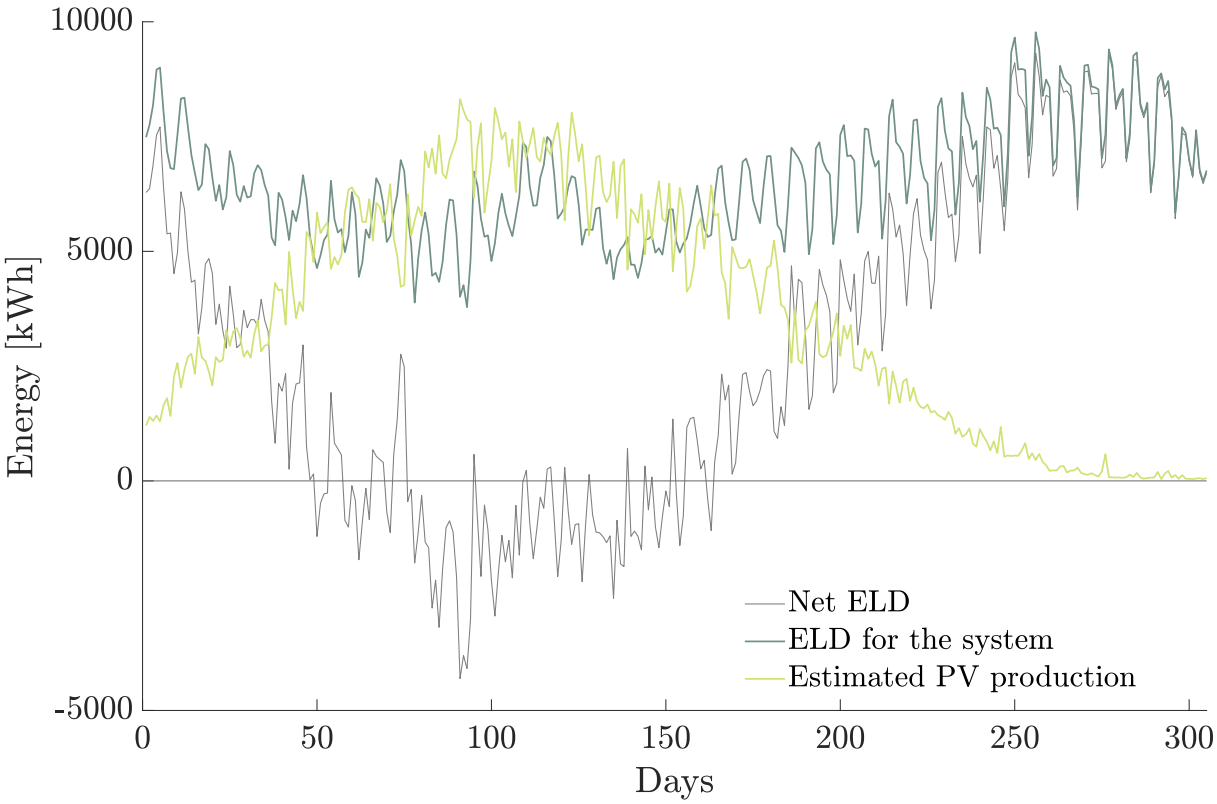

(b) *Estimated solar production scaled (×2.5) and current electricity demand.*

Figure 8.2: *ELD plotted with estimated PV production. The net ELD equals the difference between them.*

Figure 8.2b shows a production 2.5 times bigger than the planned production, which is enough to cover 55 % of the consumption. With a production of 1 105 700 kWh, there are about 100 days during the summer when the system produces surplus energy. To cover 55 % of consumption, a substantial increase in production or decrease in electricity consumption must take place in addition to what is planned. However, the production and consumption patterns are not equal and require ESS and new production methods to balance them.

During the day, two of the buildings have a high ELD which is used for electrical equipment. In Figure 6.4 the net electricity use represents the electricity used for other purposes than heating, which accounts for the majority of consumption. Other energy forms cannot meet these demands, and therefore they must be met by the local production to meet PEB requirements. Unlike the heating demand that can be covered by district heating. Although the pattern of the daily PV production (Figure 2.21) and daily consumption in an office building (Figure 2.2b) overlap, they do not overlap throughout the whole year. In the months when demand is high, solar production is low. As a result, to become a true PEB, the production pattern needs to change.

On the production side, PV panels are installed or scheduled to be installed on the roofs of all buildings. However, this production is not enough to cover the consumption. PV panels can also be installed on the facade to cover more of the consumption, but considering the position of the buildings, shadows will prevent optimal production conditions. PV panels on the facade will barley contribute to a change in the production pattern, and will mostly just increasing production during the summer. An installation of batteries or a long term energy

storage system can help change when self-produced energy is available. Other power-generating options should be explored to ensure production during winter, spring and autumn. Further development of energy production means that the buildings have to be able to share surplus energy with each other, as described in Section 2.1.4. Since the demand profile varies within the buildings, sharing energy would be a good solution. Aside from the surfaces of the buildings, there is hardly any available area at the site for energy production. Therefore, a solution could be to produce energy in a nearby location and transfer the energy to the site, as with Rye's solar production.

8.2 District Heating

District heating is used in all the heating systems at SLV 17B, including the TABS, ventilation systems and tap water, as seen in the system description (Chapter 4.1). It is mainly used for heating tap water and occasionally contributes to peak heating loads. DH is considered to be a key asset to realise the energy transition from linear to a smart integrated renewable energy system, as illustrated in Figure 2.24, so that Europe can reach the goal of being climate neutral by 2050.

DH in Trondheim mainly originates from waste incineration, which is often not viewed as renewable because of the connected emissions. Nevertheless, as mentioned in Section 2.8 the EU considers district heating to be a renewable source. DH contributes to the circular economy and is, according to the *Waste Framework Directive* created as a guideline by the EU, a better option than other ways of waste disposal and contributes to reducing emissions.

Electric energy has a higher energy quality than thermal energy. Some argue that thermal energy rather than electricity should be used for heating to save high-quality energy for uses where it is necessary. Waterborne heating solutions increase supply security when electricity demands are high, since DH decreases the ELD by covering heating demands. Heat pumps can produce more energy than they consume and are often economically profitable compared to DH in areas with low EL prices. It is however, possible to switch sources used for heating based on grid demand, known as sector coupling, which can help reduce energy costs and the load on the main grid.

District heating has to have three key elements to be competitive; market demands, pipes network, and cheap heating sources. Trondheim has a growing demand for district heating, and the infrastructure is constantly expanding. The demand for local resources increases when trying to lower electrical peak demands and is a crucial element for future innovative energy systems and beneficial for district heating. However, the pricing strategy for district heating indicates a competitive disadvantage. To improve the profitability of the sector coupling, an alternation of this price strategy may have to take place.

8.3 Further Research on TABS

The peak-shaving potential for TABS comes from the thermal lag in the concrete thermal mass. The exact value for the thermal lag depends on the thickness of the concrete floor and the operating conditions of each system. Further research should develop a model for this specific TAB system with the following control strategies. In the literature review, Section 3, it was stated that simple models have good accuracy in this context. However, these models were constructed for cooling demands and not heating demands. Therefore, simpler TABS models

may not have the same accuracy on heating. More research should be done on systems like Sluppen to ensure a reliable model. The most common control strategy, change in supply temperature and flow rate, is also used at Sluppen. However, more advanced strategies could be developed, but they demand having qualified personnel controlling the systems.

Another interesting data measure is the room temperature in 17B. No data for such temperatures were available, so it is unclear if the temperature will hold sufficiently throughout the day with the implementation of the simulations or not. As mentioned in Section 3, Michalak also experienced significant temperature variations within the room, which could be caused by less thermal mass. However, it would be interesting to review this kind of data to optimise the simulation for SLV 17B further. Temperature data would also create the opportunity to conduct further and more accurate flexibility analysis.

Although the technical chief in 2016 stated that three days went by before temperature complaints began when turning off the TABS, this is not a suggested strategy. Because of the long thermal lag, if the TABS are turned off for an extended period, it will take an equal amount of time to heat them again.

It could also be interesting to survey the employees in the buildings about the temperature, such as Namai did. However, the expectations for the environment may differ from the owners to the tenants. The owners may desire to cut costs by decreasing the temperature, while tenants want increased thermal comfort.

In the future, it would be worth developing a relationship with the owners of the other TABS buildings in Norway, for example, the passive office building in Tromsø, to share future experiences.

9 Potential Sources of Error

This section presents potential project errors that need to be considered when analysing and using the results. Furthermore, the purpose of this section is to reflect on the method implemented to get the results shown in Section 6.

Case Sluppen: System Definition

Being a part of the European +CityxChange project and focusing on technological development and utilising the local resources, many stakeholders are involved. When waiting for system descriptions and clarification regarding missing data, it would have been advantageous with a longer time frame since these tings tend to take time. The defining of Case Sluppen, Section 4, may consist of human errors as system descriptions and drawings can be challenging to comprehend for an untrained eye. The simplifications may therefore be a bit too extensive. The system for SLV 17B was facilitated in the flowchart in Figure 5.1. Although Figure 5.1 may not accurately describe all the components, these simplifications were made to conduct the simulations and may have caused errors in the results. All the received datasheet information about the components has not been used directly in the simulation but is valuable for further work. The repercussions from these errors become particularly clear in the estimated TABS matrix, which was calculated based on Figure 5.1.

Data Selection and Treatment

As mentioned in Section 5, the raw data had to go through data processing which made assumptions and estimations to make the data usable. This, of course, causes the data to be less realistic. Due to missing data from January and February in some meters, all data was adjusted to contain data from March to December. This time frame definition has most likely affected the results. As seen in Figure 2.4, January and February are months with high consumption and not including them resulted in an artificially low ELD and DHD. This data would have made the results more realistic, the values presented would be higher, and the change from the simulations would probably be more prominent.

For some short periods, for instance, during Easter, the meters did not register data. When measurements returned, the first hour of measurement showed a super peak. This super peak happened multiple times during a year and was investigated by reading papers and asking questions to professors and the industry. At first, it was suggested that it could be the starting current in components which can be high, or the SD-program as mentioned in 5.1 being sensitive once starting up. Based on this knowledge, the super peaks and other outliers were deleted, and the value after this hour-index was copied. At the end of this project, it was suggested that the SD system accumulated consumption for the entire period when there was a lapse. There was no time to take this information into consideration, but it is valuable to look into for further research.

At the beginning of the project, there were interface errors. MatLab was not importing data correctly, which resulted in a lot of **NaN***: Not a Number* values in the sheet. This was due to how MatLab imported the data but was resolved by using a different importing-data-code. However, the alternative import method made assumptions about the missing values, which may not accurately reflect reality. It can be assumed that a similar misinterpretation of data

could have happened due to the limited time on the project. Moreover, because of the size of the system, it is difficult to obtain a complete overview in the given timeframe.

It would have been an advantage to further check for missing values and categorical data. A moreover execute of statistically analyses for the raw data is recommended. For example doing an correlation analyse for the weather data, and how sensitive the used data is.

All the matrices were made to have an hourly resolution which does not translate particularly well to visual plots. Therefore, the resolution was changed by summing or calculating the average values as desired, often changing to a daily or weekly resolution. This process generalises the trends in the graphs to make them easier to read, but makes the curves less exact, which may led to false trends and thereby misinterpretation of the results. The function used for this process could probably be improved.

Base Case Definition

The national covid-lockdowns and the general recommendation to work from home could have influenced the data in March 2020, autumn 2020, spring 2021, and winter 2021. Periods of absence could have made energy demand artificially low. Data from the sub-meters were only available for 2021. It was difficult to determine how these data would have looked without covid. Based on the data from the main meter, it can be assumed that covid lowered the energy demands, but how it affected the local trends remain undetermined.

The data collected from the meter at SLV 19 was recorded from September 2019 to August 2020. When this was manipulated to match the other data, it was no longer specific to one year, implying that irradiation and temperature data from neither 2019 nor 2020 would match the SLV 19 meter. This affects, as Figure 5.1 displays, both the PV production and electricity demand for SLV 19. ELD from SLV 19 is displayed in Figure 6.2 together with ELD and DHD for the other buildings from 2021. This comparison is not realistic is the data is collected for different years, and data for ELD from SLV 19 should be obtained from the main meter for further development of the project.

Table 6.1 shows a discolouration between the yearly values presented in the table and the data used for calculations, especially for SLV 11 & 13. There is most likely an error in one of the meters which need to be resolved.

Simulations

The seasonal calculations were performed for a week, and the load shifting was done based on set time intervals. As electricity and heating demand depends heavily on the weather, the calculations may not represent other weeks in the same season or the same week in a different year since the weather can be inconsistent. Therefore, the yearly calculations are more descriptive than the weekly ones, as they iterate the change for each week. However, the time intervals are kept constant throughout the whole year. They do not consider periods of absence, public holidays, or variations in the length of the workday, which reduces the accuracy of the yearly results.

The matrix containing the estimation of heat delivered to the TABS contained negative values. These originate from the energy balance and prove that it is incorrect since *energy in* $\neq$ *energy out*. This reduces the accuracy of the TABS simulation further. The energy delivered to the TABS should be measured at the sub-meter to rightfully depict the system.

Solar production will affect the ELD, especially during summer, but is not considered in the simulations. Regulations currently prevent sharing self produced power after desire, and SLV 17B does not have its production. As PV panels are installed on SLV 17B or surplus energy can be shared within the system, the simulations should be modified. These modifications will lower the ELD but will not affect DHD.

Future aspects

The solar production estimations are simple calculations that do not include tilt or orientation. The actual production will probably share the shape of the estimated curves in Figure 8.1 but have the same variation pattern as the *SLV 19 + Rye* curve. The total yearly production will probably be lower, due to these variations and losses who the estimated curves does not take into account.

The production profile has multiple sources of error, one of them being the production from SLV 19 mentioned earlier. The rest of the production profile consists of data from the Rye microgrid. As mentioned in the methodology (Section 5), this data was manipulated to match the other datasets. This process may have wrongfully depicted some values, as the processed file had missing values and was completed with estimations which may not reflect reality. The two PV production matrices were merged, and the production profile held one matrix with data from different locations with different irradiation. Since the PV panels will stay at Rye, this was considered the best way to represent the production.

More data should be included in the simulations to improve the results. It is hard to predict how the different simulations will affect the system in the future based solely on one year of data. Temperature data should also be included to optimise the simulations further. Access to temperature data in the building would make especially the TABS simulation more accurate and presents an opportunity for further flexibility analysis on the TABS. More senors would also increase the reliability of the data and the precision of the results.

Other errors can be measurement errors in the meters, systematic errors, scientific notation and measuring sensitivity. The simulations could also be improved by including an in-depth building model, the number of building users and how this varies, air quality, and temperature. Another program for data treatment could have been used to more satisfactorily read the data without losing parts of it to **NaN**. The limitations of the thesis may have led to misinterpretation of the results.

10 Conclusion

The current system at Sluppen produces an insufficient amount of power to be qualified as a PEB. The heat pump covers most of the heating demand, while district heating is mainly used for tap water and peak heating demands. SLV 17B and 19 have relatively low demand for district heating and high electricity use as a result of this. SLV 11 & 13 have high demand because they are old buildings with a different consumption pattern than the office buildings, SLV 17B and 19. In 17B, the TABS uses 57 % of all thermal energy entering the system. Currently, there are no known measures in the system to take advantage of the thermal lag and peak shaving potential of the TABS.

The TABS simulation revealed numerous opportunities to reduce the power peaks with a smarter control of the TABS. The supply temperature during the night must be higher with this approach to ensure thermal comfort throughout the day. This simulation was based on theoretical methods and therefore had no guarantee of being representative of reality.

The heat pump simulation gave approximately the same results as the TABS simulation because of the dependency on the smart use of TABS. This option moves the electricity use of the heat pump to the night, thereby cutting electricity costs and preserving the local power grid.

The sector coupling simulation had the most potential for reducing electricity consumption. However, the total energy demand, the sum of electricity and heat energy, increases because of the heat pump's high efficiency, which requires over three times less energy than the district heating to cover the same demand. This significant increase in district heating is good for reducing electricity and the circular economy but is less profitable and could require development of the district heating grid. This simulation strategy could be used in combination with the others.

Currently, the Sluppen area does not appear to be qualified as a PEB. The existing and currently planned solar panels do not produce enough energy to cover the demands of the buildings, and the yearly consumption pattern does not fit the production pattern. Norwegian laws prohibit the sharing of surplus energy between the buildings, which is an obstacle on the way to reaching PEB requirements.

References

[1] +CityxChange. *About +CityxChange*. +CityxChange, Apr. 2020. URL: https://cityxchange.eu/about-cityxchange/ (visited on 04/11/2022).

[2] +CityxChange. *Trondheim*. +CityxChange, Jan. 2021. URL: https://cityxchange.eu/our-cities/trondheim-norwegian/ (visited on 04/11/2022).

[3] Kjeldsberg. *Sluppen*. Sluppen, Dec. 2021. URL: https://www.sluppen.no/ (visited on 02/10/2022).

[4] *Prosjekt Sluppen*. Trondheim kommune, 2021. URL: https://wwwqa.trondheim.kommune.no/aktuelt/om-kommunen/bk/barekraft/cxc/prosjekt-sluppen/ (visited on 05/12/2022).

[5] Klima- og miljødepartementet. *Klimaendringer og norsk klimapolitikk*. Regjeringen.no, Oct. 2021. URL: https://www.regjeringen.no/no/tema/klima-og-miljo/innsiktsartikler-klima-miljo/klimaendringer-og-norsk-klimapolitikk/id2636812/ (visited on 04/19/2022).

[6] Cathrine Hagem. *Figure 2: Illustration of the Scandinavian Nord Pool price areas with...* ResearchGate, Feb. 2018. URL: https://www.researchgate.net/figure/Illustration-of-the-Scandinavian-Nord-Pool-price-areas-with-external-trade-to_fig1_322911510 (visited on 04/27/2022).

[7] Olje- og energidepartementet. *Strømnettet - Energifakta Norge*. Energifakta Norge, Apr. 2019. URL: https://energifaktanorge.no/norsk-energiforsyning/kraftnett/ (visited on 05/07/2022).

[8] Trøndelag Fylkeskommune. *Klima og energi — Trøndelag i tall*. Trondelagitall.no, 2022. URL: https://trondelagitall.no/taxonomy/term/7 (visited on 04/20/2022).

[9] Norwegian Ministry of Petroleum and Energy. *Energy use by sector - Energifakta Norge*. Energifakta Norge, Aug. 2021. URL: https://energifaktanorge.no/en/norsk-energibruk/energibruken-i-ulike-sektorer/#service-industries (visited on 04/20/2022).

[10] Kein Huat Chua, Yun Seng Lim, and Stella Morris. "Energy Storage System for Peak Shaving". In: *International Journal of Energy Sector Management* 10 (Apr. 2016), pp. 3–18. DOI: 10.1108/ijesm-01-2015-0003. URL: https://bibsys-almaprimo.hosted.exlibrisgroup.com/primo-explore/openurl?url_ver=Z39.88-2004%5C&url_ctx_fmt=info:ofi%5C%2Ffmt:kev:mtx:ctx%5C&url_ctx_fmt=info:ofi%5C%2Ffmt:kev:mtx:ctx&url_tim=2022-04-26T12:37:37Z&rft.genre=article&rft_id=info:ofi%5C%2Fnam:urn:ISSN:1750-6220&rft_id=info:doi%5C%2F10.1108%5C%2FIJESM-01-2015-0003&rft.issn=1750-6220%5C&rft.atitle=Energy%5C%20storage%5C%20system%5C%20for%5C%20peak%5C%20shaving%5C&vid=NTNU_UB%5C&institution=NTNU_UB&url_ctx_val=%5C&isSerivcesPage=true (visited on 04/26/2022).

[11] Benedicte Langseth, Ingrid H. Magnussen, and Dag Spilde. *Energibruksrapporten 2013*. NVE, 2014. URL: https://publikasjoner.nve.no/rapport/2014/rapport2014_11.pdf (visited on 05/07/2022).

[12] David Roberts. *Renewable Energy and the Power Grid*. Vox, Aug. 2019. URL: https://www.vox.com/energy-and-environment/2019/8/7/20754430/renewable-energy-clean-electricity-grid-load-flexibility (visited on 01/14/2020).

[13] Jerzy Mikulik. *Energy Demand Patterns in an Office Building: a Case Study in Kraków (Southern Poland)*. July 2018.

[14] Benedicte Langseth. *Analyse av energibruk i yrkesbygg - Formålsdeling, Trender og drivere*. 2016. URL: http://publikasjoner.nve.no/rapport/2016/rapport2016_24.pdf (visited on 04/18/2022).

[15] Øystein Døhl. *Temperaturens betydning for energiforbruket*. ResearchGate, Sept. 1999. URL: https://www.researchgate.net/publication/273064080_Temperaturens_betydning_for_energiforbruket (visited on 04/25/2022).

[16] NordPool. *View monthly consumption.* Nordpoolgroup.com, 2022. URL: https://www.nordpoolgroup.com/en/Market-data1/Power-system-data/Consumption1/Consumption/NO/Hourly1111/?view=chart (visited on 04/25/2022).

[17] Meteorologisk institutt. *Historiske værdata for Trondheim*. Yr, 2021. URL: https://www.yr.no/nb/historikk/graf/1-211102/Norge/Tr%C3%B8ndelag/Trondheim/Trondheim (visited on 04/25/2022).

[18] *Historiske strømpriser*. LOS, 2022. URL: https://www.los.no/dagens-strompris/historiske-strompriser/ (visited on 04/27/2022).

[19] Eiliv Flakne. *Tenker nytt i utnyttelsen av strømnettet*. Mynewsdesk, June 28. URL: https://presse.enova.no/news/tenker-nytt-i-utnyttelsen-av-stroemnettet-248899 (visited on 05/09/2022).

[20] Knut Hofstad. *Kostnader ved produksjon av kraft og varme*. 2011. URL: https://publikasjoner.nve.no/haandbok/2011/haandbok2011_01.pdf.

[21] Raquel S. Jorge and Edgar G. Hertwich. "Environmental Evaluation of Power Transmission in Norway". In: *Applied Energy* 101 (Jan. 2013), pp. 513–520. DOI: 10.1016/j.apenergy.2012.06.004. (Visited on 04/25/2022).

[22] Stig Haugen et al. *Opprustning av kraftnettet for å redusere energitapet*. Ed. by Stig Haugen. Feb. 2004. (Visited on 04/25/2022).

[23] Trond Bjørnenak. *Forbrukerfleksibilitet: Et alternativ til nettinvesteringer?* 2018. URL: https://uia.brage.unit.no/uia-xmlui/bitstream/handle/11250/2566814/Baretto%5C%20Stian%5C%20Tveiten.pdf?sequence=1%5C&isAllowed=y%5C&fbclid=IwAR3y13NKpQGUgNmM7uur-Q5OOaaNASSalDyuO87ZuAZsJ26Ste6wAOnBZ04.

[24] Axel Gautier, Julien Jacqmin, and Jean-Christophe Poudou. "The Prosumers and the Grid". In: *Journal of Regulatory Economics* 53 (Jan. 2018), pp. 100–126. DOI: 10.1007/s11149-018-9350-5. (Visited on 05/03/2022).

[25] *Plusskunder - NVE*. www.nve.no, Dec. 2021. URL: https://www.nve.no/reguleringsmyndigheten/regulering/nettvirksomhet/nettleie/tariffer-for-produksjon/plusskunder/ (visited on 04/25/2022).

[26] Solenergiklyngen. *Hvordan kan solenergi bidra til å løse kraftkrisen?* www.youtube.com, Feb. 2022. URL: https://www.youtube.com/watch?v=jw-3IPyzUh0 (visited on 04/25/2022).

[27] Solenergiklyngen. *Dispensasjon for lokal deling av strøm i +CityxChange prosjektet – Solenergiklyngen The Norwegian Solar Energy Cluster:* Solenergiklyngen.no, Mar. 2022. URL: https://www.solenergiklyngen.no/2022/03/30/dispensasjon-for-lokal-deling-av-strom-i-cityxchange-prosjektet/ (visited on 05/13/2022).

[28] Jean-Pascal Tricoire. *Buildings are the Foundation of our Energy-Efficient Future*. World Economic Forum, Feb. 2021. URL: https://www.weforum.org/agenda/2021/02/why-the-buildings-of-the-future-are-key-to-an-efficient-energy-ecosystem/ (visited on 04/25/2022).

[29] Ragni Mikalsen et al. *Energieffektive bygg og brannsikkerhet*. Feb. 2019. URL: https://www.dsb.no/globalassets/dokumenter/rapporter/andre-rapporter/rise-rapport-2019_2-energieffektive-bygg-og-brannsikkerhet.cleaned.pdf.

[30] Passipedia - The Passive House Resource. *What is a Passive House?* Passipedia.org, Aug. 2020. URL: https://passipedia.org/basics/what_is_a_passive_house (visited on 03/29/2022).

[31] Standard Norge. *NS3701 Criteria for Passive Houses and Low Energy Buildings Non-residential buildings*. Sept. 2021.

[32] Forbrukerrådet and Meteorologisk institutt. *Norske årsmiddeltemperaturer: I alfabetisk rekkefølge*. 2015. URL: https://fil.forbrukerradet.no/wp-content/uploads/2015/11/VP_2015_%5C%C3%5C%85rsmiddel_Alfabetisk.pdf (visited on 05/03/2022).

[33] *Byggteknisk forskrift (TEK17)*. Dibk.no, 2022. URL: https://dibk.no/regelverk/byggteknisk-forskrift-tek17/ (visited on 03/28/2022).

[34] *A Norwegian ZEB-definition Embodied Emission*. ZEB Project. Sintef Academic Press, Norwegian University of Science and Technology, 2014. URL: https://ntnuopen.ntnu.no/ntnu-xmlui/bitstream/handle/11250/2388249/ZEB+rapport_no_17.pdf?sequence=3 (visited on 03/29/2022).

[35] Kaja Nordby. *Plusshus*. ZERO, Sept. 2009. URL: https://zero.no/wp-content/uploads/2016/05/plusshus.pdf (visited on 03/30/2022).

[36] *Positive Energy Block (PEB) - +CityxChange*. +CityxChange, Dec. 2020. URL: https://cityxchange.eu/knowledge-base/positive-energy-block-peb/ (visited on 03/30/2022).

[37] Frank P Incropera. *Fundamentals of Heat and Mass Transfer*. 6th. Wiley, 2013, pp. 1–13.

[38] Ibrahim Dinçer and Marc Rosen. *Thermal Energy Storage: Systems and Applications*. Second. John Wiley and Sons Ltd, 2011, pp. 32–42.

[39] Jacob J. Lamb and Bruno G. Pollet, eds. *Energy-Smart Buildings*. IOP Publishing, 2020, pp. 2.1–2.10.

[40] *What is buoyant force?* Khanacademy.org, 2022. URL: https://www.khanacademy.org/science/physics/fluids/buoyant-force-and-archimedes-principle/a/buoyant-force-and-archimedes-principle-article (visited on 04/25/2022).

[41] Merriam-Webster. *Merriam-Webster Dictionary*. Merriam-webster.com, 2022. URL: https://www.merriam-webster.com/dictionary/sensible%5C%20heat (visited on 03/28/2022).

[42] Merriam-Webster. *Merriam-Webster Dictionary*. Merriam-webster.com, 2021. URL: https://www.merriam-webster.com/dictionary/latent%5C%20heat (visited on 03/28/2022).

[43] Ioan Sarbu and Calin Sebarchievici. "A Comprehensive Review of Thermal Energy Storage". In: *Sustainability* 10 (Jan. 2018), p. 191. DOI: 10.3390/su10010191. URL: https://www.mdpi.com/2071-1050/10/1/191 (visited on 03/28/2022).

[44] Alvaro de Gracia and Luisa F. Cabeza. "Phase Change Materials and Thermal Energy Storage for Buildings". In: *Energy and Buildings* 103 (Sept. 2015), pp. 414–419. DOI: 10.1016/j.enbuild.2015.06.007. (Visited on 03/28/2022).

[45] Ahmet Akta and Yağmur Kirçiçek. *Solar Hybrid Systems : Design and Application*. Academic Press, an Imprint of Elsevier, Cop, 2021, Chapter 6 –Solar Thermal Systems and Thermal Storage. URL: https://www.sciencedirect.com/topics/engineering/thermal-energy-storage-system.

[46] *Sensible Heat*. Otherlab. URL: https://www.otherlab.com/sensible-heat (visited on 04/27/2022).

[47] Alexis Sevault. *What Are Phase Change Materials?* SINTEFblog, Aug. 2018. URL: https://blog.sintef.com/sintefenergy/energy-efficiency/phase-change-materials-pcm/.

[48] Depeng Kong et al. "A Novel Battery Thermal Management System Coupling with PCM and Optimized Controllable Liquid Cooling for Different Ambient Temperatures". In: *Energy Conversion and Management* 204 (Jan. 2020), p. 112280. DOI: 10.1016/j.enconman.2019.112280. (Visited on 04/28/2022).

[49] Chris Reardon, Caitlin McGee, and Geoff Milne. *Thermal mass — YourHome*. Yourhome.gov.au, 2013. URL: https://www.yourhome.gov.au/passive-design/thermal-mass (visited on 04/26/2022).

[50] Gohar Gholamibozanjani and Mohammed Farid. "A Comparison between Passive and Active PCM Systems Applied to Buildings". In: *Renewable Energy* 162 (Dec. 2020), pp. 112–123. DOI: 10.1016/j.renene.2020.08.007. (Visited on 04/01/2022).

[51] Gunrid Kjellmark, Matthias Haase, and Anders Homb. *Utnyttelse av termiske egenskaper i betong for redusert energibruk*. Brekkestrand.no, May 2018. URL: https://brekkestrand.no/betong-og-miljo/ (visited on 04/26/2022).

[52] Jae-Han Lim, Jin-Hee Song, and Seung-Yeong Song. "Development of Operational Guidelines for Thermally Activated Building Systems According to Heating and Cooling Load Characteristics". In: *Applied Energy* 126 (Aug. 2014), pp. 123–135. DOI: 10.1016/j.apenergy.2014.03.087. URL: https://www.sciencedirect.com/science/article/pii/S0306261914003274?casa_token=GH3PFfOuTZkAAAAA:vtysP8f3SF1LxvQi6mGcDeu7KJZAoXG0nqzvsCQW7xmn1pvWyZfSX_4ct4Xy79Zz2cknWbfsuls (visited on 04/08/2022).

[53] Robert Cubick. *The Benefits of Thermally Active Building Systems - Uponor Blog*. Uponor Blog, Feb. 2017. URL: https://web.uponor.hk/radiant-cooling-blog/the-benefits-of-thermally-active-building-systems/ (visited on 04/08/2022).

[54] Green Energy Solution. *The Working Principle Heat Pumps — Green Energy Solutions*. Green Energy Solution. URL: https://greenenergysolution.org/en/heat-pumps-en/working-principle/.

[55] Håvard Karoliussen. *Varmepumper, Bruk av Mollier diagram*. 2020.

[56] *Experimental Analysis of a Multi-Purpose Refrigerator System*. G.L Bajaj Institute of Technology and Management. Department of Mechanical Engineering, May 2018. URL: https://www.researchgate.net/publication/324908978_Experimental_Analysis_of_A_Multi-Purpose_Refrigerator_System.

[57] Thomas Leypoldt Marthinsen. *COP Og SCOP - Helt Enkelt Forklart*. tjenestetorget.no, May 2019. URL: https://tjenestetorget.no/blogg/cop-scop-enkelt-forklart#cop-varmefaktor.

[58] *ESEER Explained: European Seasonal Energy Efficiency Ratio*. LearnMetrics, Mar. 2022. URL: https://learnmetrics.com/eseer-european-seasonal-energy-efficiency-ratio/ (visited on 05/14/2022).

[59] *Heat Pump Energy Ratings Explained* -. McWilliams & Son, Feb. 2016. URL: https://www.mcwilliamsandson.com/blogs/heat-pump-energy-ratings-explained (visited on 05/14/2022).

[60] E.M. Ishiyama, W.R. Paterson, and D.I. Wilson. "Thermo-hydraulic channelling in parallel heat exchangers subject to fouling". In: *Chemical Engineering Science* 63 (July 2008), pp. 3400–3410. DOI: 10.1016/j.ces.2008.04.008. (Visited on 11/18/2019).

[61] Alireza Dehghani-Sanij and Mehdi N. Bahadori. "Chapter 3 - Artificial production of ice". In: *Ice-Houses*. Ed. by Alireza Dehghani-Sanij and Mehdi N. Bahadori. Academic Press, 2021, pp. 89–130. ISBN: 978-0-12-822275-1. DOI: https://doi.org/10.1016/B978-0-12-822275-1.00010-2. URL: https://www.sciencedirect.com/science/article/pii/B9780128222751000102.

[62] vijay. *Refrigerant Used in Heat Pumps and How to Choose It Wisely*. Aspiration Energy, Mar. 2021. URL: https://aspirationenergy.com/refrigerant-used-in-heat-pumps-and-how-to-choose-it-wisely/ (visited on 03/29/2022).

[63] A. Kayode Coker. "Chapter 17 - Refrigeration Systems". In: *Ludwig's Applied Process Design for Chemical and Petrochemical Plants (Fourth Edition)*. Ed. by A. Kayode Coker. Fourth Edition. Boston: Gulf Professional Publishing, 2015, pp. 623–727. ISBN: 978-0-7506-8524-5. DOI: https://doi.org/10.1016/B978-0-08-094242-1.00017-6. URL: https://www.sciencedirect.com/science/article/pii/B9780080942421000176.

[64] G.F. Hundy, A.R. Trott, and T.C. Welch. "Chapter 3 - Refrigerants". In: *Refrigeration, Air Conditioning and Heat Pumps (Fifth Edition)*. Ed. by G.F. Hundy, A.R. Trott, and T.C. Welch. Fifth Edition. Butterworth-Heinemann, 2016, pp. 41–58. ISBN: 978-0-08-100647-4. DOI: https://doi.org/10.1016/B978-0-08-100647-4.00003-6. URL: https://www.sciencedirect.com/science/article/pii/B9780081006474000036.

[65] D.M. van de Bor and C.A. Infante Ferreira. "Quick selection of industrial heat pump types including the impact of thermodynamic losses". In: *Energy* 53 (May 2013), pp. 312–322. DOI: 10.1016/j.energy.2013.02.065. (Visited on 04/07/2022).

[66] De Kleijn Energy Consulting B.V. *Mechanical heat pump*. Industrialheatpumps.nl. URL: https://industrialheatpumps.nl/english/operating_principle/mechanical_heat_pump/.

[67] Attila Tamas Vekony. *Heat Pumps in UK: Types, Prices, Suppliers (2020) — GreenMatch*. www.greenmatch.co.uk, Mar. 2022. URL: https://www.greenmatch.co.uk/heat-pump.

[68] Elsevier Science. *Handbook of Energy Efficiency in Buildings - a Life Cycle Approach*. Ed. by Francesco Asdrubali and Umberto Desideri. www.sciencedirect.com, 2018. URL: https://www.sciencedirect.com/topics/engineering/photovoltaic-effect.

[69] Håvard Karoliussen and Tor Hennum. *Fornybar energi grunnkurs Solenergi*. 2019.

[70] Most efficient solar panels — Clean Energy Reviews. *Most Efficient Solar Panels 2022*. Clean Energy Reviews, Mar. 2019. URL: https://www.cleanenergyreviews.info/blog/most-efficient-solar-panels.

[71] Ian Lund. *Solar Production Over Time Graph*. SunCommon, Dec. 2019. URL: https://suncommon.com/a-guide-to-your-gmp-bill-with-solar/screen-shot-2019-12-18-at-2-05-48-pm/ (visited on 04/01/2022).

[72] Nicola Mihaylov et al. “Load Profile of Typical Residential Buildings in Bulgaria”. In: *IOP Conference Series: Earth and Environmental Science* 172 (June 2018), p. 012035. DOI: 10.1088/1755-1315/172/1/012035. (Visited on 04/01/2022).

[73] Sven Werner. *District Heating and Cooling*. Ed. by Cutler J. Cleveland. ScienceDirect, Jan. 2004. URL: https://www.sciencedirect.com/science/article/pii/B012176480X00214X (visited on 04/10/2022).

[74] *Directives Directive (EU) 2018/2001 of the European Parliament and of the Council of 11 December 2018 on the promotion of the use of energy from renewable sources (recast) (Text with EEA relevance)*. Dec. 2018. URL: https://eur-lex.europa.eu/legal-content/EN/TXT/PDF/?uri=CELEX:32018L2001%5C&from=EN (visited on 04/29/2022).

[75] *District heating*. Aug. 2010. URL: https://www.statkraft.no/globalassets/old-contains-the-old-folder-structure/documents/distirict-heating-10-eng_tcm9-10832.pdf (visited on 04/28/2022).

[76] *Fjernvarme – framtid eller fortid?* Energi og Natur, July 2021. URL: https://energiognatur.no/fjernvarme-framtid-eller-fortid/ (visited on 04/27/2022).

[77] Jingjing Song, Fredrik Wallin, and Hailong Li. “District heating cost fluctuation caused by price model shift”. In: *Applied Energy* 194 (May 2017), pp. 715–724. DOI: 10.1016/j.apenergy.2016.09.073. (Visited on 05/04/2021).

[78] Heidi Rapp Nilsen. *sirkulaer oekonomi“ Store norske leksikon*. Store norske leksikon, Mar. 2020. URL: https://snl.no/sirkul%C3%A6r_%C3%B8konomi.

[79] Svein Ove Slinde. *Fjernvarme: Urban energi*. www.statkraftvarme.no, 2018. URL: https://www.statkraftvarme.no/kunnskapssenter/nyheter/2019/fjernvarme-urban-energi/ (visited on 04/26/2022).

[80] Svein Ove Slinde. *Myteknusing: Å brenne avfall for å produsere fjernvarme er ikke klimavennlig*. www.statkraft.com, 2021. URL: https://www.statkraft.no/nyheter/nyheter-og-pressemeldinger/arkiv/2019/myteknusing-a-brenne-avfall-for-a-produsere-fjernvarme-er-ikke-klimavennlig/ (visited on 04/28/2022).

[81] Hailong Li et al. “A review of the pricing mechanisms for district heating systems”. In: *Renewable and Sustainable Energy Reviews* 42 (Feb. 2015), 56â€“65. DOI: 10.1016/j.rser.2014.10.003. URL: https://www.sciencedirect.com/science/article/pii/S136403211400820X?casa_token=K_p8D4pQ6-IAAAAA:APRt-9Uy2RwSgaFgkyau1m6MNUMj-Ak8m2cBz7Ffhmk1a5_rQERFs_wHp0C4LNq0dbg-MrEJ1dFY (visited on 05/01/2022).

[82] Hans M. Jordheim. *NVE vil ha ny pris for alle fjernvarmekunder*. e24.no, Nov. 2021. URL: https://e24.no/privatoekonomi/i/eEkrLg/nve-vil-ha-ny-pris-for-alle-fjernvarmekunder (visited on 05/10/2022).

[83] Statskraft Varme. *Fjernvarmetariff BT1V til næringskunder i Trondheim*. Statskraft Varme, July 2021. URL: https://www.statkraftvarme.no/globalassets/0/statkraft-varme/produkter-og-tjenester/prisark/juli-2021/trondheim-bedrift-med-volumledd-bt1v.pdf (visited on 05/16/2022).

[84] *Prismodell*. Statkraftvarme.no, 2022. URL: https://www.statkraftvarme.no/kundeservice/priser/prismodell/ (visited on 05/16/2022).

[85] Ellen Synnøve Viseth. *Hvorfor følger fjernvarmeprisen strømprisen?* Tu.no, Oct. 2021. URL: https://www.tu.no/artikler/hvorfor-folger-fjernvarmeprisen-stromprisen/514367 (visited on 05/16/2022).

[86] Frazer Norwell. *ENERGY: What Norway's new grid rent model means for you.* The Local Norway, May 2022. URL: https://www.thelocal.no/20220509/energy-prices-what-the-new-grid-rent-model-in-norway-means-for-you/ (visited on 05/16/2022).

[87] Troms Kraft. *Grid Rental - Price information - Private customers.* Tromskraftnett.no, 2020. URL: https://www.tromskraftnett.no/privat/english/nettognettleie (visited on 05/16/2022).

[88] NVE. *Strømkunder.* www.nve.no, 2012. URL: https://www.nve.no/energi/virkemidler/elsertifikater/stroemkunder/ (visited on 05/16/2022).

[89] Statskraft Varme. *Fjernvarmetariff PT1 til privatkunder i Trondheim.* Statskraft Varme, July 2021. URL: https://www.statkraftvarme.no/globalassets/0/statkraft-varme/kundeservice/priser/2022/trondheim-privatkunder-pt1.pdf (visited on 05/16/2022).

[90] Statskraft Varme. *Fjernvarmetariff PT1V til fellesmålte borettslag/sameier i Trondheim.* Statskraft Varme, July 2021. URL: https://www.statkraftvarme.no/globalassets/0/statkraft-varme/kundeservice/priser/2022/trondheim-borettslag-pt1v.pdf (visited on 05/16/2022).

[91] *Fjernkontrollen.no.* www.fjernkontrollen.no, 2021. URL: https://www.fjernkontrollen.no/ (visited on 04/26/2022).

[92] Rockwool. *Nytt samarbeid: overskuddsvarme fra AS ROCKWOOL til norske boliger.* www.rockwool.com, Jan. 2016. URL: https://www.rockwool.com/no/om-oss/nyheter/2016/nytt-samarbeid-overskuddsvarme-fra-as-rockwool-til-norske-boliger/ (visited on 05/01/2022).

[93] Statkraft Varme. *Overskuddsvarme utnyttes til fjernvarmeproduksjon.* www.statkraftvarme.se, Oct. 2016. URL: https://www.statkraftvarme.se/no/om-statkraftvarme/presse/nyheter/avtale-med-rockwool/ (visited on 05/01/2022).

[94] NTNU and Idun Haugan. *Smarte bydeler i Trondheim er fÃ¸rst i verden med kjÃ¸p og salg av strÃ¸m i nabolaget.* forskning.no, Mar. 2022. URL: https://forskning.no/energi-ntnu-partner/smarte-bydeler-i-trondheim-er-forst-i-verden-med-kjop-og-salg-av-strom-i-nabolaget/1998237 (visited on 05/01/2022).

[95] Joshua Roberts et al. *Energy Community Definitions.* 2019. URL: https://www.compile-project.eu/wp-content/uploads/Explanatory-note-on-energy-community-definitions.pdf (visited on 04/05/2022).

[96] Knut Samdal. *Energisystem - SINTEF.* SINTEF, Nov. 2021. URL: https://www.sintef.no/felles-fagomrade/energisystem/ (visited on 04/05/2022).

[97] EUROPEAN COMMISION. *Press corner.* European Commission - European Commission, July 2020. URL: https://ec.europa.eu/commission/presscorner/detail/en/fs_20_1295?fbclid=IwAR0Zyx0pHTueGWdOrLQ6MFkghLoM8G-tvXhAPU6aaK4aFHEujX4ynZFEqDE (visited on 05/02/2022).

[98] Berlin Energy Transition Dialogue. *Explainer: Sector Coupling.* www.youtube.com, July 2020. URL: https://www.youtube.com/watch?v=sm4wbsAhEd4 (visited on 05/02/2022).

[99] Rongling Li et al. “Case-study of Thermo Active Building Systems in Japanese Climate”. In: *Energy Procedia* 78 (Nov. 2015), pp. 2959–2964. DOI: 10.1016/j.egypro.2015.11.679. URL: https://www.sciencedirect.com/science/article/pii/S187661021502411X (visited on 05/03/2022).

[100] International Organization for Standardization (ISO). *ISO 11855-4:2021 Building environment design — Embedded radiant heating and cooling systems — Part 4: Dimensioning and calculation of the dynamic heating and cooling capacity of Thermo Active Building Systems (TABS)*. ISO, 2021. URL: https://www.iso.org/standard/74686.html (visited on 05/03/2022).

[101] VVS Akktuelt. *Termoaktive betongdekker*. VVS aktuelt, 2016. URL: https://www.vvsaktuelt.no/termoaktive-betongdekker-106312/nyhet.html (visited on 04/21/2022).

[102] Joaquim Romaní, Alvaro de Gracia, and Luisa F. Cabeza. “Simulation and Control of Thermally Activated Building Systems (TABS)”. In: *Energy and Buildings* 127 (Sept. 2016), pp. 22–42. DOI: 10.1016/j.enbuild.2016.05.057. URL: https://www.sciencedirect.com/science/article/pii/S0378778816304261 (visited on 05/04/2022).

[103] Piotr Michalak. “Selected Aspects of Indoor Climate in a Passive Office Building with a Thermally Activated Building System: A Case Study from Poland”. In: *Energies* 14 (Feb. 2021). Ed. by Andrea Ferrantelli, p. 860. DOI: 10.3390/en14040860. URL: https://www.mdpi.com/1996-1073/14/4/860 (visited on 05/03/2022).

[104] Toshiki Namai et al. “Measurement and Operational Improvement in an Office with Thermo Active Building System”. In: *E3S Web of Conferences* 111 (2019). Ed. by S.I Tanabe et al., p. 02065. DOI: 10.1051/e3sconf/201911102065. URL: https://www.e3s-conferences.org/articles/e3sconf/abs/2019/37/e3sconf_clima2019_02065/e3sconf_clima2019_02065.html (visited on 05/04/2022).

[105] D.O. Rijksen, C.J. Wisse, and A.W.M. van Schijndel. “Reducing Peak Requirements for Cooling by Using Thermally Activated Building Systems”. In: *Energy and Buildings* 42 (Mar. 2010), pp. 298–304. DOI: 10.1016/j.enbuild.2009.09.007. URL: https://www.sciencedirect.com/science/article/pii/S0378778809002217?via%3Dihub (visited on 05/03/2022).

[106] Amelia Natalie Lisiecka. “Optimalisering av effekttopper i kontorbygg ved hjelp av termoaktive dekker og varmepumper”. In: *Ntnu.no* 3271 (2021). DOI: no.ntnu:inspera:80324182:35959661. URL: https://ntnuopen.ntnu.no/ntnu-xmlui/handle/11250/2788861 (visited on 04/26/2022).

[107] Lasse Simonsen. “Analysis of a Thermo-Active Building System in a Modern Norwegian Office Building”. In: *Ntnu.no* 3271 (2021). DOI: no.ntnu:inspera:80323884:47571426. URL: https://ntnuopen.ntnu.no/ntnu-xmlui/handle/11250/2787162 (visited on 04/26/2022).

[108] Headspin Productions AS. *Kjeldsberg – Sluppen*. Kjeldsberg, 2015. URL: https://www.kjeldsberg.no/?s=sluppen (visited on 04/12/2022).

[109] Kjersti Lunden Nilsen. *Denne gården drives med sol, vind og hydrogen*. Tu.no, Nov. 2021. URL: https://www.tu.no/artikler/denne-garden-drives-med-sol-vind-og-hydrogen/515059 (visited on 05/18/2022).

[110] European Commission. *Waste Framework Directive*. ec.europa.eu, 2021. URL: https://ec.europa.eu/environment/topics/waste-and-recycling/waste-framework-directive_en.

[111] *ArcGIS Web Application*. statkrafteu.maps.arcgis.com, 2022. URL: https://statkrafteu.maps.arcgis.com/apps/webappviewer/index.html?id=4f17d9af01884fc1b98708105a227dc3.

A Waste Framework Directive

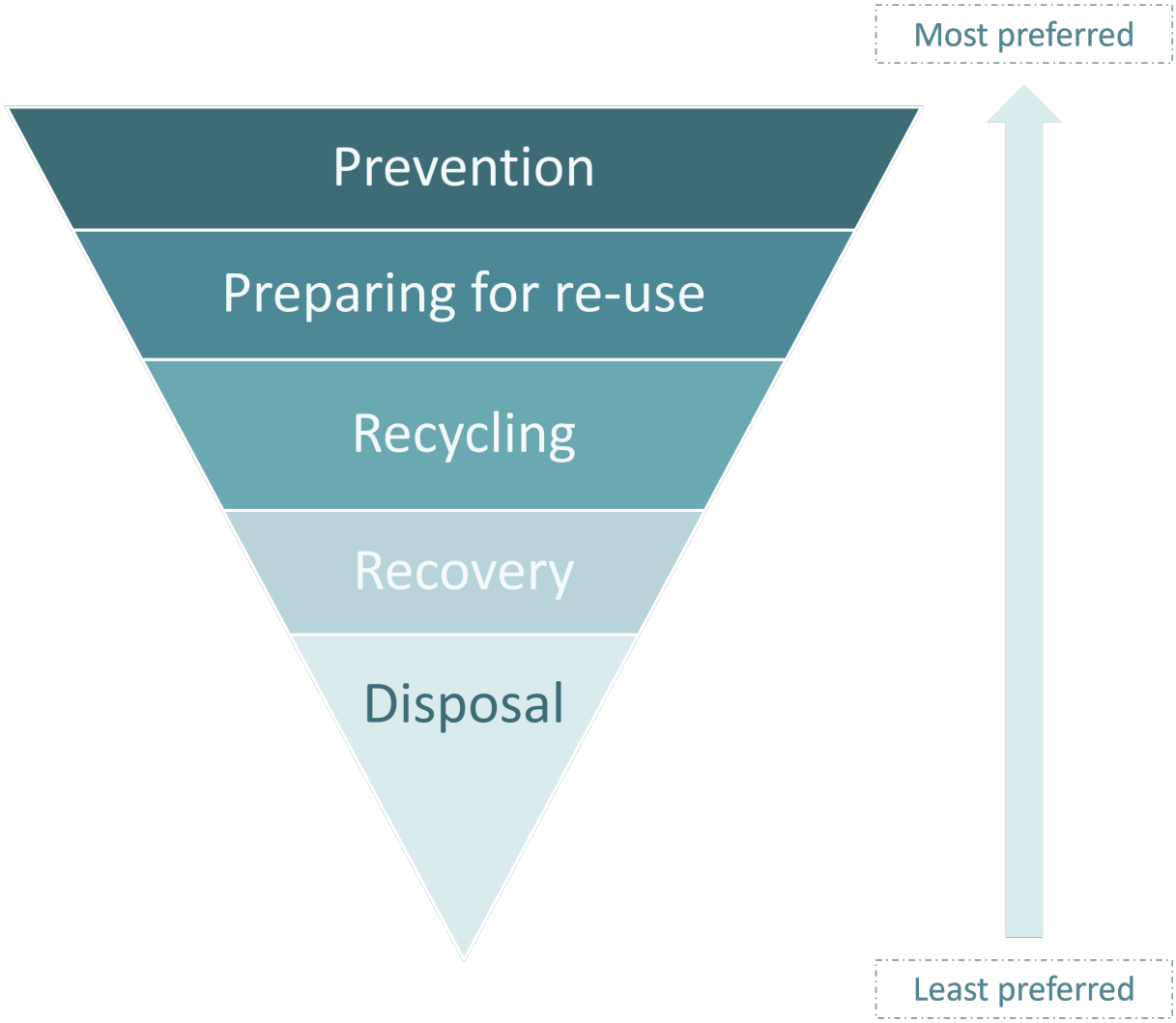

Figure A.1: *Waste Framework Directive, a part of waste prevention and management strategy for EU, inspired by [110].*

B Map of District Heating, Trondheim

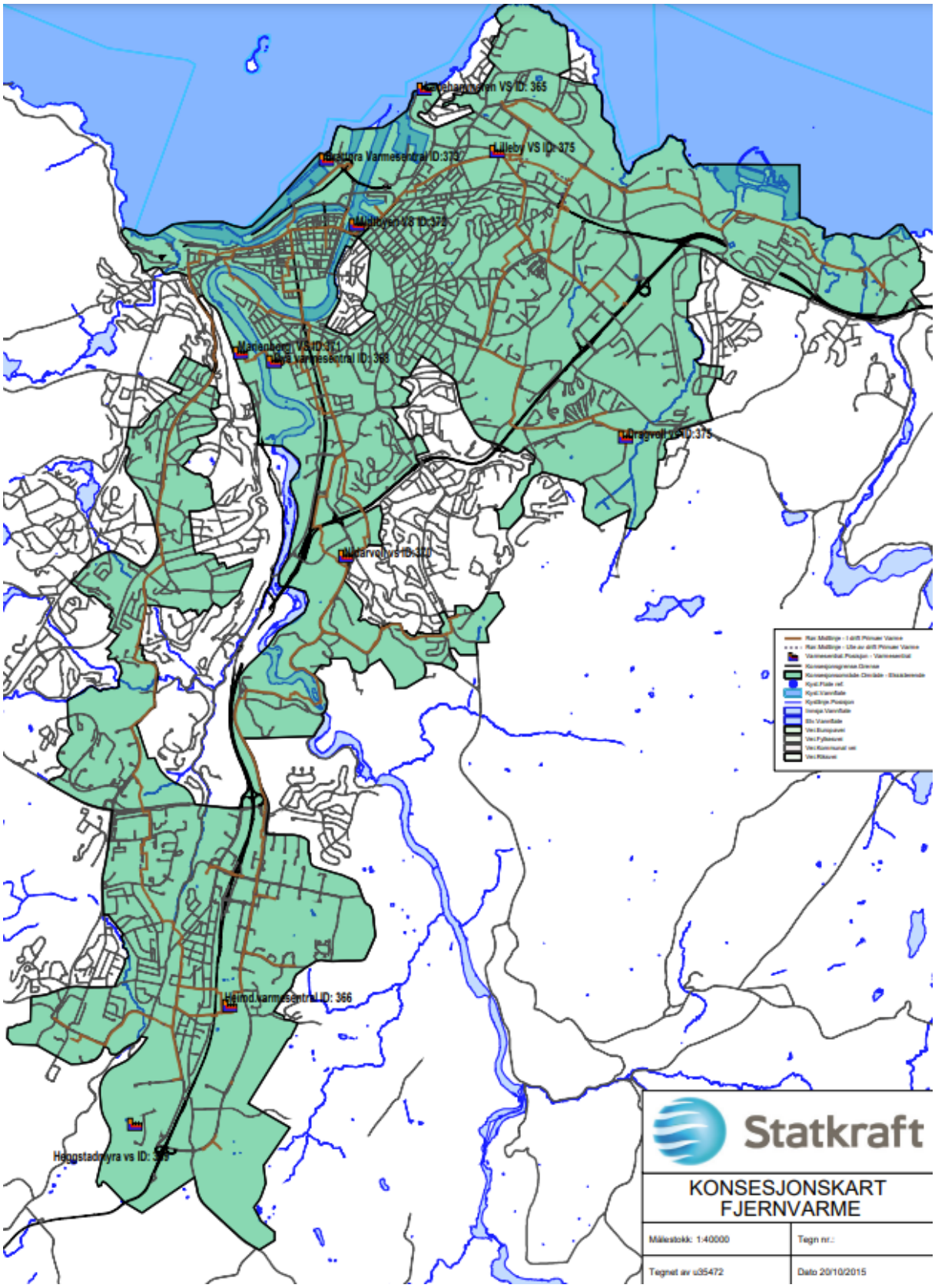

Figure B.1: *Map of district heating in 2015, Trondheim [111].*

C Map of District Heating, Sluppen

Figure C.1: *Map of the district heating distribution at Sluppen, and the nearby heating plant at Nidardvoll [111].*

D Pressure Enthalpy Diagram for Refrigerant R410A

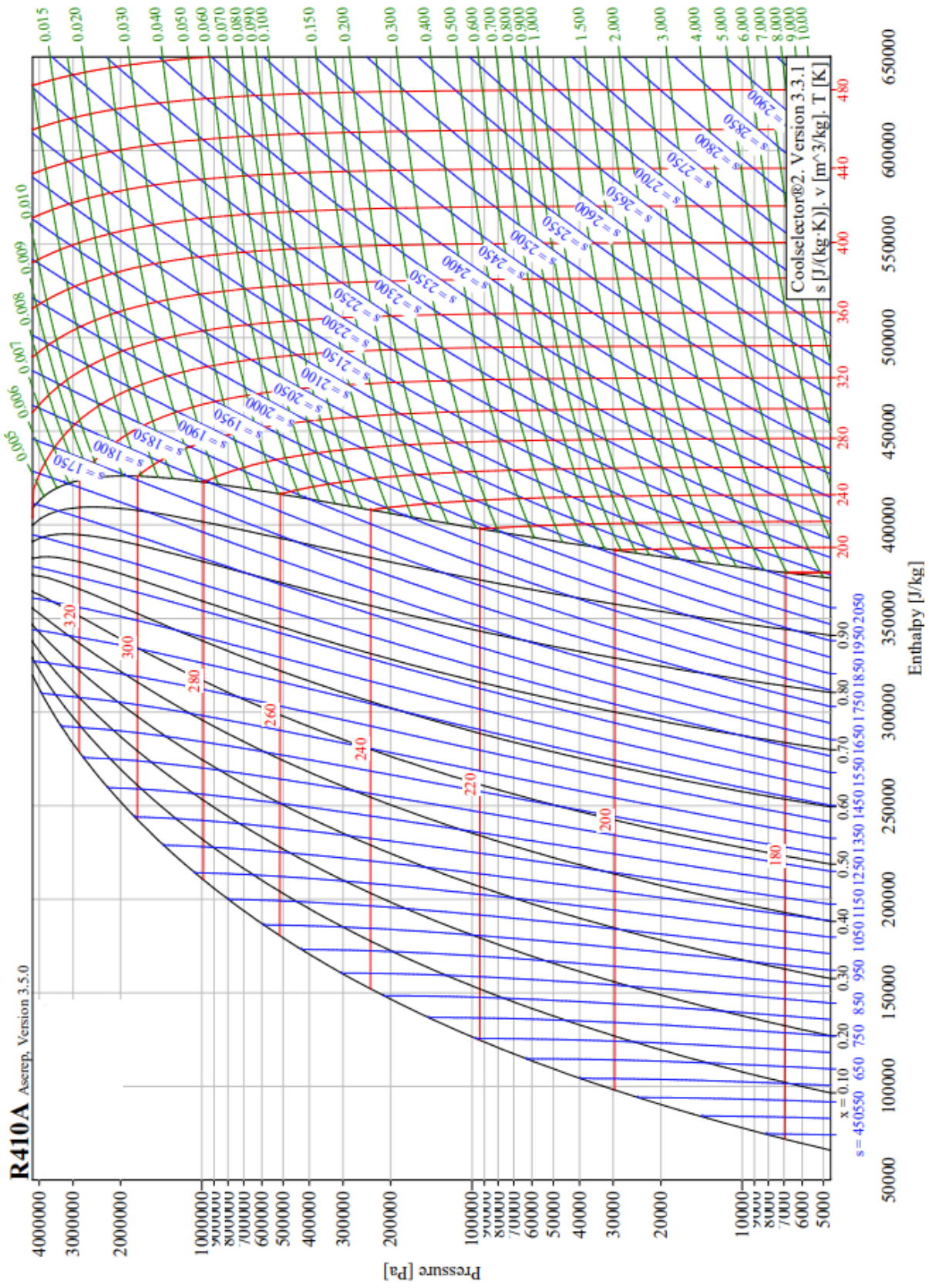

Figure D.1: *Pressure enthalpy diagram for refrigerant R410A*

E MatLab - Data Treatment

```
%% Data treatment
% All data if nothing else is stated, used in this script is confidential
% and supplied by external supervisors.

%% Temperature data
Weather     = readtable('w3.csv');
% from Norsk KlimasService Senter, seklima.met.no
w3          = Weather(24:7344,:);
w3          = w3(:,4);
w3          = table2array(w3);
w3          = func_commatoperiod(w3);
w3(5880,:)  = [];
save('temp.mat','w3')

function ut = func_commatoperiod(x)
x = char(x);
for i =1:size(x,1)
for j = 1:length(x(i,:))
    if x(i,j) == ','
        x(i,j) = '.';
    end
end
end
ut = str2num(x);
end

%% Main meters Sluppen
% EL = electricity load, mesured by the
% FJV = district heating load
%%% 2019 %%%%%%%%%%%%%%%%%%%%%%%%%%%%%%%%%%%%%%%%%%%%%%%%%%%%%%%%%%%%%%%%%%%%
%%%% Starts 01.03.19 00:00
%%%% Ends 31.12.19 00:00
C19      = readtable("Mainmeter2019.csv");
C19_17B  = table2array(C19(1417:8736,[8 9]));
% EL, FJV
C19_19   = table2array(C19(1417:8736,[11]));
%     FJV
C19_11   = table2array(C19(1417:8736,[14 15]));
% EL, FJV
C19_13   = table2array(C19(1417:8736,17));
% EL
%%% 2020 %%%%%%%%%%%%%%%%%%%%%%%%%%%%%%%%%%%%%%%%%%%%%%%%%%%%%%%%%%%%%%%%%%%%
%%%% Starts 01.03.20 00:00
%%%% Ends 31.12.20 00:00
```

```
C20      = readtable("Mainmeter2020.csv");
C20_17B  = table2array(C20(1417:8736,[8 9]));
% EL, FJV
C20_19   = table2array(C20(1417:8736,[11]));
%     FJV
C20_11   = table2array(C20(1417:8736,[14 15]));
% EL, FJV
C20_13   = table2array(C20(1417:8736,17));
% EL
%%% 2021 %%%%%%%%%%%%%%%%%%%%%%%%%%%%%%%%%%%%%%%%%%%%%%%%%%%%%%%%%%%%%%%%%%%%%%%
%%%% Starts 01.03.21 00:00
%%%% Ends 31.12.21 00:00
C21      = readtable("Mainmeter2021.csv");
C21_17B  = table2array(C21(1417:8736,[8 9]));
% EL, FJV
C21_19   = table2array(C21(1417:8736,[11]));
%     FJV
C21_11   = table2array(C21(1417:8736,[14 15]));
% EL, FJV
C21_13   = table2array(C21(1417:8736,17));
% EL

%% Production profile
% PV data Sluppenvegen 19 %%%%%%%%%%%%%%%%%%%%%%%%%%%%%%%%%%%%%%%%%%%%%%%%%%%%
%%%% Starts 01.09.19 00:00
%%%% Ends 31.08.20 00:00
Sol_1           = readtable("Sluppenvegen19.xlsx");
colNames        = {'Sum','Mean','Max','Min','Antall'};
%%%% Starts 01.03.20 00:00
%%%% Ends 31.12.19 00:00
Sol_2           = readtable('Sluppenvegen19_treated.xlsx');
Sol             = Sol_2(1441:8760,:);

SolEV           = Sol(:,3);
SolEV           = table2array(SolEV);
save('SolEV.mat','SolEV')

DCprod          = Sol(:,6);
DCprod          = table2array(DCprod);
DCprod          = DCprod(:,1);

% PV data Rye %%%%%%%%%%%%%%%%%%%%%%%%%%%%%%%%%%%%%%%%%%%%%%%%%%%%%%%%%%%%%%%%
RYEprod         = load('RYEprod.mat');
RYEprod         = RYEprod.RYEprod;
RYEprod         = RYEprod./1000; %kWh

```

```
% Total PV production %%%%%%%%%%%%%%%%%%%%%%%%%%%%%%%%%%%%%%%%%%%%%%%%%%%%%%%%%%%%
prod = DCprod + RYEprod;
for i = 2:length(prod) % Removes errors in the data set
    if prod(i) > 200
        prod(i) = prod(i-1);
    end
end

for i = 5000:length(prod)
    if prod(i) > 73
        prod(i) = prod(i-1);
    end
end

%% Load profile
%%% Mean total values %%%%%%%%%%%%%%%%%%%%%%%%%%%%%%%%%%%%%%%%%%%%%%%%%%%%%%%%%%%%
CEL_17B     = mean([C19_17B(:,1) C20_17B(:,1) C21_17B(:,1)],2);
CFJV_17B    = mean([C19_17B(:,2) C20_17B(:,2) C21_17B(:,2)],2);

SolEV       = load('SolEV.mat');SolEV    = SolEV.SolEV;
CEL_19      = SolEV;
CFJV_19     = mean([C19_19 C20_19 C21_19],2);

CEL_11      = mean([C19_11(:,1) C20_11(:,1) C21_11(:,1)],2);
CFJV_11_13  = mean([C19_11(:,2) C20_11(:,2) C21_11(:,2)],2);

CEL_13       = mean([C19_13 C20_13 C21_13],2);

CEL         = sum([CEL_17B CEL_19 CEL_11 CEL_13],2);
CFJV        = sum([CFJV_17B CFJV_19 CFJV_11_13],2);

%%% Yearly values %%%%%%%%%%%%%%%%%%%%%%%%%%%%%%%%%%%%%%%%%%%%%%%%%%%%%%%%%%%%%%%%
CEL_17B_y   = [C19_17B(:,1) C20_17B(:,1) C21_17B(:,1)];
CFJV_17B_y  = [C19_17B(:,2) C20_17B(:,2) C21_17B(:,2)];
CEL_19_y    = CEL_19;
CFJV_19_y   = [C19_19 C20_19 C21_19];
CEL_11_y    = [C19_11(:,1) C20_11(:,1) C21_11(:,1)];
CFJV_11_13_y= [C19_11(:,2) C20_11(:,2) C21_11(:,2)];
CEL_13_y    = [C19_13 C20_13 C21_13];

%% Sub-meters Sluppenvegen 17B
%%% Starts 01.03.21 00:00
%%% Ends 31.12.21 00:00
B17     = readtable('Sub_meters_17B.csv');

% Electric energy consumption, heat pump:
```

```
137 EL7     = table2array(B17(:,9));
138 EL7     = [EL7(1:5878,1); EL7(5878); EL7(5879:7319,1)];
139 % Delivered heat %%%%%%%%%%%%%%%%%%%%%%%%%%%%%%%%%%%%%%%%%%%%%%%%%%%%%%%%%%%%
140 % Delivered heat to heating system from district heating:
141 VAR2    = table2array(B17(:,39));
142 % Delivered heat to heating system by heat pump:
143 VAR8    = table2array(B17(:,45));
144 VAR8    = [VAR8(1:5878,1); VAR8(5878); VAR8(5879:7319,1)];
145 % Delivered heat to ventilation system:
146 VAR9    = table2array(B17(:,46));
147 VAR9    = [VAR9(1:5878,1); VAR9(5878); VAR9(5879:7319,1)];
148
149 % Tapwater %%%%%%%%%%%%%%%%%%%%%%%%%%%%%%%%%%%%%%%%%%%%%%%%%%%%%%%%%%%%%%%%%
150 TAPP    = table2array(B17(:,38));
151
152 % Rermoves peaks from inrush current measurment errors %%%%%%%%%%%%%%%%%%%%%
153 VAR9    = peakdelete(VAR9,90);
154 VAR8    = peakdelete(VAR8,90);
155 EL7     = peakdelete(EL7,60);
156 TAPP    = peakdelete(TAPP,50);
157 TAPP    = peakdelete(TAPP,50);
158 NFJV    = peakdelete(NFJV,60);
159 RAD     = peakdelete(RAD,15);
160 RAD     = peakdelete(RAD,15);
161
162 %%% Estimated heat deliverd to TABS, based on energy balance
163 tabs    = VAR8 + VAR2 - VAR9 - TAPP;
164 % removing negative values
165 for i = 1:length(tabs)
166     if tabs(i) < 0
167         tabs(i) = 0;
168     end
169 end
170 % Functions %%%%%%%%%%%%%%%%%%%%%%%%%%%%%%%%%%%%%%%%%%%%%%%%%%%%%%%%%%%%%%%%%
171 function matrise = peakdelete(matrise,max)
172     L = find(matrise > max);
173     for i = 1:length(L)
174         matrise(L(i),1) = matrise(L(i)+1,1);
175     end
176 end
```

F MatLab - Additional Solar Production

```
%% Import data
Sun2 = readtable('Sundata.csv');
NaN  = sum(isnan(table2array(Sun2(:,9))));
% NaN has to be equal to zero for the code to run correctly

%% Reoranise the matrix to have hourly values
soll     = Sun2(1:2559725,[1 5 7 9]);
soll.Properties.VariableNames = {'x_localdate_' 'prod1' 'prod2' 'prod3'};
vars     = {'prod1' 'prod2' 'prod3'};
solll    = soll{:,vars};
soll{:,vars} = solll;
soll     = convertvars(soll, @isdatetime, @(t) datetime(t, 'Format', 'yyyy-MM-dd-HH'));
soll.x_localdate_ = string(soll.x_localdate_);
sollmean = grpstats(soll,'x_localdate_','mean');
soll     = table2array(soll(:,2:4));

%% Fixing the number of rows
prod     = table2array(sollmean(:,3:5));
RYEprod  = sum(prod,2);
RYEprod1 = [RYEprod(1:272,1);(RYEprod(272));RYEprod(273:295,1);RYEprod(295);...
    RYEprod(296:655,1);RYEprod(655)  ;RYEprod(656:2669,1);RYEprod(2669);...
    RYEprod(2670:3436,1);RYEprod(3436)  ;RYEprod(3437:3458,1);RYEprod(3458);...
    RYEprod(3458:3480,1);RYEprod(3480)  ;RYEprod(3481:5036,1);RYEprod(5036);...
    RYEprod(5037:6043,1);RYEprod(6043)  ;RYEprod(6044:6591,1);RYEprod(6591);...
    RYEprod(6591)+2;RYEprod(6591)+3;RYEprod(6591)+4;RYEprod(6591)+5;...
    RYEprod(6591)+6;RYEprod(6591)+7;RYEprod(6592:7299,1)];
RYEprod2 = [RYEprod1(1:681);RYEprod1(681);RYEprod1(682:3441);RYEprod1(3441);...
    RYEprod1(3442:3465);RYEprod1(3465)  ;RYEprod1(3466:3488);RYEprod1(3488);...
    RYEprod1(3489:5045);RYEprod1(5045)  ;RYEprod1(5046:6053);RYEprod1(6053);...
    RYEprod1(6054:7316)];
RYEprod3 = [RYEprod2(1:3468);RYEprod2(3468)  ;RYEprod2(3469:7322)];
RYEprod4 = [RYEprod3(1:3466);RYEprod3(3469:7321)];
RYEprod5 = [RYEprod4(1:7319);RYEprod4(7319)  ;0];
RYEprod5(723) = [];
RYEprod = RYEprod5;
save('RYEprod.mat','RYEprod')
```

G MatLab - TABS

```
clear; close; clc
%%% Yearly electricty, AMS meter [kWh/h], 7320x3, main meter
    CEL_17B_y = load('CEL_17B_y-mat.mat');
    CEL_17B_y = CEL_17B_y.CEL_17B_y;
    C21_17B_2 = load('C21_17B_2.mat');
    C21_17B_2 = C21_17B_2.C21_17B_2;
    CEL_17B_2 = C21_17B_2(:,1);
%%% Estimated heat deliverd to TABS based on energy balance
    TAB       = load('TAB.mat');
    TAB       = TAB.TAB;
%%% Analysis 1, TABS %%%%%%%%%%%%%%%%%%%%%%%%%%%%%%%%%%%%%%%%%%%%%%%%%%%%%%%%%%%%
%% March
% Defining variables for desired period of time
inex_march    = 170:337;
TAB_march     = TAB(inex_march);
% Finding peakhours
ph            = peakhours(inex_march);
ph            = ph.*TAB_march;
% Defining timeperiod, moved back 24h
inex_march    = (170-24):(337-24);
EL            = CEL_17B_y(:,3);
EL_march      = EL(inex_march);
% Creating zeros matrix to move peaks
zero          = zeros(12,1);
% Adding back sunday
EL_march      = [EL_march;zero;zero];
% Valley hours, hours which are to be filled
vh            = [zero;ph.*1.1;zero]; % Adding 10% losses
% Peak hours, hours which are to be shaved
ph            = [zero;zero;ph];
% Shaving peaks and filling valleys
New           = [EL_march vh ph (vh-ph)];
                % org demand, filling vallies, shaving peaks, combined
New           = EL_march + New(:,4);
% Comparison
des_march     = describe(EL_march,New);

%% June
% Defining variables for desired period of time
index_june    = 2354:2521;
TAB_june      = TAB(index_june);
% Finding peakhours
ph            = peakhours(index_june);
ph            = ph.*TAB_june;
```

```
% Defining timeperiod, moved back 24h
index_june    = (2354-24):(2521-24);
EL            = CEL_17B_y(:,3);
EL_june       = EL(index_june);
% Moving peaks
zero          = zeros(12,1);
EL_june       = [EL_june;zero;zero];vh = [zero;ph.*1.1;zero]; % Adding 10% losses
ph            = [zero;zero;ph];
New           = [EL_june vh ph (vh-ph)];New = EL_june + New(:,4);
% Comparison
des_june = describe(EL_june,New);

%% September
% Defining variables for desired period of time
index_sep     = 4538:4705;
TAB_sep       = TAB(index_sep);
% Finding peakhours
ph            = peakhours(index_sep);
ph            = ph.*TAB_sep;
% Defining timeperiod, moved back 24h
index_sep     = (4538-24):(4705-24);
EL            = CEL_17B_y(:,3);
EL_sep        = EL(index_sep);
% Moving peaks
zero          = zeros(12,1);
EL_sep        = [EL_sep;zero;zero];vh = [zero;ph.*1.1;zero]; % Adding 10% losses
ph            = [zero;zero;ph];
New           = [EL_sep vh ph (vh-ph)];New = EL_sep + New(:,4);
% Comparison
des_sep       = describe(EL_sep,New);

%% December
% Defining variables for desired period of time
index_dec     = (6721):(6888);
TAB_dec       = TAB(index_dec);
% Finding peakhours
ph            = peakhours(index_dec);
ph            = ph.*TAB_dec;
% Defining timeperiod, moved back 24h
index_dec     = (6721-24):(6888-24);
EL            = CEL_17B_y(:,3);
EL_dec        = EL(index_dec);
% Moving peaks
zero          = zeros(12,1);
EL_dec        = [EL_dec;zero;zero];vh = [zero;ph.*1.1;zero]; % Adding 10% losses
ph            = [zero;zero;ph];
```

```
New           = [EL_dec vh ph (vh-ph)];New = EL_dec + New(:,4);
% Comparison
des_dec = describe(EL_dec,New);

%% Whole year
% Defining variables for desired period of time
TAB_y         = TAB; % whole year, Monday(1/3/21) to Thursday (30/12/21)
% Defining time period, moved back 24h
EL_y          = CEL_17B_2; % from Sunday (28/2/21) to Wednesday (29/12/21)

    hours_t   = [0:23];
    hours     = repmat(hours_t,1,7); % week 9
    hours     = hours';
    ph        = [hours hours]; % peak hours
    for i = 1:length(hours)
        if ph(i,2) ~= [7:16]
            ph(i,2) = 0;
        else
            ph(i,2) = 1;
        end
    end
    ph(length(ph)-48:length(ph),2) = 0; % removing the weekend
    ph = ph';
    ph = repmat(ph,1,43); % Repeats a week 43 time to crate week 9-51
    ph = ph'; % Ends Sunday 26/12/21
    % Have to add on 4 day to get to midnight 31/12/21
    ph2 = repmat(hours_t,1,4); % week 52
    for i = 1:length(ph2)
        if ph2(i) ~= [7:16]
            ph2(i) = 0;
        else
            ph2(i) = 1;
        end
    end
    ph2 = ph2';
    ph = [ph(:,2);ph2]; % from Monday 1/3/21 to Thursday 30/12/21
    ph  = ph.*TAB_y;

% Creating zeros matrix to move peaks
zero          = zeros(12,1);
% Adding back thursday
EL_y          = [EL_y(1:24);CEL_17B_y(:,3)];% from Sunday (28/11/21) to Thursday (30/12/21)
% Valley hours, hours which are to be filled
% adding the start of the extra Sunday at the beginning
% moving the load
vh            = [zero;ph.*1.1;zero]; % Adding 10% losses, Sunday (28/2/21)
```

```
%                                                   to Thursday (30/12/21)
% Peak hours, hours which are to be shaved
% adding extra Sunday
ph              = [zero;zero;ph]; % Sunday (28/2/21) to Thursday (30/12/21)
% Shaving peaks and filling valleys
New             = [EL_y vh ph (vh-ph)];
                % org demand, filling valleys, shaving peaks, combined
New             = EL_y + New(:,4);
% Comparison
des_y = describe(EL_y,New);

%% Functions %%%%%%%%%%%%%%%%%%%%%%%%%%%%%%%%%%%%%%%%%%%%%%%%%%%%%%%%%%%%%%%%%%%%
function peakhours = peakhours(Season)
    hours = [0:23];
    hours = repmat(hours,1,length(Season)/24);
    hours = hours';
    ph = hours; %peak hours
    for i = 1:length(hours)
        if ph(i) ~= [7:16]
            ph(i) = 0;
        else
            ph(i) = 1;
        end
    end
    ph(length(ph)-48:length(ph)) = 0; % removing the weekend
    peakhours = ph;
end

function ut = describe(Current,New)
    for i = 1:length(New)
        if New(i) < 0
            disp('ERROR!!!!')
        end
    end
     disp('Current')
     colNames = {'Mean','Min','Max','Sum'};
     ut = [mean(Current) min(Current(Current>0))  max(Current) sum(Current)];
     ut = array2table(ut,'VariableNames',colNames)
     disp('New')
     colNames = {'Mean','Min','Max','Sum'};
     ut = [mean(New) min(New(New>0))  max(New) sum(New)];
     ut = array2table(ut,'VariableNames',colNames)
     diff = Current - New;
     for i = 1:length(diff)
        if diff(i) < 0
            diff(i) = 0;
```

```
183             end
184         end
185         disp(['Max peak reduction = ',num2str(max(diff)),' kWp',' at ', ...
186         num2str(find(diff == max(diff)))])
187         disp(['Average peak reduction = ',num2str(mean(diff)),' kWh/h'])
188     end
```

H MatLab – Heat Pump

```
clear;close;clc
%%% Yearly electricty, AMS meter [kWh/h], 7320x3, main meter
    CEL_17B_y   = load('CEL_17B_y-mat.mat');
    CEL_17B_y   = CEL_17B_y.CEL_17B_y; %starts 01.03.21 00:00, ends 31.12.21 00:00
    C21_17B_2   = load('C21_17B_2.mat');
    C21_17B_2   = C21_17B_2.C21_17B_2;
    CEL_17B_2   = C21_17B_2(:,1); % starts 28.02.21 00:00, ends 30.12.21 00:00
%%% ELVARP - The heat pumps electricity demand
    ELVARP      = load('EL7.mat');
    ELVARP      = ELVARP.EL7;
%%% Analysis 2, HP %%%%%%%%%%%%%%%%%%%%%%%%%%%%%%%%%%%%%%%%%%%%%%%%%%%%%%%%%%%%
%% March
% Defining variables for desired period of time
index_march     = 170:337;
ELVARP_march    = ELVARP(index_march);
% Finding peakhours
ph              = peakhours(index_march);
ph              = ph.*ELVARP_march;
% Defining timeperiod, moved back 24h
index_march     = (170-24):(337-24);
EL              = CEL_17B_y(:,3);
EL_march        = EL(index_march);
% Creating zeros matrix to move peaks
zero            = zeros(12,1);
% Adding back Sunday
EL_march        = [EL_march;zero;zero];
% Valley hours, hours which are to be filled
vh              = [zero;ph.*1.1;zero]; % Adding 10% losses
% Peak hours, hours which are to be shaved
ph              = [zero;zero;ph];
phHP            = ph.*0.1; % 10% of the peaks shall not be shaved
% Shaving peaks and filling valleys
New             = [EL_march vh ph (vh-(ph-phHP))];
New             = EL_march + New(:,4);
% Comparison
% desEL_march     = describe(EL_march);
desNew_march    = describe(EL_march,New);

%% June
% Defining variables for desired period of time
index_june      = 2354:2521;
ELVARP_june     = ELVARP(index_june);
% Finding peakhours
ph              = peakhours(index_june);
```

```
ph              = ph.*ELVARP_june;
% Defining timeperiod, moved back 24h
index_june      = (2354-24):(2521-24);
EL              = CEL_17B_y(:,3);
EL_june         = EL(index_june);
% Creating zeros matrix to move peaks
zero            = zeros(12,1);
% Adding back Sunday
EL_june         = [EL_june;zero;zero];
% Valley hours, hours which are to be filled
vh              = [zero;ph.*1.1;zero]; % Adding 10% losses
% Peak hours, hours which are to be shaved
ph              = [zero;zero;ph];
phHP            = ph.*0.1; % 10% of the peaks shall not be shaved
% Shaving peaks and filling valleys
New             = [EL_june vh ph (vh-(ph-phHP))];
New             = EL_june + New(:,4);
% Comparison
des_june        = describe(EL_june,New);

%% September
% Defining variables for desired period of time
index_sep       = 4538:4705;
ELVARP_sep      = ELVARP(index_sep);
% Finding peakhours
ph              = peakhours(index_sep);
ph              = ph.*ELVARP_sep;
% Defining timeperiod, moved back 24h
index_sep       = (4538-24):(4705-24);
EL              = CEL_17B_y(:,3);
El_sep          = EL(index_sep);
% Creating zeros matrix to move peaks
zero            = zeros(12,1);
% Adding back Sunday
El_sep          = [El_sep;zero;zero];
% Valley hours, hours which are to be filled
vh              = [zero;ph.*1.1;zero]; % Adding 10% losses
% Peak hours, hours which are to be shaved
ph              = [zero;zero;ph];
phHP            = ph.*0.1; % 10% of the peaks shall not be shaved
% Shaving peaks and filling valleys
New             = [El_sep vh ph (vh-(ph-phHP))];
New             = El_sep + New(:,4);
% Comparison
des_sep         = describe(El_sep,New);

```

```
%% December
% Defining variables for desired period of time
index_dec       = (6721):(6888);
ELVARP_dec      = ELVARP(index_dec);
% Finding peakhours
ph              = peakhours(index_dec);
ph              = ph.*ELVARP_dec;
% Defining timeperiod, moved back 24h
index_dec       = (6721-24):(6888-24);
EL              = CEL_17B_y(:,3);
EL_dec          = EL(index_dec);
% Creating zeros matrix to move peaks
zero            = zeros(12,1);
% Adding back Sunday
EL_dec          = [EL_dec;zero;zero];
% Valley hours, hours which are to be filled
vh              = [zero;ph.*1.1;zero]; % Adding 10% losses
% Peak hours, hours which are to be shaved
ph              = [zero;zero;ph];
phHP            = ph.*0.1; % 10% of the peaks shall not be shaved
% Shaving peaks and filling valleys
New             = [EL_dec vh ph (vh-(ph-phHP))];
New             = EL_dec + New(:,4);
% Comparison
des_dec         = describe(EL_dec,New);

%% Whole year
% Defining variables for desired period of time
ELVARP_y        = ELVARP; %for hele året, mandag(1/3/21) til torsdag (30/12/21)
% Defining timeperiod, moved back 24h
EL_y            = CEL_17B_2; % fra en dag før og slutter en dag før,
                             % fra søndag (28/2/21) til onsdag (29/12/21)

    hours_t     = [0:23];
    hours       = repmat(hours_t,1,7); % week 9
    hours       = hours';
    ph          = [hours hours]; % peak hours
    for i = 1:length(hours)
        if ph(i,2) ~= [7:16]
            ph(i,2) = 0;
        else
            ph(i,2) = 1;
        end
    end
    ph(length(ph)-48:length(ph),2) = 0; % removing the weekend
    ph = ph';
```

```
    ph = repmat(ph,1,43); % Repets a week 43 time to crate week 9-51
    ph = ph'; % Ends Sunday 26/12/21
    % Have to add on 4 day to get to midnight 31/12/21
    ph2 = repmat(hours_t,1,4); % week 52
    for i = 1:length(ph2)
        if ph2(i) ~= [7:16]
            ph2(i) = 0;
        else
            ph2(i) = 1;
        end
    end
    ph2 = ph2';
    ph = [ph(:,2);ph2]; % from Monday 1/3/21 to Thursday 30/12/21
    ph  = ph.*ELVARP_y;
% Creating zeros matrix to move peaks
zero          = zeros(12,1);
% Adding back thursday
EL_y          = [EL_y(1:24);CEL_17B_y(:,3)];% fron Sunday (28/11/21) to Thursday (30/12/21)
% Valley hours, hours which are to be filled
% adding the start of the extra sunday at the beginning
% moving the load
vh            = [zero;ph.*1.1;zero]; % Adding 10% losses, Sunday (28/2/21)
%                                                    to Thursday (30/12/21)
% Peak hours, hours which are to be shaved
% adding extra sunday
ph            = [zero;zero;ph]; % Sunday (28/2/21) to Thursday (30/12/21)
% Shaving peaks and filling valleys
New           = [EL_y vh ph (vh-ph)];
              % org demand, filling vallies, shaving peaks, combined
New           = EL_y + New(:,4);
% Comparison
des_y         = describe(EL_y,New);

%% Functions %%%%%%%%%%%%%%%%%%%%%%%%%%%%%%%%%%%%%%%%%%%%%%%%%%%%%%%%%%%%%%%%
function peakhours = peakhours(Season)
    hours = [0:23];
    hours = repmat(hours,1,length(Season)/24);
    hours = hours';
    ph = hours; %peak hours
    for i = 1:length(hours)
        if ph(i) ~= [7:16]
            ph(i) = 0;
        else
            ph(i) = 1;
        end
    end
```

```
183         ph(length(ph)-48:length(ph)) = 0; % removing the weekend
184         peakhours = ph;
185     end
186     function ut = describe(Current,New)
187         for i = 1:length(New)
188             if New(i) < 0
189                 disp('ERROR!!!!')
190             end
191         end
192          disp('Current')
193          colNames = {'Mean','Min','Max','Sum'};
194          ut = [mean(Current) min(Current(Current>0))  max(Current) sum(Current)];
195          ut = array2table(ut,'VariableNames',colNames)
196          disp('New')
197          colNames = {'Mean','Min','Max','Sum'};
198          ut = [mean(New) min(New(New>0))  max(New) sum(New)];
199          ut = array2table(ut,'VariableNames',colNames)
200          diff = Current - New;
201          for i = 1:length(diff)
202             if diff(i) < 0
203                 diff(i) = 0;
204             end
205          end
206     end
```

I MatLab – Sector Coupling

```
clear;close;clc
%%% Yearly electricty, AMS meter [kWh/h], 7320x3, main meter
    CEL_17B_y   = load('CEL_17B_y-mat.mat');
    CEL_17B_y   = CEL_17B_y.CEL_17B_y;
    CEL         = CEL_17B_y(:,3);
%%% VARP - Heat deliverd by heat pump
    VARP        = load('VAR8.mat');
    VARP        = VARP.VAR8;
%%% ELVARP - The heat pumps ELD
    ELVARP      = load('EL7.mat');
    ELVARP      = ELVARP.EL7;
%%% District heating in
    FJV         = load('VAR2.mat');
    FJV         = FJV.VAR2;
    FJV         = peakdelete(FJV,120);
    FJV         = peakdelete(FJV,120);

%%% Analysis 3, no HP %%%%%%%%%%%%%%%%%%%%%%%%%%%%%%%%%%%%%%%%%%%%%%%%%%%%%%%%
%% March
% Defining variables for desired period of time
CEL             = CEL_17B_y(:,3);
index_march     = 170:337;
EL              = CEL(index_march) - ELVARP(index_march);
HEAT_IN         = FJV(index_march) + VARP(index_march);
% Comparison
desEL_march     = describe(CEL(index_march));
desEL           = describe(EL);
desFJV_march    = describe(FJV(index_march));
desHEATIN       = describe(HEAT_IN);

%% June
% Defining variables for desired period of time
CEL             = CEL_17B_y(:,3);
index_june      = 2354:2521;
EL              = CEL(index_june) - ELVARP(index_june);
HEAT_IN         = FJV(index_june) + VARP(index_june);
% Comparison
for i = index_june(1):index_june(length(index_june))
    if VARP(i) == 0
        ELVARP_d(i) = 0;
    end
    EL_d = CEL(index_june) - ELVARP_d(index_june);
end

```

```
desEL_june      = describe(CEL(index_june));
desEL           = describe(EL_d);
desFJV_june     = describe(FJV(index_june));
desHEATIN       = describe(HEAT_IN);

%% September
% Defining variables for desired period of time
CEL             = CEL_17B_y(:,3);
index_sep       = 4538:4705;
EL              = CEL(index_sep) - ELVARP(index_sep);
HEAT_IN         = FJV(index_sep) + VARP(index_sep);
% Comparison
desEL_sep       = describe(CEL(index_sep));
desEL           = describe(EL);
desFJV_sep      = describe(FJV(index_sep));
desHEATIN       = describe(HEAT_IN);

%% December
% Defining variables for desired period of time
CEL             = CEL_17B_y(:,3);
index_dec       = (6721):(6888);
EL              = CEL(index_dec) - ELVARP(index_dec);
HEAT_IN         = FJV(index_dec) + VARP(index_dec);
% Comparison
desEL_dec       = describe(CEL(index_dec));
desEL           = describe(EL);
desFJV_dec      = describe(FJV(index_dec));
desHEATIN       = describe(HEAT_IN);

%% Whole year
% Defining variables for desired period of time
CEL             = CEL_17B_y(:,3);
EL              = CEL - ELVARP;
HEAT_IN         = FJV + VARP;

% Comparison
for i = 1:length(CEL) % makes sure not to move days where the EL is only used for cooling
    if VARP(i) == 0
        ELVARP(i) = 0;
    end
    EL = CEL - ELVARP;
end
desEL_year      = describe(CEL);
desEL           = describe(EL);
desFJV_year     = describe(FJV);
desHEATIN       = describe(HEAT_IN);
```

```
%% Function %%%%%%%%%%%%%%%%%%%%%%%%%%%%%%%%%%%%%%%%%%%%%%%%%%%%%%%%%%%%%%%%%%%%
function matrise = peakdelete(matrise,max)
    finne = find(matrise > max);
    for i = 1:length(finne)
        matrise(finne(i),1) = matrise(finne(i)+1,1);
    end
end

function ut = describe(matrise)
    colNames = {'Mean','Min','Max','Sum'};
    ut = [mean(matrise) min(matrise(matrise>0))  max(matrise) sum(matrise(:))];
    ut = array2table(ut,'VariableNames',colNames);
end
```

J MatLab - PV Estimation

```
clear;close;clc

%%% Estimation of PV production

%% Loading data
%   Irradiance for the area, collected from NASA
    IRRD         = readtable('IRRD2.csv');
    IRRD         = table2array(IRRD);
    IRRD         = IRRD(24:7344,5);
    IRRD(5879,:) = [];

%% Production from SLV19 and Rye
    prod         = load('prod.mat');
    prod         = prod.prod;

%% Defining variables
%   Area of new PV panels
    A11          = 1600;
    A17          = 666;

%   Efficiency of panels on SLV19
    eta          = 22.1/100;

%% Estimating production
    estP_11      = IRRD.*A11.*eta/1000;
    estP_17      = IRRD.*A17.*eta/1000;
    estP_tot     = estP_11 + estP_17 + prod;
    optprod      = sum(estP_tot)*2.5;
    % Optimized production, based on irradiation and demand
```

J. H. Evenstuen, P. S. Pedersen, I. M. Thrane

NTNU
Kunnskap for en bedre verden